Chapter 4

Results and Discussion

4.1. Characterization of BD and TEL

4.1.1. Physicochemical characterization

I. Organoleptic properties

The collected samples of BD and TEL were physically characterized and identified based on numerous factors. The results are shown in table 4.1, confirming the authenticity of these two medicine.

Sr. No.	Description	BD	TEL
1.	Color	Yellowish	White to slightly yellowish
2.	Odor	Odorless	Odorless
3	Nature	Powder	Powder
4.	Solubility	Soluble in methanol	Soluble in methanol

Table 4.1: Physicochemical characterization of BD and TEL

II. Solubility of BD and TEL

BD and TEL solubility was examined in water and methanol. The solubility of BD in water is 0.14 ± 0.051 µg/mL, whereas the solubility of TEL in water is 0.11 ± 0.020 mg/mL. The solubility of BD in methanol is 50.85 ± 0.012 mg/mL, whereas TEL has a solubility of 20.25 ± 0.213 mg/mL. The research findings confirmed that both drugs were soluble in methanol, as shown by the provided data.

4.1.2. Identification test using spectrum analysis of BD and TEL

BD and TEL were identified using UV spectroscopy, FT-IR spectroscopy, and DSC analysis.

I. UV spectroscopy

The maximum absorbance (λmax) of BD and TEL in methanol by UV spectroscopy was found to be 237 and 254 nm respectively (table 4.2 and figure 4.1). The obtained

λmax of BD and TEL in solvent was concordant with reference λmax of respective drug samples which validated the purity of the drugs.

Drug	Solvent system	Reported Value	Obtained Value
Benidipine	Methanol	237	237
Telmisartan	Methanol	254	254

Table 4.2: Reported and obtained value of λmax for BD and TEL

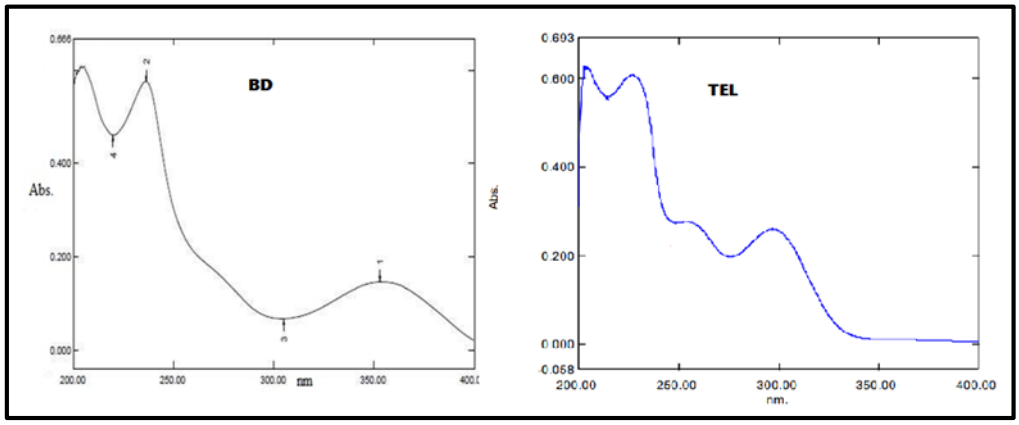

Figure 4.1: UV spectroscopy of BD and TEL

II. FTIR

The FTIR spectra of BD and TEL were captured for comparison with the respective reference spectra displayed in figure 4.2 (a) and 4.2 (b).

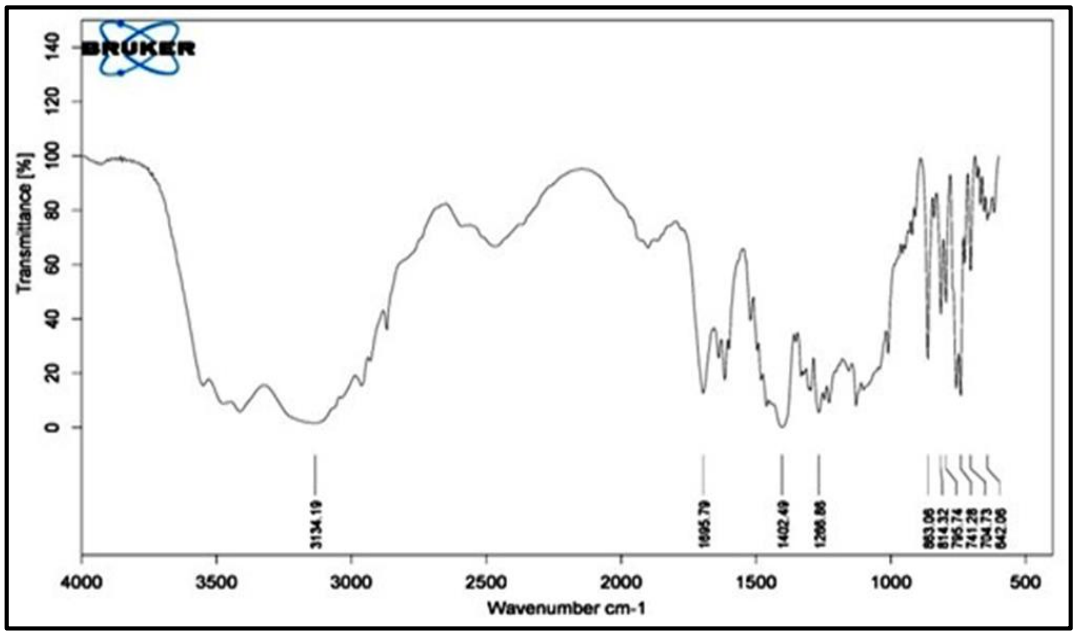

Figure 4.2(a): FTIR spectra of BD

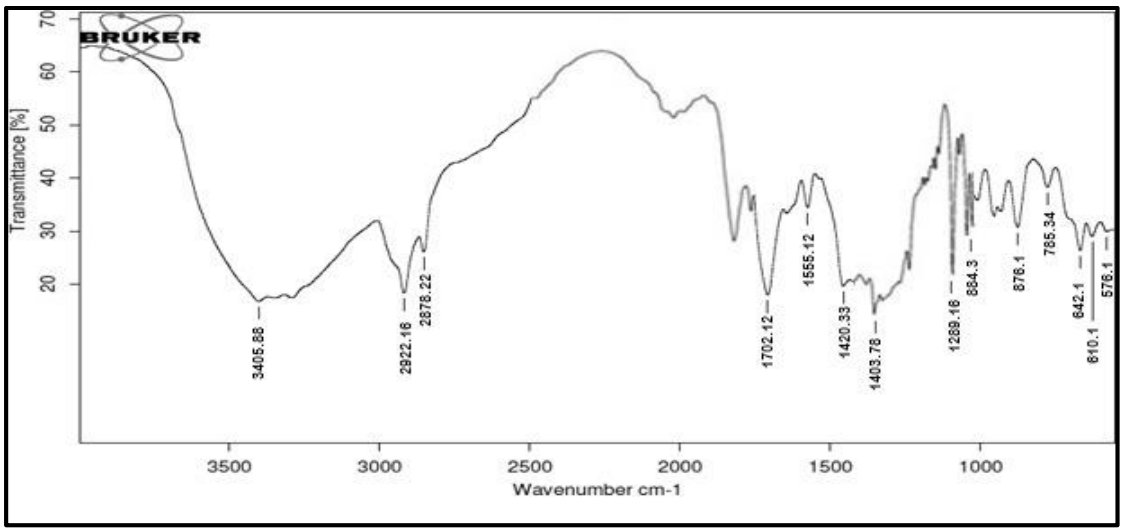

Figure 4.2(b): FTIR spectra of TEL

The characteristic peaks of both drugs are displayed in Table 4.3. From this data, it can be concluded that the FTIR spectrum of the sample medicine was similar to the reference spectra, which validated the identity and purity of the samples of BD and TEL.

BD		**TEL**	
Wave number (cm^{-1})	**Functional group**	**Wave number (cm^{-1})**	**Functional group**
3401	Aromatic N-H stretching	1895	C-H stretching
1708	C=O stretching	1266	C-N stretching
1574	C=C stretching	3134	Aromatic N-H stretching
2852	N=O stretching	1402	C=O stretching
1165	N=O stretching	883	C=C stretching
1018	N=C stretching	741	C=O stretching
777	C=C stretching		

Table 4.3: FTIR bands with characteristic functional group of BD and TEL

III. DSC

The thermal behavior of BD and TEL is depicted in figure 4.3. The DSC curves of BD and TEL indicated a pronounced endothermic peak at 172°C and 262°C, respectively, which is consistent with the given values in the literature, i.e., 193°C for BD and 262°C for TEL. These evaluations showed the purity of the drug samples.

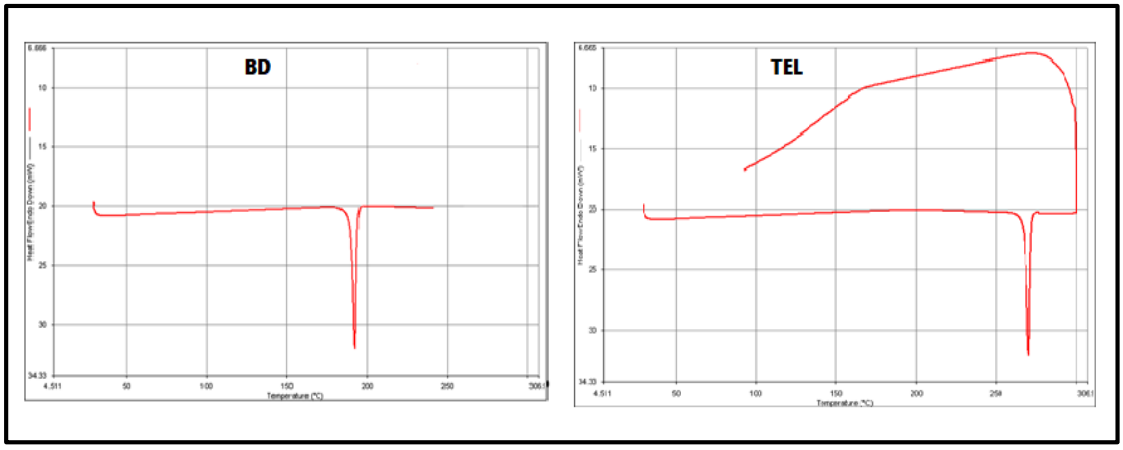

Figure 4.3: DSC spectrum of BD and TEL.

Conclusion

It confirmed that, on the basis of the physical-chemical characteristics investigation and identification test by the spectrum analysis, the obtained pharmaceuticals, including BD and TEL, have been found to be acceptable and pure and may be employed for further studies.

4.1.3. Analytical technique development and validation for the determination of BD and TEL

The analytical technique was designed and verified for the estimation of BD and BD with TEL using UV spectroscopy.

A) Analytical method development and validation for the determination of BD

The λmax was determined by scanning a 10 µg/mL solution of the test medium in the range of 200–400 nm employing a UV visible spectrophotometer against the identical blank. The λmax was found to be 237 nm for the methanol and 0.1N HCl, respectively. So, a further research employing the UV visible spectrophotometer was done at 237 nm wavelength for both 0.1N HCl and methanol.

The absorbance values (mean of three measurements) with their standard deviation at different concentrations in the range of 3–15 µg/mL for methanol and 3–15 µg/mL for 0.1N HCl are presented in tables 4.4 and 4.5. The drug was determined to be in accordance with Lambert's law in the concentration range. The correlation coefficient (R^2) for BD was found to be 0.9986 in methanol and 0.9991 in 0.1N HCl (Figure 4.4). Linear regression analysis for all calibration curves of BD is presented in Table 4.6. So, this equation has been used for the calculation of the solubility of the drugs in various solvents, drug content, and drug release.

Concentration (µg/ml)	**Absorbance**
0	0
3	0.189±0.002
6	0.334±0.003
9	0.492±0.001
12	0.640±0.002
15	0.796±0.003

Table 4.4: Data of standard calibration curve of BD in methanol at 237 λmax

Concentration (µg/ml)	**Absorbance**
0	0
3	0.177±0.03
6	0.325±0.08
9	0.462±0.06
12	0.621±0.04
15	0.768±0.12

Table 4.5: Data of standard calibration curve of BD in 0.1N HCl at 237 λmax

Solvent	**Slope**	**Intercept**	**R^2**
Methanol	0.0523	0.0163	0.9986
0.1N HCl	0.0506	0.0118	0.9991

Table 4.6: Linear regression analysis for calibration curve of BD

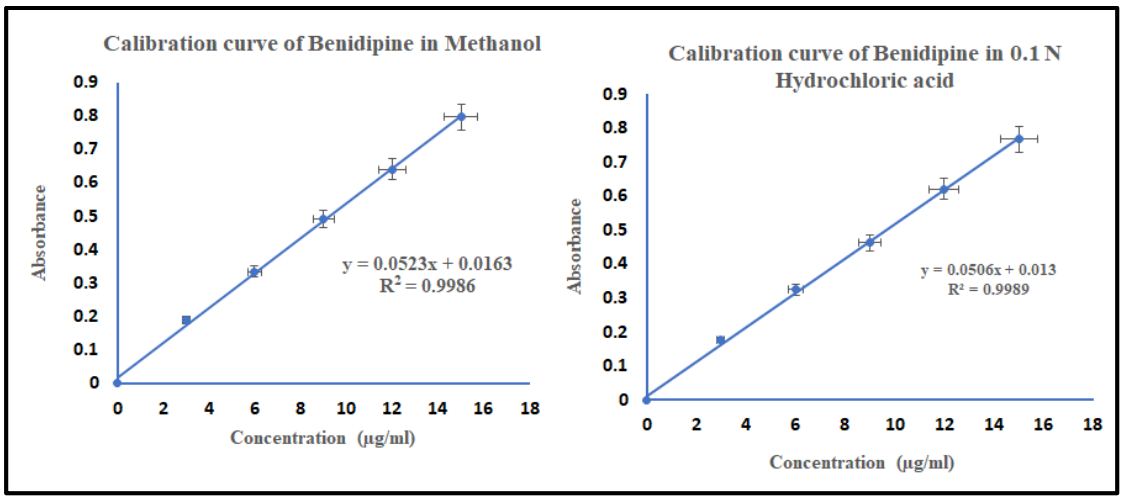

Figure 4.4: Standard calibrations Curve of BD in methanol and 0.1N HCl

B) Analytical technique development and validation for estimation of BD with TEL

To identify the wavelength for measurement, BD (5 µg/ml) and TEL (50 µg/ml) solutions were scanned between 400 and 200 nm. From the overlain spectra, as shown in figure 4.5, four wavelengths—229.30 nm and 246.32 nm for BD and 280.10 nm and 315.29 nm for TEL—were chosen for estimation of both drugs using the dual wavelength spectrophotometric method. The quantitative measurement of BD was carried out by comparing the absorbance differences at λmax of 229.30 nm and 246.32 nm when TEL showed a similar absorbance value. The quantitative measurement of TEL was carried out by measuring the absorbance difference at 280.10 nm and 315.29 nm, while BD exhibited a similar absorbance value at both wavelengths.

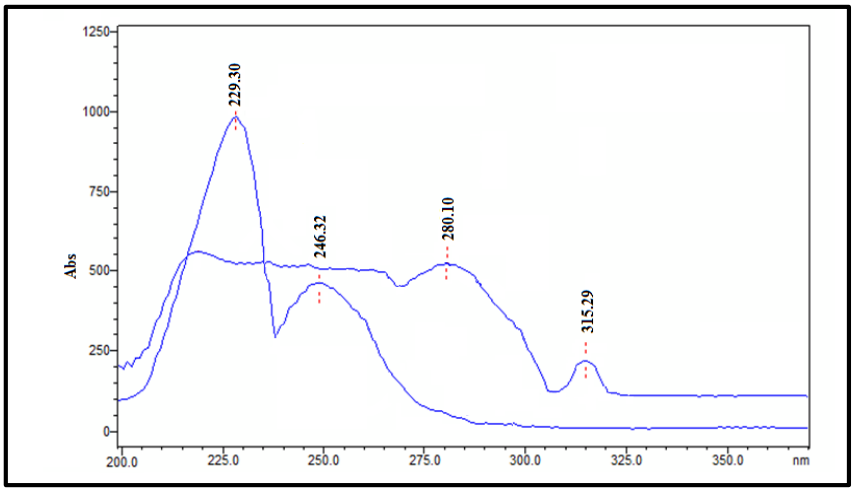

Figure 4.5: Overlain spectra of BD (5 µg/ml) and TEL (50 µg/ml)

The linearity of BD and TEL was discovered to be in the region of 1–5 µg/ml and 10–50 µg/ml, respectively. Linearity was examined in terms of slope, intercept, and correlation coefficient for both drugs, as given in Table 4.7.

Parameters	BD	TEL
Wavelength	229.30 nm and 246.32	280.10 nm and 315.29 nm
Beer's law limit **(**µg/ml)	1-5	10-50
Regression equation (y = mx + c)	y = 0.0054x + 0.004	y = 0.0046x + 0.0534
Slope (m)	0.0081	0.0073
Intercept (c)	0.008	0.0562
Correlation coefficient (r^2)	0.992	0.990
Repeatability (% RSD, n=3)	1.12	0.58

Table 4.7: Data indicating recovery studies of BD and TEL

Drug	**% level of recovery**	**Amount of drug taken (µg/ml)**	**Amount of drug added (µg/ml)**	**Total amount found (µg/ml)**	**%Recovery**
Benidipine	50	2	1	2.90	98.25
	100	2	2	4.10	101.30
	150	2	3	5.11	100.65
Telmisartan	50	20	10	30.10	100.76
	100	20	20	39.10	99.07
	150	20	30	49.53	99.14

Table 4.8: Data indicating recovery studies of BD and TEL

The accuracy of the technique was verified by recovery assessments of marketed formulations at three levels (80%, 100%, and 120%).The percentage recovery for BD and TEL was found to be 98.25–101.30% for both medicines, as indicated in table 4.8.

Conclusion

The developed dual-wavelength spectrophotometric method is adequate for the simultaneous measurement of BD and TEL in a complex formulation without significant cross-interference. It was demonstrated that a dual-wavelength spectrophotometric approach is acceptable for measuring the drug content and studying the in vitro release of BD using TEL SNEDDS.

4.1.4. Compatibility studies

Compatibility of BD and TEL

After a period of 12 hours, the color and texture of the combination, including BD and TEL, remained unaltered, demonstrating that there was no indication of interaction between the two compounds. This compatibility was further verified by the use of DSC, XRD, and FTIR spectrum analysis.

1. DSC

Differential scanning calorimetry (DSC) analysis is used to analyze the physical state of medicines in order to determine their compatibility when mixed with other drugs. According to reports, if both medicines are compatible with each other, the thermal characteristics of their combination may be determined via combining the thermal properties of each individual drug. Figure 4.3 exhibits the thermal properties of BD and TEL, however their combination in Figure 4.6 especially demonstrates the thermal behavior of their mixture. The differential scanning calorimetric (DSC) curves of BD and TEL displayed a significant endothermic peak at 172°C and 262°C, respectively, which matches with the values given in the literature. The thermogram of the combination of both medicines also displayed the same endothermic peaks without any change in height or shape of the peak.

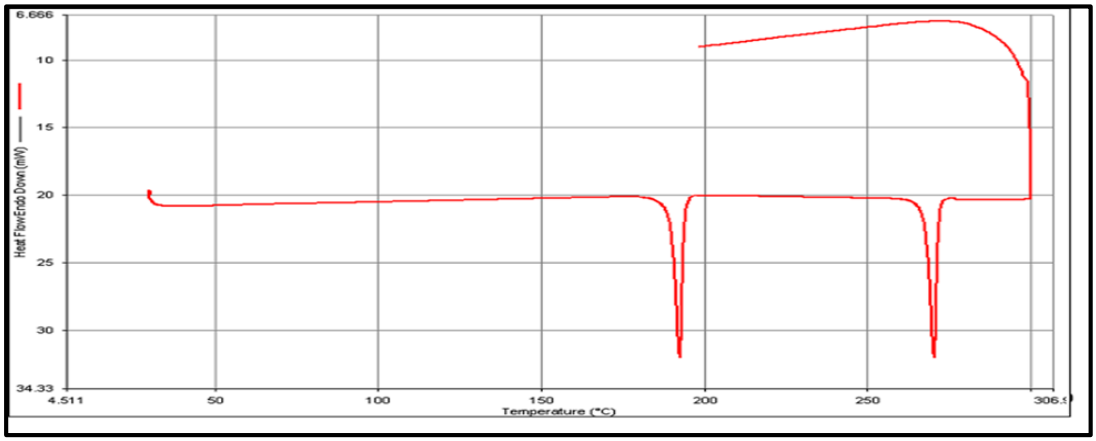

Figure 4.6: DSC spectrum of mixture of BD and TEL

The use of DSC for indicating solid-state compatibility between medicines and excipients is more useful than other analytical techniques, since the time required for this study is decreased and the sample size is minimal. It also provides important information with regard to the interaction between the two drugs so that the combination of drugs might be rejected in the initial stages of formulation development. Here, the DSC of the combination of medicine with no changes in the peak position

revealed that neither drug interacted with the other and remained intact in its crystalline form and stable in its solid state.

II. FTIR

The FTIR spectra of BD, TEL, and their combination are presented in figures 4.2(a), 4.2(b), and 4.7. BD possesses characteristic peaks of C=C stretching, N=C stretching, N=O stretching, C=O stretching, and aromatic N-H stretching at the frequencies of 777 cm^{-1},1018 cm^{-1},1165 cm^{-1}, 2852 cm^{-1} 1574 cm^{-1}, 1708 cm^{-1}, 3401 cm^{-1}, respectively, whereas TEL has characteristic peaks of C=O stretching, C=C stretching, aromatic N-H stretching, C-N stretching, and C-H stretching at 741 cm^{-1}, 883 cm^{-1}, 1402 cm^{-1}, 3134 cm^{-1}, 1266 cm^{-1}, 1895 cm^{-1} , respectively. The combination of BD and TEL demonstrated the existence of distinctive peaks in both medicines, which suggested that these two drugs were not interacting.

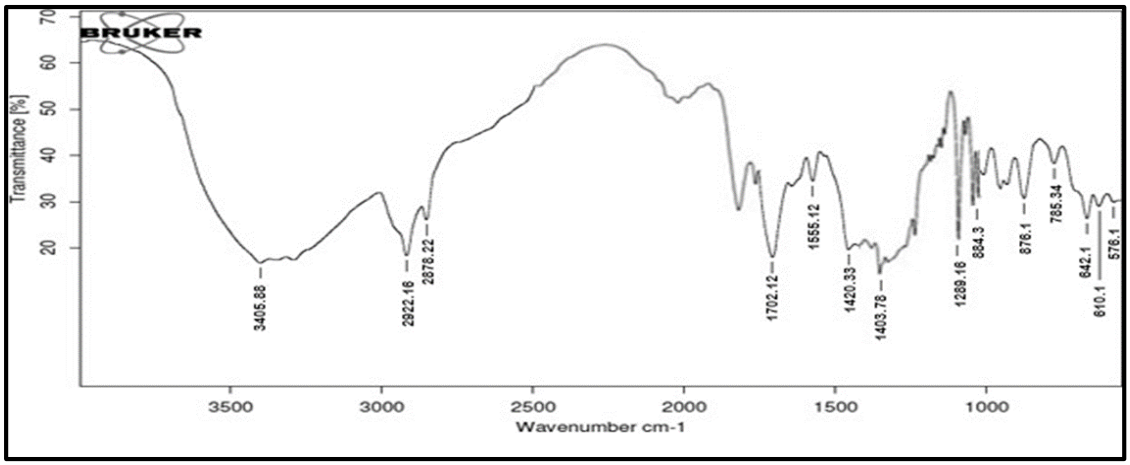

Figure 4.7: FTIR spectrum of mixture of BD and TEL

4.2. QbD approach

4.2.1. QTPP (Quality target product profile)

The key attributes of the L-SNEDDS of BD and BD with TEL are outlined in Table 4.9, including the manufacturing method, therapeutic dosage and strength, action mechanisms and processes, pharmacokinetics, packaging, and storage specifications.

4.2.2. CQAs (Critical quality attributes)

The main characteristics of the L-SNEDDS of BD and BD with TEL were identified as the Critical Quality Attributes (CQAs) derived from the Quality Target Product Profile

(QTPP) components analyzed in the formulation. In addition, the justification for using Critical Quality Attributes (CQAs) and their impact on the therapeutic effectiveness of the L-SNEDDS of BD and BD with TEL was investigated and documented in Table 4.10. The fishbone diagram, shown in figure 4.8, was created to demonstrate the impact of significant material characteristics and manufacturing process factors on the production of S-SNEDDS for BD and BD with TEL. Furthermore, a sequential exercise was carried out to identify the components that exhibited a significant risk by establishing a risk assessment.

4.2.3. Risk Evaluation

The Ishikawa fishbone diagram was created to illustrate the causal relationship between each of the components that might influence the critical quality attributes (CQAs) of the S-SNEDDS drug formulation. The critical quality attributes (CQAs) of BD-S-SNEDDS and BD with TEL-S-SNEDDS, together with a summary of each, were analyzed for early risk assessment studies. Three parameters, including the lipid quantity, surfactant, and co-surfactant, were shown to be causing major risks due to Critical Quality Attributes (CQAs).

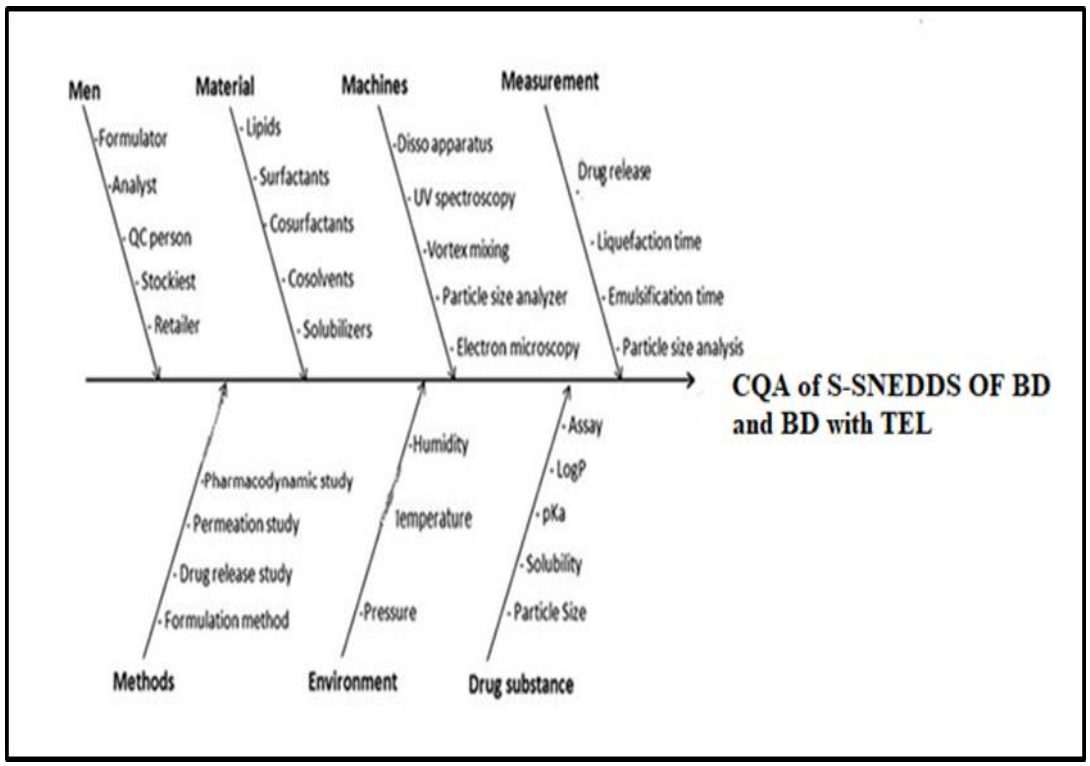

Figure 4.8: Ishikawa Fishbone diagram portraying causes and sub causes influencing S-SNEDDS of BD and BD with TEL quality attributes

QTTP Elements	**Target**	**Justification**
Dosage type	Rapid release	More therapeutic effects are achieved with a quicker beginning of action.
Dosage form	S-SNEDDS	The oral bioavailability of the medicine benidipine would be augmented by its application of a lipid-based solid self-nano emulsifying tool.
Dosage strength	4 mg BD(For BD SNEDDS) and 4 mg BD with 40 mg TEL(For BD SNEDDS)	The development and implementation of S-SNEDDS include a unit dosage of benidipine.
Route of administration	Oral	The most effective way to administer benidipine to achieve antihypertensive effects.
Pharmacokinetics	Higher Cmax and AUC	To improve therapeutic efficacy, drug levels in the systemic circulation must be higher.
Packaging	HPMC capsule	For better patient compliance, mobility, and manufacturing simplicity, the S-SNEDDS may be conveniently packed into HPMC capsules.
Container closure system	Air-tight glass bottle	To safeguard medicine and lipids avoiding deterioration in the presence of the air.
Different approaches to administering	Solid dispersion, inclusion complex, salts, polymorphs, nanocrystals, and co-crystals	These methods may ultimately increase the rate of oral absorption, yet they will only improve the degree of the drug's dissolution.
Contraindications	None	None
Stability	In compliance with the ICH stability studies' guidelines	To identify a potential hazardous trend in the drug and excipients contained in the formulation.

Table 4.9: Quality Target Product Profile (QTPP) of Benidipine S-SNEDDS and Benidipine with Telmisartan S-SNEDDS

Quality attributes of the drug product	**Target**	**Is this a CQA?**	**Justification(s)**
Physical attributes Colour Odour Appearance	 Acceptable to Patient No unpleasant odour Acceptable to Patient	 No	Since that they are not promptly related to patient efficacy and safety, color, odor, and design were not deemed important.
Assay and content uniformity	100%	No	While test variability and content homogeneity regularly have an impact on the effectiveness and safety of medications, they were still seen to be possibly important for the S-SNEDDS because they were homogeneous dispersions at the drug solubilized in a combination of lipidic excipients.
Globule size (Dnm)	< 200 nm	Yes	It was believed that a smaller globule size was particularly significant because it facilitates penetration through the GI epithelial membrane and paracellular pathways.
Zeta potential	≥ + 20Mev	Yes	Target zeta potential required to ensure distributed system stability
Liquefaction time	Low	Yes	A lowered liquefaction time value is required for a faster release of the medication from the dosage form. As a result, it was thought of as crucial.
Emulsification time	Low	Yes	Since shorter emulsification time values make it easier to make nanoemulsion, they were thought to be of utmost significance.
Mean dissolution time	Low	Yes	It is considered to be especially significant since it is a sign of a quicker and more comprehensive drug release solubilization in the dissolving solution.
Drug release in 60 min (Rel_{60min})	100%	Yes	The drug release rate was thought to be relatively high because it is required for improved blood bioavailability of medicine.
Transmittance (%)	> 95 %	Yes	The product's clarity guarantees that the globule size is kept to a minimum.

Table 4.10: Critical quality attributes (CQAs) for S-SNEDDS of BD and BD with TEL and their justifications

4.3. Formulation and development of SNEDDS

4.3A Formulation and development of benidipine SNEDDS

4.3A1. Screening of Oil, Surfactants, and Co-Surfactants

Oil is a very crucial excipient of the formulation as it effects the release of drugs throughout the body. The major criteria for the selection of oil were based on the maximum solubility of each of the drugs in the oil so as to generate an efficient, self-emulsifying formulation. Throughout the formulation and development of SNEDDS, it is vital to choose oils so that the drugs to be loaded are freely soluble, as the required solubility due to the presence of surfactants and co-surfactants might result in the precipitation of drugs on diluting with the contents of the gastro-intestinal tract. The maximum solubility of drugs is also responsible for the maximum loading of drugs in the developed SNEDDS.

Usually, medium-chain triglycerides are readily emulsified in the aqueous medium when compared to long-chain triglycerides, owing to decreased interfacial tension, higher water solubility, and better partitioning ability. However, semisynthetic medium-chain triglycerides have greater self-emulsifying characteristics because of their amphiphilic nature as compared to synthetic and natural oils. Due to these advantages, semisynthetic medium-chain triglycerides were also examined together with different other triglycerides for the selection of the oil. Additionally, different types of oils were included in this research, such as synthetic oils, natural oils, synthetic monoglycerides, synthetic diglycerides, and synthetic triglycerides. The information regarding the BD solubility in various oils is presented in Table 4.11 and Figure 4.9(a), which suggest significant differences between the lowest and maximum solubility of drugs in oils. Figure 4.9a displays the bar chart illustrating the solubility of BD in various oils, which was determined to be in the following order: eucalyptus oil, <sunflower oil, sesame oil, castor oil, peanut oil, olive oil, soybean oil, oleic acid, and Labrafil M 2125 CS. Labrafil M 2125 CS has been chosen as the oil having the highest solubility for the drug 98.34 ± 1.4 mg/mL, being utilized [30].

Sr.No.	Oil	Solubility of Benidipine (mg/mL)
1	Oleic acid	9.1± 1.14
2	Sunflower oil	2.31 ± 1.2
3	Olive oil	7.11 ± 1.4
4	Castor oil	3.45 ± 1.5
5	Sesame oil	3.11 ± 0.12
6	Peanut oil	5.73 ± 0.45
7	Eucalyptus oil	2.13 ± 0.76
8	Cottonseed oil	7.12± 1.34
9	Soyabean oil	8.8 ± 1.14
10	Labraill M 2125 CS	98.34 ± 1.4

Table 4.11: Solubility of Benidipine in various oil
Each value represents the mean ± SD, n = 3

The selection of surfactant was based on its emulsification capacity with the specified oil, i.e., Labraill M 2125 CS. For the generation of oil in water nanoemulsions, numerous surfactants with varied HLB values ranging from 8–16 having cation, ionic, and non-ionic natures may be utilized. Non-ionic surfactants are typically used for oral consumption as they have been considered to be safer than ionic surfactants. They are additionally anticipated to improve the nanoemulsions stability throughout a greater pH and ionic strength range. Additionally, they may reversibly modify the gut mucosa to improve the absorption of any co-administered medicine [38].

The data of BD solubility in various surfactant is provided in table 4.12 and figure 4.9(b), which shown the considerable difference between the lowest and highest solubility of medicines in surfactant. The bar chart in Figure 4.9b represents the drug's solubility in surfactants, which were discovered to be in the following sequence: Tween 20< Span 20 < Tween 80 < Span 80 < Solutol HS 15< Cremophor RH 40< Kolliphor EL. BD solubility studies were done in various excipients and buffers at 37°C.

Amongst these, Kolliphor EL was chosen, as it resulted in the creation of a transparent mixture with oil, had a solubility of 88.35± 1.87 mg/mL, and had a transmittance of 98.50%. Kolliphor EL is a promising surfactant because of its high HLB value, i.e., 12–

14, in contrast to the HLB value of Labraill M 2125 CS, i.e., 9, attributed to which it exhibits a better emulsifying property that ensues in a decrease in interfacial tension, low entropy, and quick dispersion of oil globules in the aqueous phase that eventually offers stable microscopic oil in water nanoemulsion. Considering Kolliphor EL is non-ionic in nature, it generates a low magnitude of charge over the nanoparticle, which minimizes the possibility of agglomeration, leading to the stabilization of the formulation. It is described as a less harmful and preferable surfactant for oral intake [39]. The power of the surfactant to spontaneously emulsify oil when diluted with distilled water was considered one of the selection criteria. The number of inversions and the percentage transmission employed to establish the emulsification abilities of different surfactants and co-surfactants have been documented.

Sr.No.	Surfactant	Solubility of Benidipine (mg/mL)
1	Cremophor RH 40	80.34 ± 2.5
2	Kolliphor EL	88.35± 1.87
3	Tween 20	18.23± 0.16
4	Tween 80	22.21± 3.15
5	Span 20	21.11± 1.15
6	Span 80	28.56± 1.29
7	Solutol HS 15	56.34± 2.12

Table 4.12: Solubility of Benidipine in various Surfactant
Each value represents the mean ± SD, n = 3

Therefore, based on the outcomes of the emulsification and solubility examinations, Kolliphor EL was chosen as a surfactant for further study.

The selection of co-surfactant was decided based on its emulsification capabilities with the specified oil and surfactant, i.e., Labrafil M 2125 CS and Kolliphor EL, respectively. Co-surfactants are short-chain amines or alcohols, which help stabilize the nanoformulations. The co-presence of surfactants gives the surfactant layer the requisite flexibility, which assists in the creation of the varied curvatures required for the synthesis of nanoemulsions in a range of compositions. The co-surfactant enhances the

area available for the production of nanoemulsion by reducing surface tension even more while fluidizing the surfactant layer [40].

The emulsification ability of co-surfactant is given in table 4.13 and Figure 4.9 (C). Figure 4.9(C) portrays a bar graph exhibiting a drug's solubility in co-surfactants, with all of the co-surfactants that were examined having the drug's solubility in the following order: PEG-400< PEG-200< PG< Transcutol P. Transcutol P was chosen as a co-surfactant as it emulsified both the selected oil and the surfactant and resulted in the development of a clear emulsion with a transmittance higher than 98.34 ± 0.3%. It is a potential co-surfactant since it assists in stabilizing the interfacial layer along with the surfactant owing to its low HLB value of 4.2.

Sr.No.	Co-Surfactant	Solubility of Benidipine (mg/mL)	% Transmittance	No. of Inversion
1	Transcutol P	64.35± 1.15	98.34± 1.70	5
2	Propylene glycol	44.23± 1.21	87.25± 0.25	12
3	PEG-200	34.12± 1.16	64.55± 0.50	25
4	PEG-400	37.23± 1.19	55.25± 2.05	33

Table 4.13: Selection of Co-surfactant on the basis of solubility and % T

Conclusion: Finally, Labrafil M 2125 CS, Kolliphor EL, and Transcutol P had been selected as the oil, surfactant, and co-surfactant, respectively, based on the results of the tests of solubilization capacity and emulsification efficiency.

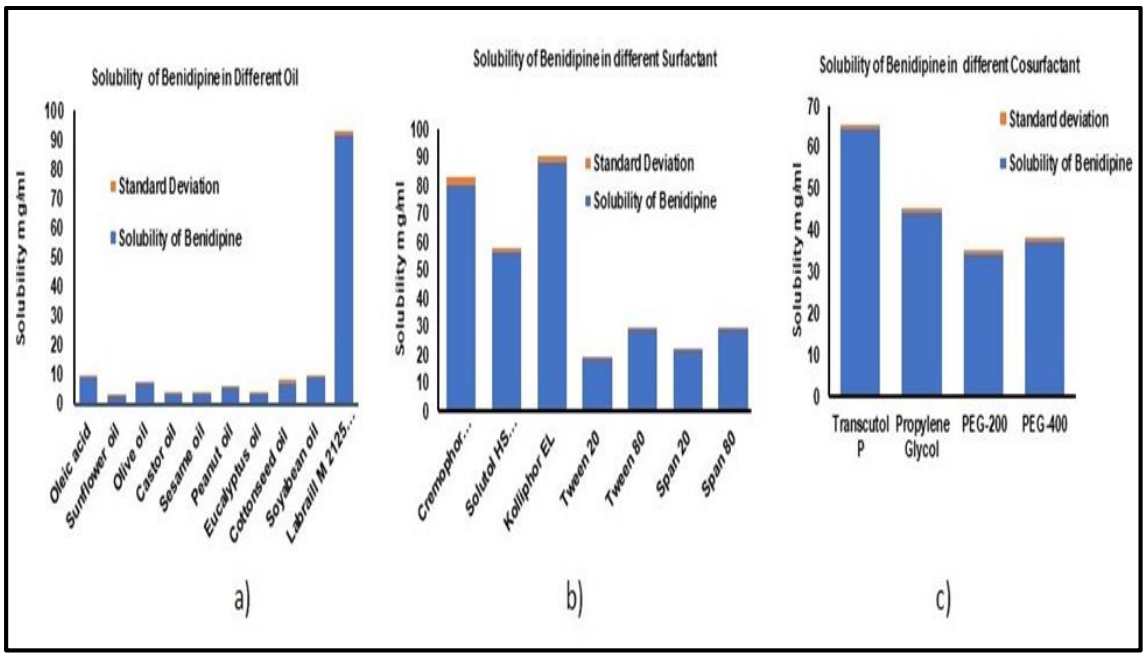

Figure 4.9: a) Solubility of BD in various oil, b) solubility of BD in different surfactants and c) solubility of BD in different co-surfactants

4.3A2. Building of a Ternary Phase Diagram

In the initial stages, ternary phase diagrams were produced employing Labrafil M 2125 CS (oil), Kolliphor EL (surfactants), and Transcutol P (co-surfactant) at 1:1, 2:1, and 3:1 ratios for identifying the largest area for the production of thermodynamically stable nanoemulsion, as shown in Figure 4.10. The oil and Smix have been combined in different proportions, ranging from 9:1 to 1:9. An outstanding nanoemulsion area was identified between Labrafil M 2125 CS, Kolliphor EL, and Transcutol P, which may be attributable to the emulsification of oil by only one surfactant and a co-surfactant.

After being diluted with 100 mL of water and 0.1 mL of SNEDDS, each sample received a score based on its estimated opacity and transmittance. For further investigation and drug loading, only clear and transparent mixtures were chosen. The ratio of 3:1 amongst the three combinations has been shown to be the most effective region for nanoemulsion. The self-nano emulsifying system's transparency improved when the concentration of Smix increased while the concentration of oil was lowered. Additionally, the surfactant lowered the interaction between the oil and the water, allowing SNEDDS to disperse more quickly in an aqueous medium and reducing particle size when diluted with water [41].

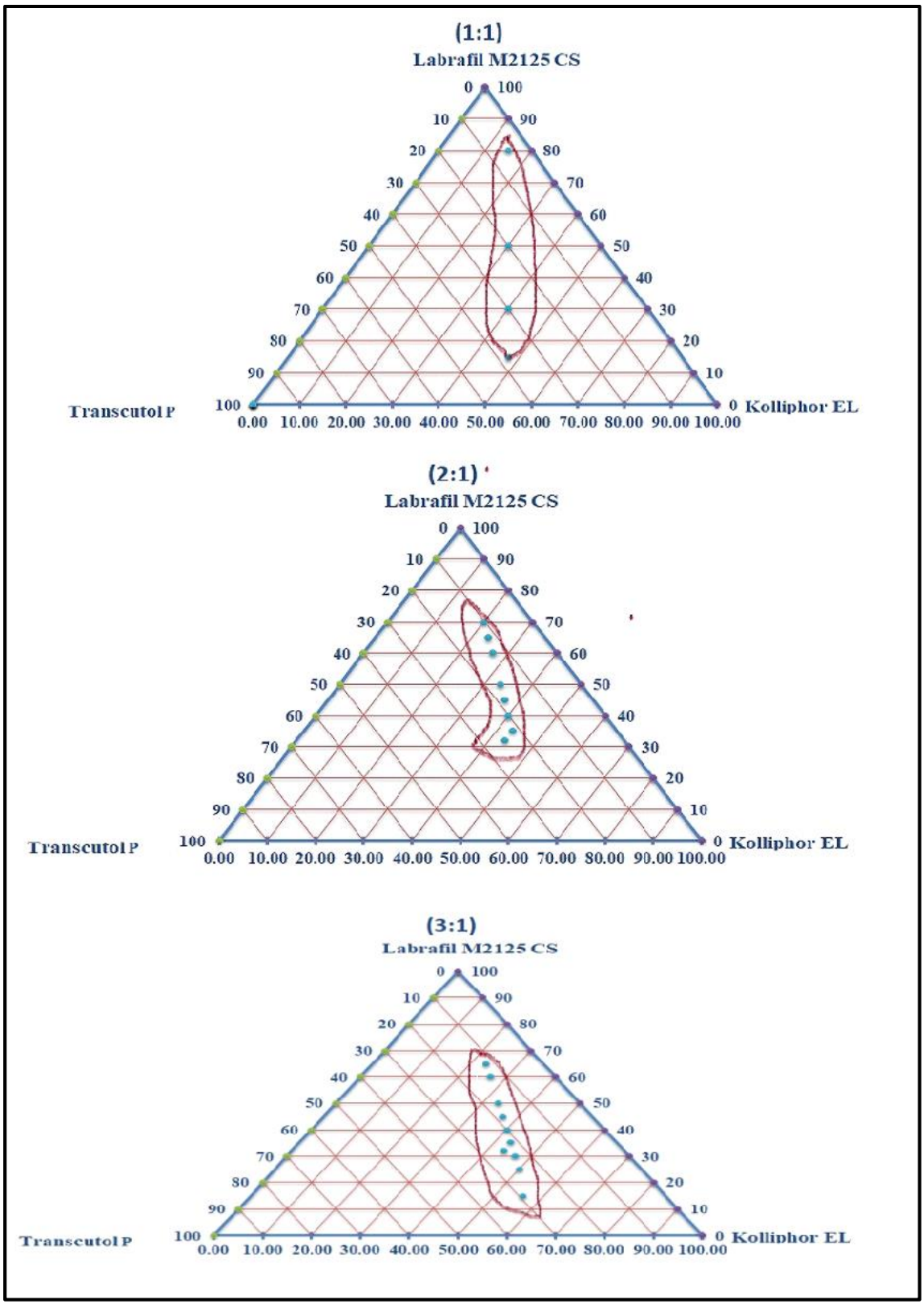

Figure 4.10: Ternary phase diagrams of the o/w emulsified regions of 1:1, 2:1, and 3:1 ratios of Labrafil M 2125 CS, Kolliphor EL, and Transcutol P

Effect of BD on the phase diagram

Figure 4.10 displays the way various quantities were taken into consideration when analyzing the quantity of oil, surfactant, and co-surfactant that should be included in the BD nanoemulsion system. The primary three formulation ingredients of the nanoemulsion were Transcutol P, Kolliphor EL, and Labrafil M 2125 CS. When a hydrophobic drug (BD) is entrapped in the SNEDDS, the self-emulsifying performance reduces. In addition, the drug may precipitate in a 1:1 ratio. In the present investigation, incorporation with BD in the 1:1 ratio lowered the efficient self-emulsifying efficiency, whereas there was no change in the 3:1 ratio.

4.3A3. Optimization of SNEDDS Employing Experimental Design

Design Expert 13 had been assigned to build the experimental pattern. Table 4.14 offers a summary of the CQAs observed for formulations of BD created in accordance with the CCD design for the response variables (Y_1), transmittance percentage (Y_2), self-emulsification time (Y_3), and percentage of drug release in 15 minutes (Y_4). Other features, such as the utilization of multiple regression analysis, have been used to assess the generated SNEDDS, and the CCD model has been constructed to match the 2nd-order polynomial model. The findings of a regression analysis of the CCD categories of BD-loaded SNEDDS are presented in Table 4.15.

The mathematical link between the evident replies and a polynomial equation was identified. Quadratic polynomial equation-according to the following equation:

$$Y_1 \text{ (Emulsification time)} = 68.987 + 8.295 X_1 - 1.947 X_2 - 1.827 X_3 - 0.045 X_1 X_2 + 0.867 X_2X_3 + 0.02 X_1 X_3 + 6.075 X_1^2 + 1.463 X_2^2 - 0.150 X_3^2 \quad \text{……(4.1)}$$

$$Y_2 \text{ (Droplet size)} = 159.595 + 4.364 X_1 + 2.830 X_2 - 1.469 X_3 - 0.496 X_1 X_2 + 0.431 X_2 X_3 - 0.541 X_1X_3 + 12.798 X_1^2 + 10.510 X_2^2 + 1.930 X_3^2 \quad \text{……..… (4.2)}$$

$$Y_3 \text{ (\% Drug release at 15min)} = 90.264 + 0.769 X_1 + 0.222 X_2 + 0.320 X_3 + 0.296 X_1 X_2 - 1.081 X_2 X_3 + 0.426 X_1 X_3 - 6.719 X_1^2 - 2.550 X_2^2 + 1.499 X_3^2 \quad \text{…..…… (4.3)}$$

$$Y_4 \text{ (\%Transmittance)} = 98.203 - 2.636 X_1 - 0.780 X_2 + 0.099 X_3 - 0.547 X_1 X_2 + 0.99 X_2 X_3 - 1.085 X_1 X_3 - 2.639 X_1^2 - 2.418 X_2^2 + 0.236 X_3^2 \quad \text{….....(4.4)}$$

Formulation	Average ± SD (n=3)				
	T_{emul} (sec)	D_{nm} (nm)	$R_{el15min}$ (%)	T (%)	Polydispersity Index
BD1	75.67±2.10	186.01±3.10	82.17±1.90	95.67±0.90	0.454
BD2	87.71±2.40	195.23±3.25	83.14±1.95	93.10±0.70	0.258
BD3	68.58±2.25	183.14±3.00	86.11±2.10	98.25±0.50	0.264
BD4	82.12±2.20	191.32±3.30	87.12±1.95	88.00±0.40	0.425
BD5	69.31±2.05	184.23±3.20	84.12±1.90	98.05±0.10	0.331
BD6	83.11±2.80	192.23±3.10	85.65±2.15	85.65±0.90	0.256
BD7	67.37±2.25	184.03±2.90	82.59±1.95	99.10±0.30	0.260
BD8	79.31±2.15	189.10±2.80	86.45±2.10	90.00±0.25	0.265
BD9	67.36±1.90	182.43±2.75	67.25±1.80	91.10±0.50	0.454
BD10	104.21±3.10	199.75±2.90	69.12±1.85	90.10±0.60	0.464
BD11	75.17±2.15	170.12±2.70	81.21±1.75	95.25±0.20	0.421
BD12	70.31±2.80	199.12±2.60	78.74±1.65	87.20±0.30	0.325
BD13	71.14±2.30	164.50±2.50	90.21±1.65	97.67±0.90	0.299
BD14	65.21±1.95	156.20±2.40	92.65±1.70	99.80±0.70	0.250
BD15	69.12±2.05	161.21±2.50	91.32±1.80	98.25±0.50	0.415

Table 4.14: An overview of the CQAs observed for formulations of BD created by the CCD design

In contrast to a negative symbol, which represents an antagonistic impact, a positive sign suggests a synergistic effect. Table 4.15 illustrates the outcomes of the ANOVA study for BD-loaded SNEDDS. Using contour plots and response surface plots, the relationship between the dependent and independent variables has been further examined.

Co-efficients	T_{emul} (sec)(Y_1)		D_{nm} (Y_2)		%$Rel_{15\ min}$ (Y_3)		%T (Y_4)	
	FM[a]	RM[b]	FM	RM	FM	RM	FM	RM
b_0	68.987	70.604	159.595	175.26	90.264	88.940	98.203	93.812
b_1	8.295	8.295	4.364	–	0.769	–	-2.636	-2.636
b_2	-1.947	–	2.830	2.830	0.222	0.222	-0.780	–
b_3	-1.827	–	-1.469	–	0.320	0.320	0.099	–
b_4[c]	-0.045	–	-0.496	–	0.296	–	-0.547	–
b_5[c]	0.867	–	0.431	–	-1.081	–	0.99	–
b_6 [c]	0.02	–	-0.541	–	0.426	–	-1.085	–
b_7	6.075	5.572	12.798	8.028	-6.719	-6.316	-2.639	–
b_8	1.463	–	10.510	–	-2.550	–	-2.418	–
b_9	-0.150	–	1.930	–	1.499	–	0.236	–

Table 4.15: Regression analysis of the CCD categories of BD-loaded SNEDDS
[a] FM, Full model, [b] RM, Reduced model.,
[c] Non-significant (P > 0.05) coefficients

a) Composition Elements' Impact on Responses

The regression analysis results indicate that X_1 (oil) exhibited a positive coefficient, whereas X_2 (surfactant) and X_3 (co-surfactant) exhibited negative coefficients. Investigations have shown that variations in the quantity of oil and surfactant have a significant impact on the size of the drops, compared to other independent parameters. For Self-Emulsification Time (Y_1), Droplet size (Y_2), % $Rel_{15\ min}$ (Y_3), and %T (Y_4) coefficients b_4 ,b_5 and b_6 were found to be insignificant (P > 0.05) and hence, these terms were separated from their respective full model in order to develop a reduced model. The removal of insignificant terms was further justified by executing an ANOVA test.

(I) Self-Emulsification Time

The emulsification process evidently suffered a reduction in speed and efficacy as the amount of oil in the formulation got higher, resulting in larger droplet sizes and a greater degree of lipophilicity [42]. Rising oil content resulted in larger and more lipophilic droplets, possibly speeding up the emulsification process. In this manner, the

nanoemulsion formation was a result of the composition of the system, where the existence of the nanoemulsion formation could be recognized with the aid of the ternary phase diagram. Inasmuch as the ordering of the mixing of the different components contributed absolutely nothing in regards to impacting the creation of the nanoemulsion, the system was able to continue to be thermodynamically stable.

Figure 4.11 presents a contour plot, whereas Figure 4.15 provides a 3D surface response plot. These figures indicate the influence of oil concentration, surfactant concentration, and co-surfactant concentration on the emulsification time. Emulsification of liquid SNEDDS preconcentrates results in a clear dispersion with a high percentage of transmittance (%T) as well as a tiny droplet size, which reveals a blue tint, as mentioned in Table 4.14. In most instances, the %T was, in most instances, >90%, which is a sign of a rapid and repeatable emulsification process. The modified R^2 and the projected R^2 indicate significant agreement with each other's criteria.

(II) Droplet size

The droplet size is a key component in the SNEDDS since it determines the speed and magnitude of drug release. The droplets comprise a broad variety of nanoscale sizes, resulting in a considerable amount of surface area accessible for drugs and gastrointestinal absorption [43]. The droplet sizes in the emulsion varied between 156.20±2.40 and 199.75±2.90 nm. The quadratic polynomial equation stated before has been utilized for determining the size of droplets. On the other hand, an increase in the quantity of Transcutol P has a detrimental influence on drop size, resulting in a reduction in drop size [40].

Figure 4.12 presents a contour plot, whereas Figure 4.16 provides a 3D surface response plot. These figures show how oil concentration, surfactant concentration, and co-surfactant concentration affect the size of droplets. Droplet size increased with an increase in the concentration of oil, while it decreased with an increase in the concentration of Smix. The significance of the model was assessed by its F value of 1.4865, while the relevance of each parameter in the model was highlighted by their p values being less than 0.05. The predicted R^2 is substantially similar to the adjusted R^2, confirming their practical compliance with the standard as experimentally coded.

Model	df[c]	SS[d]	MS[e]	R^2
T_{emul} (sec) (Y_1)				
Regression				
FM[a]	9	1426.438	158.4931	0.9509
RM[b]	2	1298.969	649.4844	0.8659
Residual				
FM	5	73.7113	14.7423	Fcal = 1.2352
RM	12	201.1803	16.7650	Fcritical = 4.88 df= (7,5)
Dnm(µ) (Y_2)				
Regression				
FM	9	2028.2927	225.3659	0.9025
RM	2	855.0392	427.5196	0.8648
Residual				
FM	5	563.7756	112.7551	Fcal = 1.4865
RM	13	1737.0292	144.7524	Fcritical = 4.88 df = (7,5)
%$Rel_{15\ min}$ ($Y3$)				
Regression				
FM	9	616.350	68.483	0.9229
RM	3	463.466	154.488	0.9201
Residual				
FM	5	107.208	21.441	Fcal = 1.1884
RM	11	260.092	23.645	Fcritical = 8.94 df = (6,3)
%T ($Y4$)				
Regression				
FM	9	225.910	25.102	0.9255
RM	1	94.906	94.907	0.8378
Residual				
FM	5	95.953	19.190	Fcal = 0.05202
RM	13	226.956	17.458	Fcritical = 3.73 df = (8,7)

Table 4.16: Outcomes of the ANOVA test for the BD-loaded SNEDDS

[a]FM, Full model; [b]RM, Reduced model; [c]df, Degree of freedom; [d]SS, Sum of squares; [e]MS, Mean of squares.

(II) Drug release at 15 min

For the intended batches, a range of 78.74% to 92.65% of the drugs were released at the stipulated 15-minute interval. The only independent variable whose change

considerably influenced CPR_{15} was the oil concentration. To form a nanoemulsion, the compositions needed to be mixed effectively; increasing the amount of any one composition would have an effect on the system's overall balance, which was essential to maintaining the drugs solubilized [44].

Figure 4.13, contour plot, and Figure 4.17, 3D surface response plot, demonstrate the influence of concentrations of oil, surfactant, and co-surfactant on drug release. The quadratic polynomial equation described previously may be utilized to compute the drug release percentage after 15 minutes. The model's F value of 1.1884 was evaluated using an ANOVA and was shown to be significant. If the p-value is less than 0.05, the model terms (independent variables) could be advantageous for forecasting the result. It was readily apparent that the independent factors significantly impacted result prediction, with an R^2 of 0.9229. There is a remarkable degree of uniformity between the calculated R^2 and the adjusted R^2.

(III)Percentage Transmittance

The outcomes for percent transmittance varied between 85.65±0.90 to 99.80±0.70%. The SNEDDS dispersion was transparent and clear, with an extensive selection of nanometer-sized droplets and a transmittance score based on a percentage of approximately 100%. Clear solutions have greater transmittance values than turbid solutions owing to the increased scattering of the radiation that enters. Figure 4.14 displays a contour plot, while figure 4.18 shows a 3D surface response plot. These plots illustrate the impact of oil concentration, surfactant concentration, and co-surfactant concentration on the percent transmittance.

The impact of parameters on the response rate of transmittance is seen in the cubic polynomial equation for calculating transmittance. The outcomes of the regression analysis demonstrated that although the amount of co-surfactant had no impact on transmission, the percentage of oil to surfactants was affected. The oil quantity displayed an insufficient relationship with the outcome measure, as demonstrated by the oil amount's (X_1) negative coefficient. The transmission percentage decreased as the amount of oil increased in the constant-weight formulation. This was made practicable because when the composition changed, the oil level increased, becoming less transparent and more lipophilic [43].

(b) Response Surface and Contour Plot Analysis

To highlight the link between the dependent and independent components and investigate their interactions, two-dimensional contour plots and three-dimensional surface response plots were developed. Figures 4.11 to 4.14 present contour plots demonstrating the impact of oil concentration, surfactant concentration, and co-surfactant concentration on emulsification time, droplet size, percentage of drug release at 15 minutes, and percent transmittance. Figures 4.15–4.18 show the response surface for the influence of oil concentration, surfactant concentration, and co-surfactant concentration on emulsification time, droplet size, drug release at 15 minutes, and transmittance percentage, respectively.

The simultaneous reduction in globule size with the decrease in oil concentration may be explained by an instantaneous rise in surfactant concentration, which may quickly emulsify the oil phase and lower the globule size. The absence of surfactant may have contributed to the prolongation of the emulsification process as the oil content increased. In order to reduce the amount of free interfacial energy and act as a mechanical barrier that slows emulsion coalescence, surfactant molecules adhere to the outermost emulsion droplets. As an outcome, a finite thermodynamic dispersion developed [44]. Consequentially, greater concentrations promote emulsification and drug absorption.

(c) Identification and Evaluation of Optimum Formulation Using Desirability Function

All of the respondents in the present experiment were subject to obstacles, and a technique of desired functionality was used. An appropriate formulation has been developed based on the needed functions and response characteristics. Globule size, % transmittance, self-emulsification time, and % drugs dissolved in 15 min were measured. The relationship between the predicted and actual variable components was explored as seen in figure 4.19.

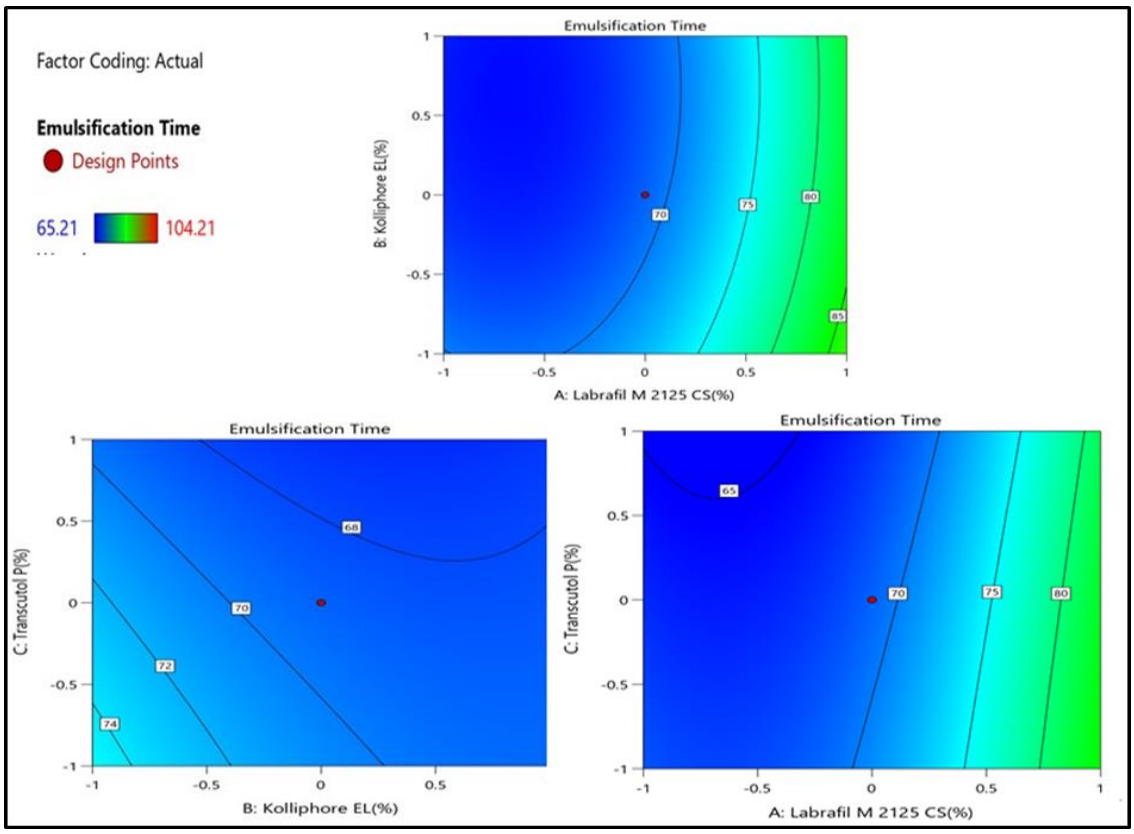

Figure 4.11: 2D contour plot response for emulsification time of BD SNEDDS

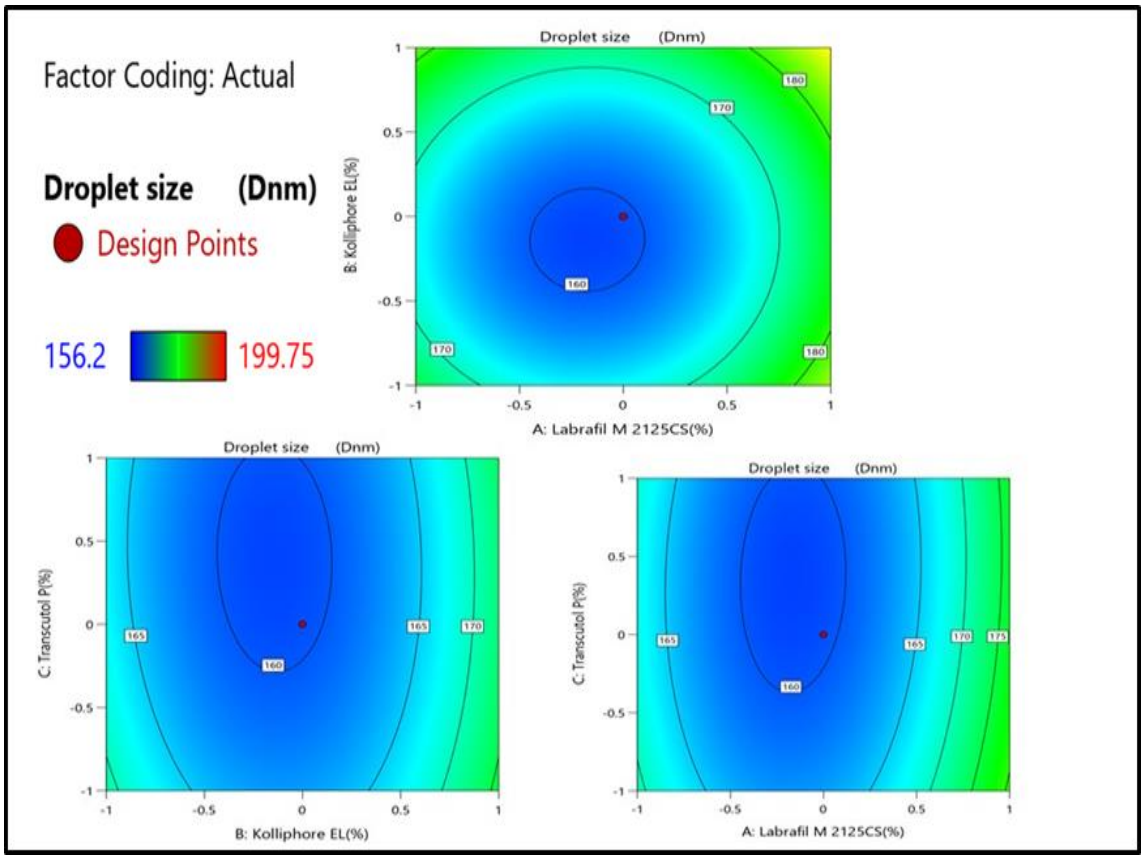

Figure 4.12: 2D contour plot response for droplet size of BD SNEDDS

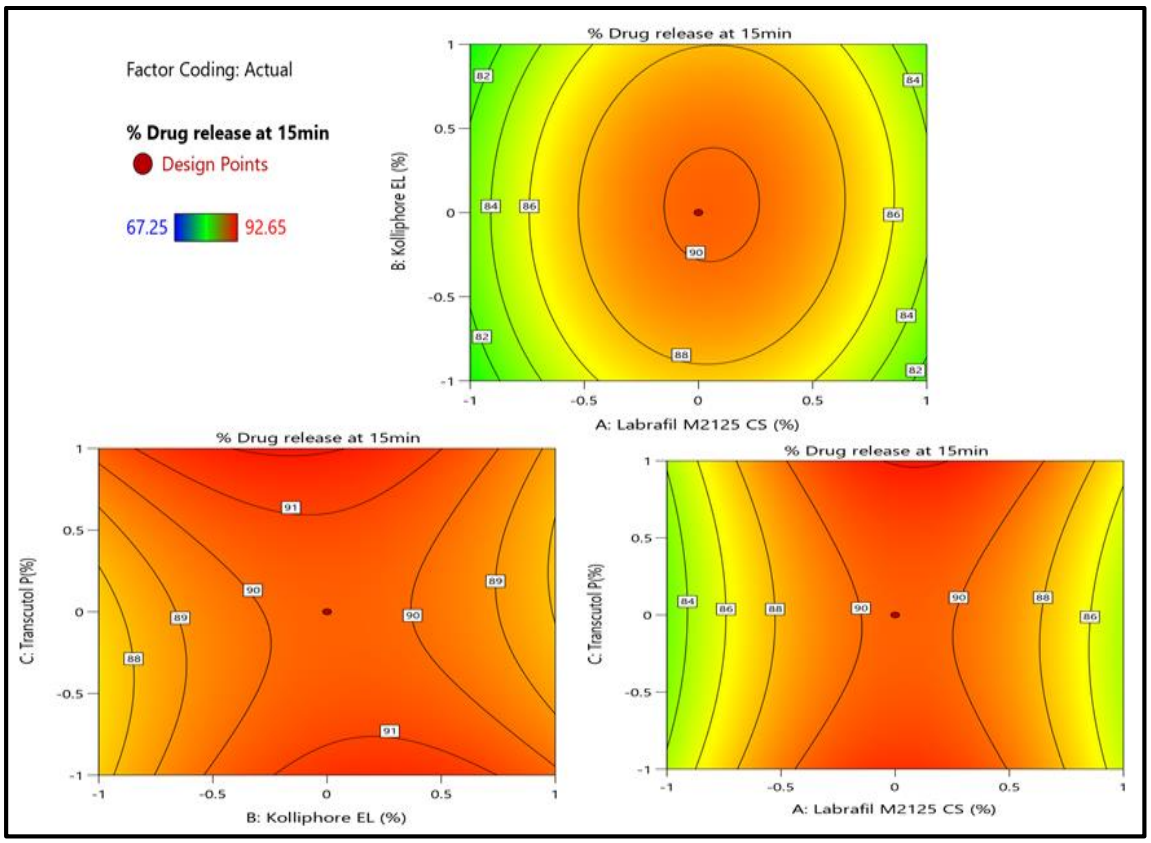

Figure 4.13: 2D contour plot response for drug release at 15 min of BD SNEDDS

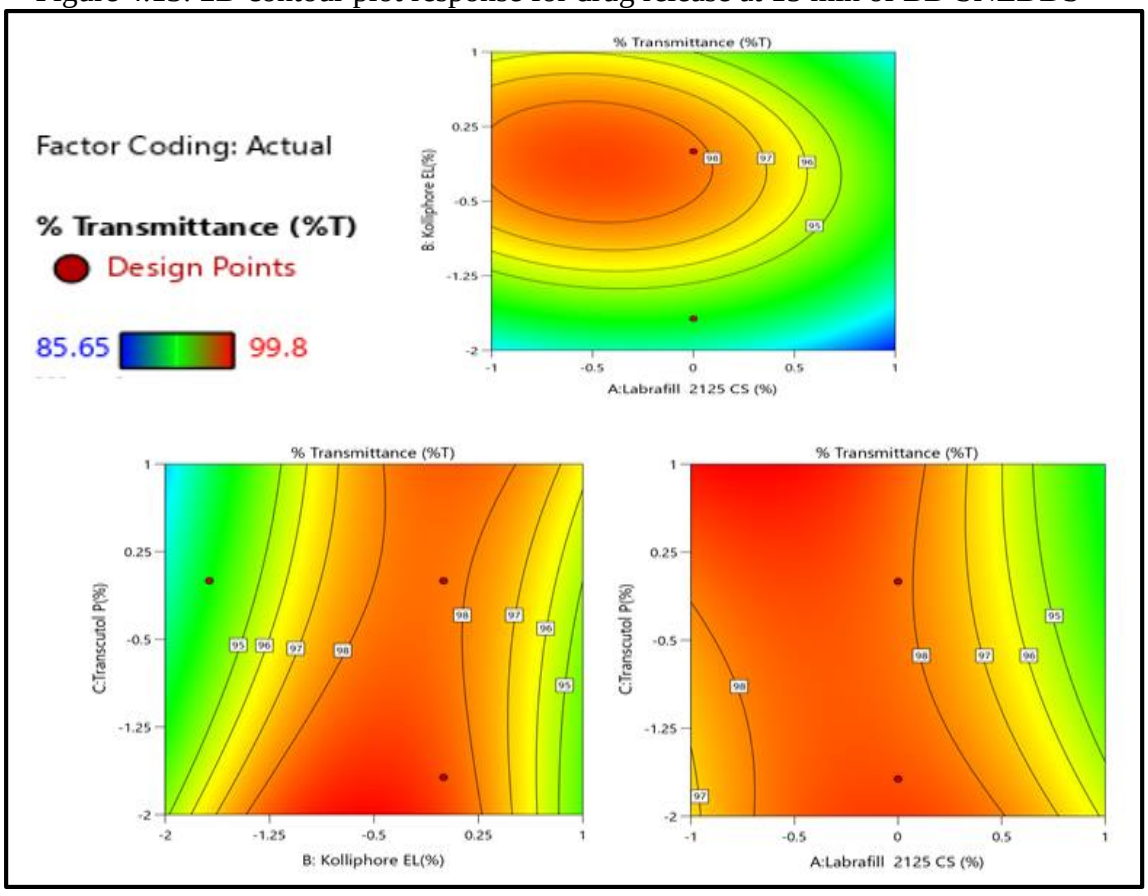

Figure 4.14: 2D contour plot response for %transmittance of BD SNEDDS

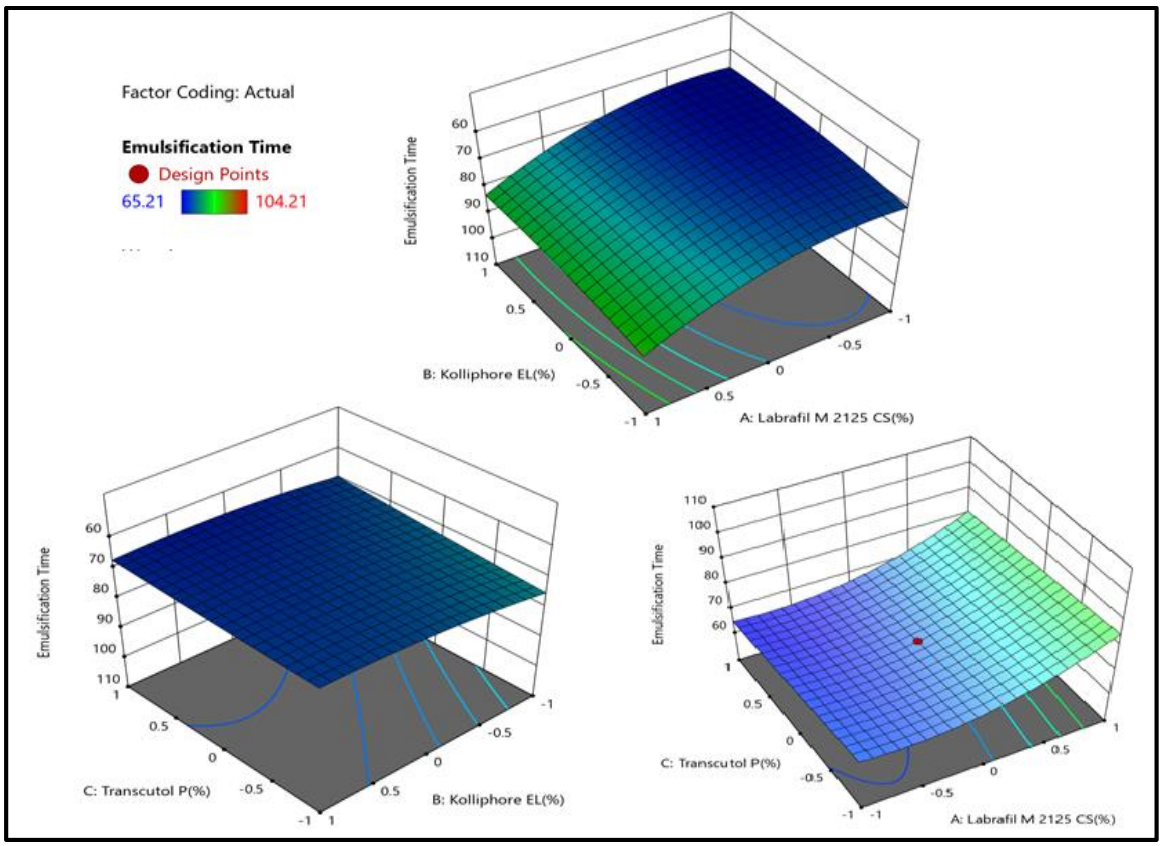

Figure 4.15: Response surface plots for emulsification time of BD SNEDDS

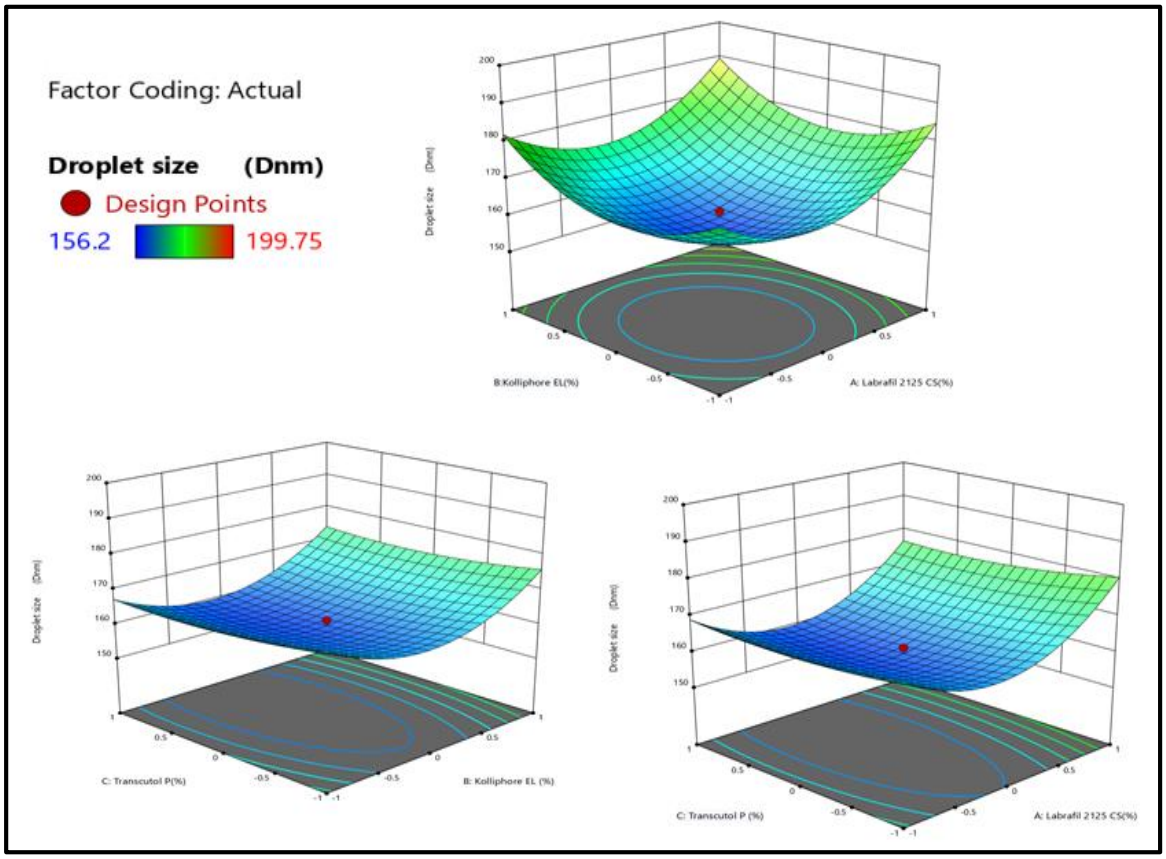

Figure 4.16: Response surface plots for droplet size of BD SNEDDS

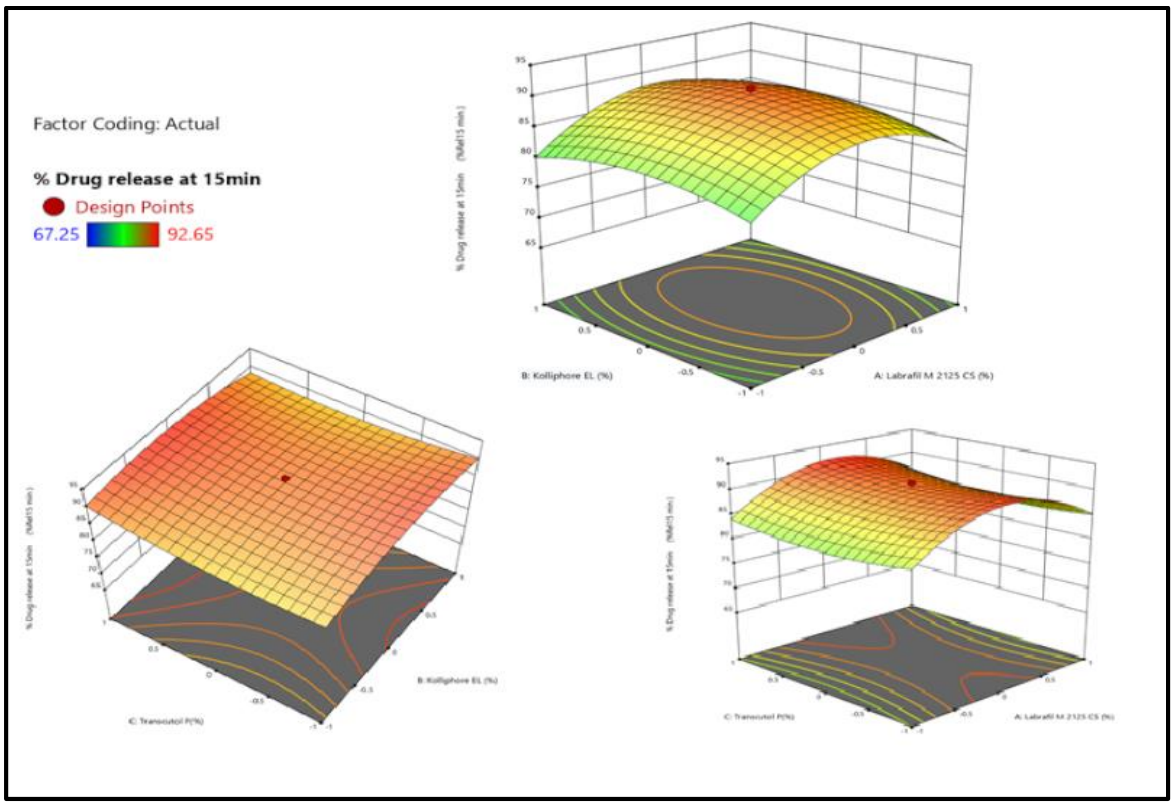

Figure 4.17: Response surface plots for drug release at 15 min of BD SNEDDS

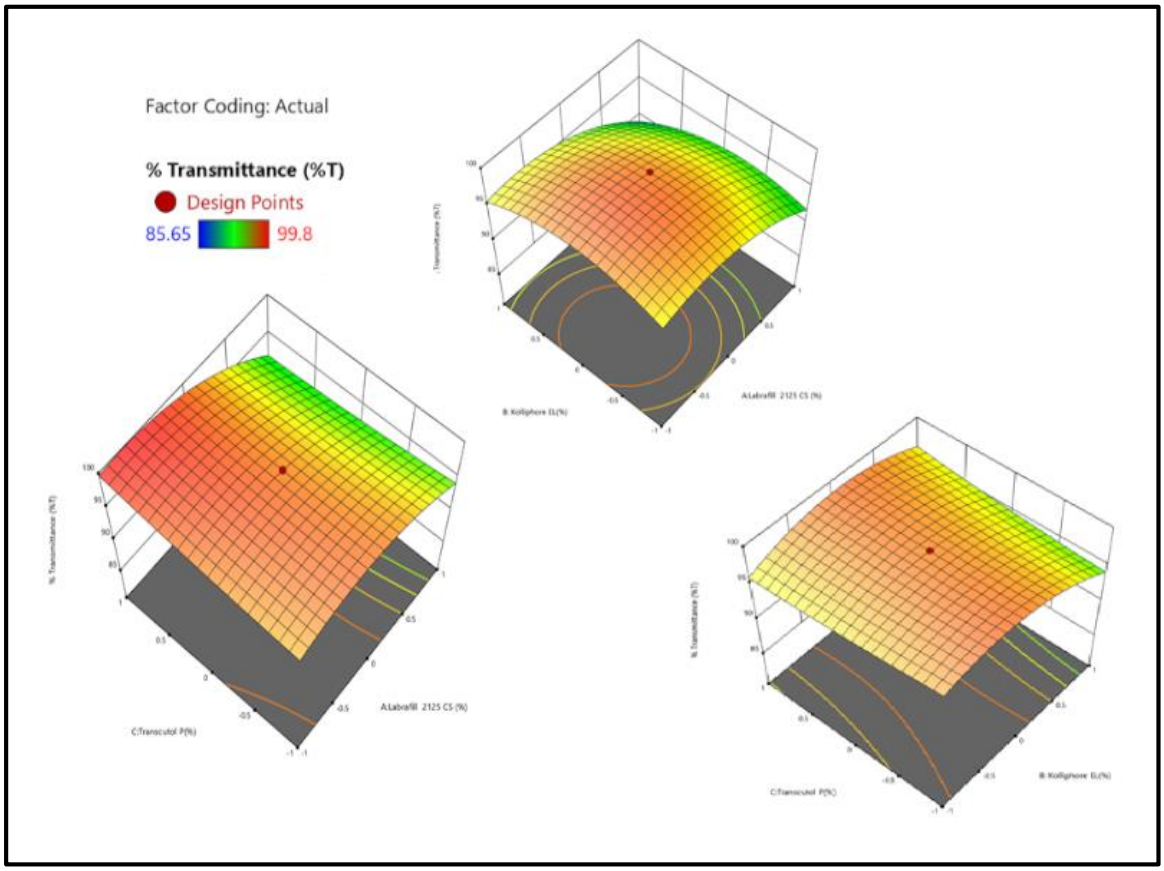

Figure 4.18: Response surface plots for %transmittance of BD SNEDDS

Additional aspects of the modified composition have been investigated. The mean droplet size and emulsification time decreased in the responses while increasing transmittance as well as drug release within 15 minutes. The formulation that attained all of the maximum response variables and produced the optimal desirability function was selected. X_1 = 30.0%, X_2 = 38.0%, and X_3 = 40% w/w of the selected formulation were determined to have an overall effect of 0.987. For the responses from Y_1, Y_2, Y_3, and Y_4, Table 4.17 demonstrates both the expected and actual values.

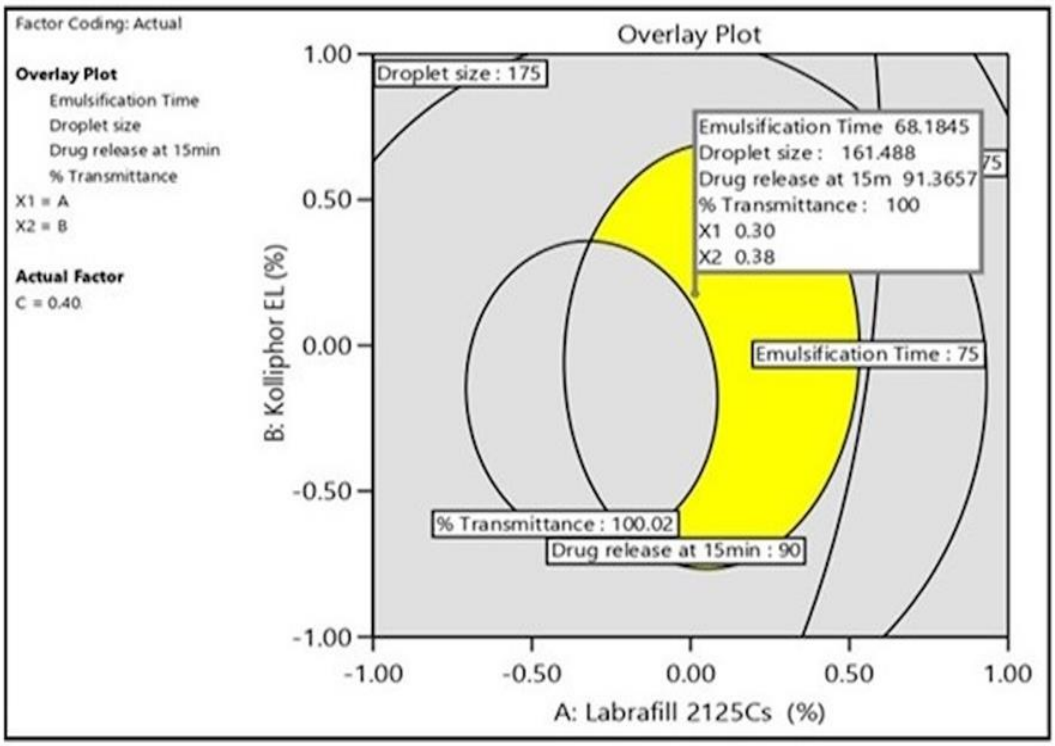

Figure 4.19: Overlay plot for optimized formulation of BD-loaded-SNEDDS

Response	Predicted value	Experimental value[a]	% Relative error
T_{emul} (sec) (Y_1)	68.1845	67.25±1.875	1.389
Dnm(μ) (Y_2)	161.488	162.25±3.50	-0.478
$\%Rel_{15\ min}$ (Y_3)	91.3657	90.15±2.15	1.33
%T (Y_4)	100	99.50±1.78	0.5

Table 4.17: Predicted and measured values for optimized BD-loaded SNEDD
[a]Values are of mean ± SD (n=3), SD: Standard deviation

The overlay plot of the optimized batch is presented in Table 4.16 and Figure 4.13. The predicted batch demonstrates significant reproducibility within the percentage

deviation. From the result, it shows that the prediction value is close to the experimental value, therefore the design is significant.

Conclusion: According to the desirability index, formulation BD14 was considered to be an optimum batch with a desirability index of 0.987. Formulation BD14 contained Benidipine (4mg), Labrafil M2125 Cs (30%), Kolliphor EL (45%), and Transcutol P (50%) with globule size of 162.25nm, release of drug within 15 minutes, 90.15%, self-emulsification time of 67.25 sec, and %transmittance (99.50).

4.3B Formulation and development of benidipine with telmisartan SNEDDS

4.3B1. Screening of Oil, Surfactants, and Co-Surfactants

The solubility of the drugs in the oil is an important factor in determining the degree to which the SNEDDS formulation keeps the drug in the solubilized condition throughout retention. Oil has been indicated to increase the medicine's intestinal permeability while also delivering the highest pharmacological solubility feasible.

The data on BD and TEL solubility in various oils is provided in Table 4.18 and Figure 4.20, which reveal a considerable difference between the lowest and maximum solubility of both drugs in oils. Figure 4.20 indicates the bar chart illustrating the solubility of BD in various oils, which was determined to be in the following order: Soybean oil, <sunflower oil, sesame oil, cotton seed oil < castor oil < peanut oil < olive oil < oleic acid < eucalyptus oil < labrafil M 2125 CS.

Sr.No.	Oil	Solubility of Benidipine (mg/mL)	Solubility of Telmisartan (mg/mL)
1	Oleic acid	6.0 ± 1.1	11.2 ± 1.2
2	Sunflower oil	3.3± 0.4	10.4 ± 0.8
3	Olive oil	5.5 ± 1.5	13.2 ± 0.6
4	Castor oil	4.5 ± 0.12	10.3 ± 0.3
5	Sesame oil	4.3 ± 0.45	15.1 ± 0.5
6	Peanut oil	5.5 ± 0.75	12.1 ± 1.1
7	Eucalyptus oil	6.5± 1.1	18.3 ± 1.2

8	Cotton seed oil	4.5 ± 0.5	11.2 ± 1.2
9	Soyabean oil	3.1 ± 0.4	14.12 ± 1.1
10	Labraill M 2125CS	8.4 ± 0.8	14.2 ± 0.8

Table 4.18: Solubility of Benidipine with Telmisartan in various Oil
Each value represents the mean ± SD, n = 3

The solubility of TEL in different oils was discovered to be in the following order: Castor oil < sunflower oil < peanut oil < olive oil < soybean oil < labrafil M 2125 CS < sesame oil < cotton seed oil < eucalyptus oil. So eucalyptus oil has been chosen as the oil having the highest solubility for the drug being utilized [40].

The strategy of selection of the surfactant and cosurfactant in subsequent studies has been determined by the efficacy of emulsification with the specified oil, i.e., eucalyptus oil and the solubilization capability of BD with TEL. For the generation of oil in water nanoemulsions, numerous surfactants with varied HLB values ranging from 8–16 having cation, ionic, and non-ionic natures may be utilized. Non-ionic surfactants are typically used for oral consumption as they have been considered to be safer than ionic surfactants [38].

In the beginning, the surfactant was chosen with focus given to the continuous phase of the nanoemulsion, with the hydrophilic surfactant for the nanoemulsion and the aqueous phase as the state of dispersion, and vice versa. Table 4.19 highlight the emulsification studies of Eucalyptus oil for the surfactant and cosurfactant selection of Benidipine and Telmisartan. The solubility of the drugs in surfactants and cosurfactants, coupled with the number of inversions and the percentage of transmission, was employed to assess the emulsification capacities of various surfactants and co-surfactants [45].

The power of the surfactant to spontaneously emulsify oil when diluted with distilled water was considered one of the selection criteria. The number of inversions and the percentage transmission employed to establish the emulsification abilities of different surfactants and co-surfactants have been documented. The bar chart in Figure 4.20 represents the drug's solubility in surfactants, which were discovered to be in the following sequence: Tween 80< Cremophor RH 40< Span 20< Tween 20 <Solutol HS

15< Span 80 < Kolliphor EL. Amongst these, Kolliphor EL was chosen, as it resulted in the creation of a transparent mixture with oil and had a transmittance of 99.50%.

Kolliphor EL is a promising surfactant because of its high HLB value, i.e., 12–14, in contrast to the HLB value of eucalyptus oil, i.e., 9.2, attributed to which it exhibits a better emulsifying property that ensues in a decrease in interfacial tension, low entropy, and quick dispersion of oil globules in the aqueous phase that eventually offers stable microscopic oil in water nanoemulsion. Considering Kolliphor EL is non-ionic in nature, it generates a low magnitude of charge over the nanoparticle, which minimizes the possibility of agglomeration, leading to the stabilization of the formulation. It is described as a less harmful and preferable surfactant for oral intake [39].

Surfactant	**No. of Inversion (BD)**	**(%)Transmitance (BD)**	**No. of Inversion (TEL)**	**(%)Transmitance (TEL)**
Cremophor RH40	35	84.5	38	83.1
Tween 20	21	87.3	24	86.65
Tween 80	45	82.2	49	80.3
Span 20	22	85.5	24	84.65
Span 80	18	96.5	20	97.2
Solutol HS 15	20	92.5	23	93.5
Kolliphor EL	17	99.5	19	99.65
Cosurfactant				
PEG-200	27	94.25	25	92.25
Transcutol P	15	97.5	13	98.85
PEG-400	21	96.75	18	95.5
Propylene Glycol	35	92.25	32	90.65

Table 4.19: Emulsification study of Eucalyptus oil for the surfactant and cosurfactant selection of Benidipine and Telmisartan

Thus, considering the results of the emulsification and solubility tests, Kolliphor EL was selected as a surfactant for future studies. The co-presence of surfactants provides the surfactant layer with the requisite flexibility and facilitates the creation of the different curvatures necessary for the synthesis of nanoemulsions in a variety of compositions. The co-surfactant enhances the area accessible for the production of nanoemulsions by decreasing surface tension even further while fluidizing the surfactant layer [46]. All of the co-surfactants that were examined influenced the drug's solubility in the following sequence: propylene glycol < PEG-400 <PEG-200<

Transcutol P. Transcutol P was chosen as a co-surfactant based on solubility and its percentage of transparency of the created emulsions.

Conclusion: As a consequence, Eucalyptus oil, Kolliphor EL, and Transcutol P have been chosen as the oil, surfactant, and co-surfactant, accordingly, on the basis of the results of solubilization capacity and emulsification efficiency.

4.3B2. Building of a Ternary Phase Diagram

The purpose of generating phase diagrams was to study the maximum nanoemulsification. The research focused on the fact that the larger the field of nano-emulsification, the better the nano-emulsification performance of the system. It was also revealed that if the length of the chain was extended, there was an increase in the area of the presence of the nanoemulsion. This means that the nanoemulsions development depends on the system's composition, and the existence of the nanoemulsions development has been confirmed with the help of the ternary phase diagram. In the same way as the process of mixing each component provided little in terms of changing the production of the nanoemulsion, the system was kept in a thermodynamically stable state that was pH-independent [47].

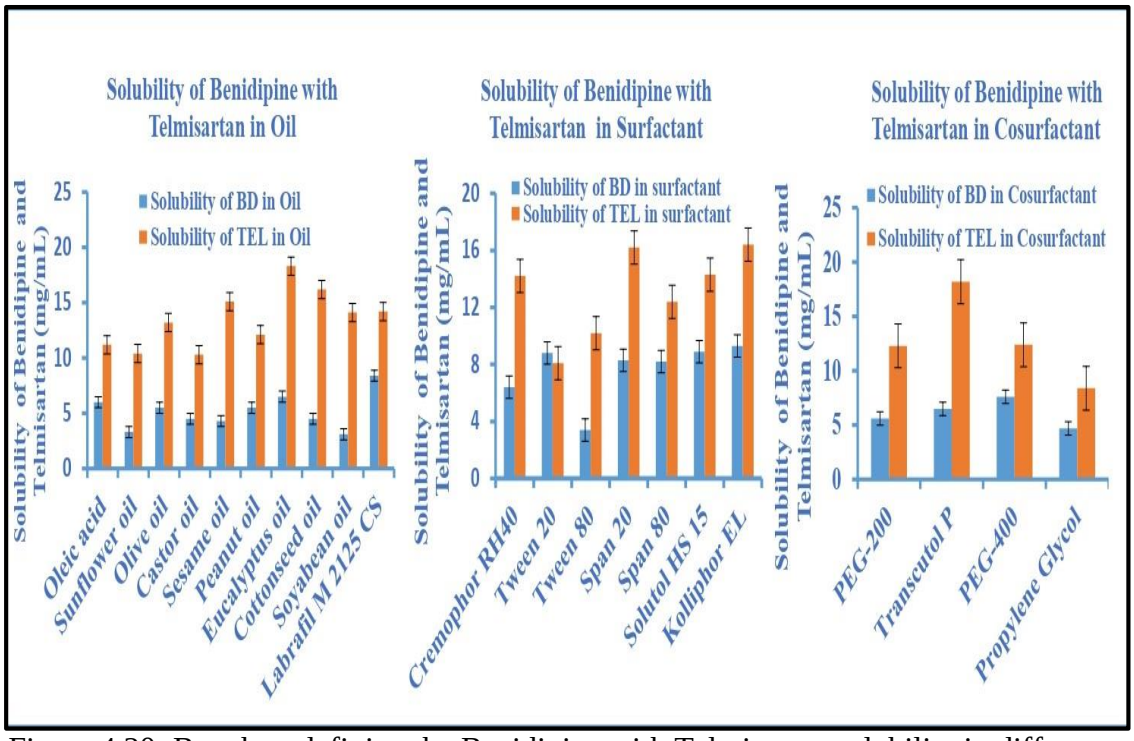

Figure 4.20: Bar chart defining the Benidipine with Telmisartan solubility in different oils, surfactants and co-surfactants

The second interesting finding was that there was no evident change from the w/o to the o/w nanoemulsion. The remaining half of the region of the phase diagram was characteristic of turbid and conventional emulsions. There was also a thorough examination of the formulations in order to ensure that the metastable complexes were not selected, even though the free energy that was expended in the production of the nanoemulsion was fairly low.

For further optimization of the system, the influence of the surfactant and cosurfactant ratios on nanoemulsion fabrication was determined. A total of five phase diagrams were developed employing varied ratios of oil phase, surfactant, and cosurfactant (1:1, 2:1, 3:1, 1:3, and 1:2) as displayed in figure 4.21. According to the results, the second phase diagram with the (2:1) ratio showed the fewest nano-emulsification zones, but the phase diagram with the (3:1) ratio offered the best phase diagram. The additional phase diagrams with (1:2) and (1:3) ratios showed considerable nano-emulsification regions as compared to the least emulsified parts (2:1). From the data collected, the phase diagram with the (3:1) ratio and the maximum quantity of nano-emulsification zones had been selected for the BD and TEL-SNEDDS formulation development.

Effect of BD with TEL on the phase diagram

Figure 4.21 shows the various quantities that were considered while determining the appropriate amounts of oil, surfactant, and co-surfactant for the BD with TEL nanoemulsion system. Three primary ingredients—eucalyptus oil, Kolliphor EL, and Transcutol P—formed the nanoemulsion's structure. A decrease in self-emulsifying performance is seen when hydrophobic drugs, such as BD with TEL, become trapped in the SNEDDS. Additionally, the ratio of 2:1 may be seen for the drug precipitation. The current study discovered that the effective self-emulsifying efficiency was reduced when BD and TEL were incorporated in a 2:1 ratio, while the remaining ratio remained unchanged.

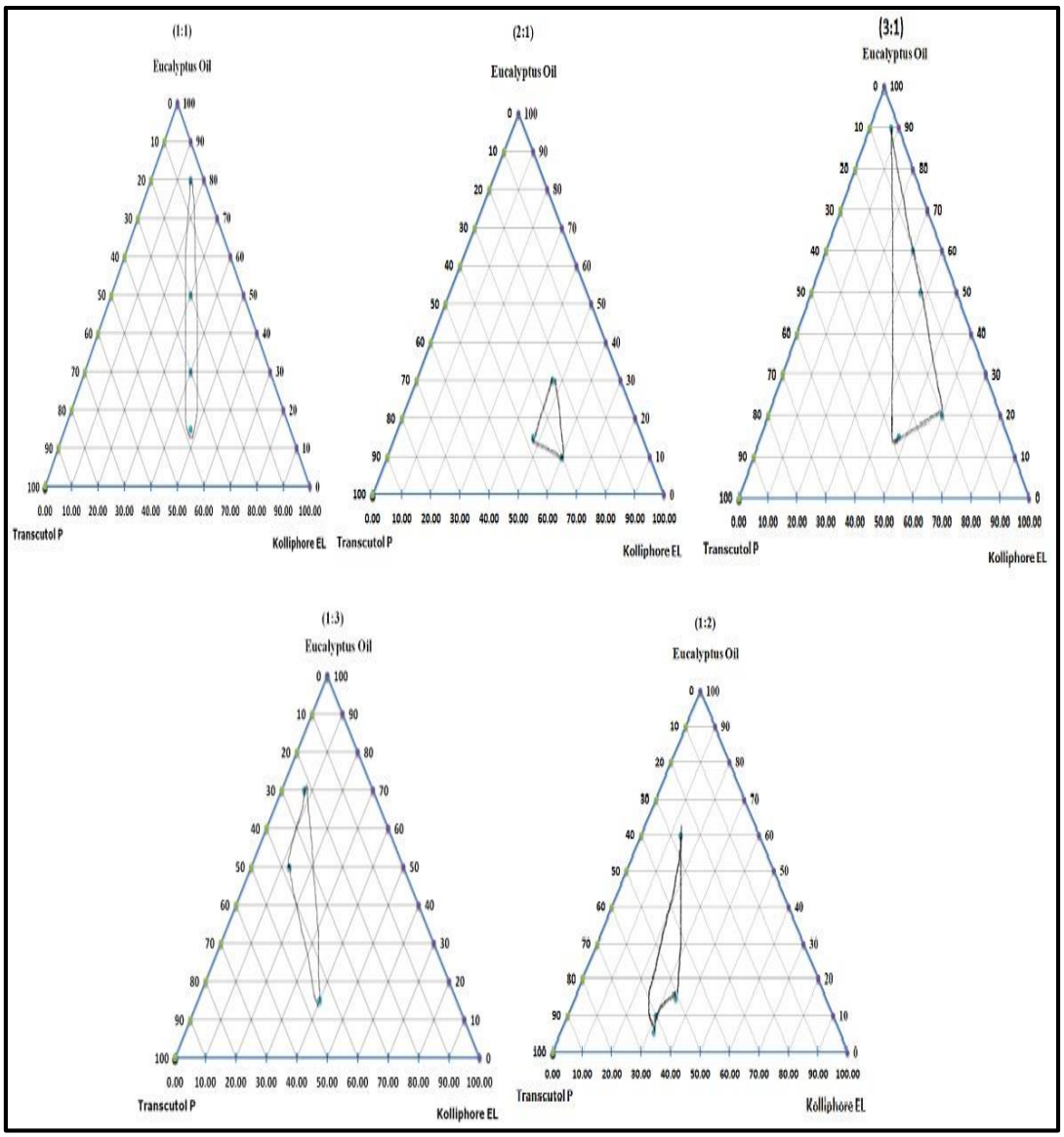

Figure 4.21: Ternary phase diagrams of the o/w emulsified regions of 1:1, 2:1, 3:1, 1:3 and 1:2 ratios of Eucalyptus oil, Kolliphor EL, and Transcutol P

4.3B3. Optimization of SNEDDS Employing Experimental Design

Design Expert 13 had been chosen to design the trial pattern. Summary of CQAs achieved for BD with TEL formulations generated as per the BBD design for the response self-emulsification time (Y_1), droplet size Dnm (Y_2), percentage of BD release in 15 minutes (Y_3), percentage of TEL release in 15 minutes (Y_4), and % transmittance %T (Y_5) are provided in Table 4.20. Prepared SNEDDS have been examined by several aspects, such applying multiple regression analysis. The BBD model was created to suit the 2nd-order polynomial model. Table 4.21 displays the results of a regression analysis

on designing batches of BD with TEL-loaded SNEDDS. A polynomial equation was constructed as the mathematical connection for possible responses.

Formulation	Average ± SD (n=3)				
	T_{emul} (sec)	D_{nm} (nm)	%Rel 15 min		%Transmittance (%)
			BD	TEL	
BT1	60.60±2.03	186.01±3.10	91.5±1.2	92.7±0.5	97.1±1.47.
BT2	57.71±2.10	195.23±3.25	92.3±1.4	92.9±1.9	89.1±1.2
BT3	58.50±2.15	183.14±3.00	89.7±0.6	89.5±1.2	92.3±0.5
BT4	53.12±2.10	191.32±3.30	91.6±1.3	92.4±1.1	96.1±1.9
BT5	55.10±2.05	184.23±3.20	91.6±0.9	91.6±1.7	95.3±1.2
BT6	61.15±2.10	192.23±3.10	91.7±1.7	92.4±1.6	96.9±1.5
BT7	57.30±2.15	184.03±2.90	92.3±0.8	92.9±1.2	89.2±0.4
BT8	56.22±2.10	189.10±2.80	92.5±0.6	92.9±1.4	98.2±1.1
BT9	55.16±1.95	182.43±2.75	91.9±0.4	91.7±1.4	96.1±1.7
BT10	62.90±2.50	199.75±2.90	92.1±1.6	92.1±1.6	92.9±1.6
BT11	53.00±2.10	175.12±2.70	93.5±0.8	93.7±0.7	99.6±0.3
BT12	60.30±2.10	199.12±2.60	91.4±1.5	92.5±0.5	86.5±0.5
BT13	57.10±2.20	164.50±2.50	92.3±0.6	93.0±1.6	89.0±0.6
BT14	59.25±1.97	156.20±2.40	91.3±1.2	91.6±0.2	88.6±0.7
BT15	60.12±2.00	161.21±2.50	91.8±0.6	91.9±0.4	93.9±0.4

Table 4.20: An overview of the CQAs observed for formulations of BD with TEL created by the BBD design

All the values are in mean ±SD (n=3), BT: Benidipine with Telmisartan

Quadratic polynomial equation-according to the following equation

Y_1 (Emulsification time) = $52.779+0.355\ X_1-0.921\ X_2+0.026\ X_3+1.125X_1\ X_2-1.375\ X_2\ X_3+0.02\ X_1\ X_3+1.0271\ X_1^2+1.895\ X_2^2-1.718X_3^2$ …….....(4.5)

Y_2 (Droplet size) = $184.50+0.118\ X_1+0.977\ X_2-0.311\ X_3+1.054X_1\ X_2+0.379X_2\ X_3-0.741X_1\ X_3+12.657\ X_1^2+11.523\ X_2^2+1.673\ X_3^2$ ....……..... (4.6)

Y_3 (% BD release at 15min) = $86.768+3.322\ X_1-0.011X_2-1.112X_3-5.795\ X_1\ X_2-2.066\ X_2\ X_3-2.827\ X_1\ X_3-0.518X_1^2-0.845\ X_2^2-1.754\ X_3^2$ ……. (4.7)

Y_4 (% TEL release at 15min) = $162.30+6.62\ X_1-57.31\ X_2-2.69X_3-43.87\ X_1\ X_2-6.70X_2\ X_3-20.20X_1\ X_3+42\ X_1^2+19.21X_2^2+0.451\ X_3^2$ ..…… (4.8)

Y_5 (%Transmittance) = $97.73-2.852\ X_1+2.268\ X_2+0.396X_3+2.975X_1\ X_2-0.35\ X_2\ X_3+0.6\ X_1\ X_3-2.2923\ X_1^2-1.794X_2^2-0.643X_3^2$ …….……(4.9)

A positive sign in research indicates that the effects are synergistic, while a negative sign suggests that the effects are antagonistic. The findings of the analysis of variance (ANOVA) for BD with TEL-loaded SNEDDS are shown in Table 4.22. A greater comprehension of the connection between the dependent and independent variables was achieved through the use of response surface plots and contour plots in further research.

The assessment of response result variability was conducted using the R^2 and adjusted R^2 values. R^2 and adjusted R^2 values over 0.9 suggest a significant level of agreement between the experimental data and the fitted values for each response. The statistical models' ability to move through the design space was evaluated by testing their precision against acceptable levels of accuracy. An integer greater than 4 indicated that the statistical model might be effectively used for exploring the design space. Remarkably, all the statistical models exhibited comparable R^2 and adjusted R^2 values, with a difference of less than 0.2 between the two. This reveals a strong correspondence between all the models, indicating that the experimental data closely matched the values that were estimated.

Co efficients	**T_{emul} (sec) (Y_1)**		**Dnm (Y_2)**		**BD%$_{Rel\ 15\ min}$ (Y_3)**		**TEM%$_{Rel\ 15min}$ (Y_4)**		**%T (Y_5)**	
	FM[a]	**RM[b]**	**FM**	**RM**	**FM**	**RM**	**FM**	**RM**	**FM**	**RM**
b_0	52.779	70.604	184.50	185.53	86.768	92.940	162.30	185.53	97.73	98.812
b_1	0.355	8.295	0.118	–	3.322	–	61.62	–	-2.852	-2.636
b_2	-0.921	–	0.977	0.723	-0.011	0.279	-57.31	0.237	2.268	–
b_3	0.026	–	-0.311	–	-1.112	0.335	-2.69	0.279	-0.396	–
b_4[c]	1.125	–	1.054	-	-5.795	–	-43.87	–	2.975	–
b_5[c]	-1.375	–	0.379	–	-2.066	–	-6.70	–	-0.35	–
b_6[c]	0.02	–	-0.741	–	-2.827	–	-20.20	–	0.6	–
b_7	1.0271	–	12.657	6.834	-0.518	-8.316	42.00	-6.834	-2.923	–
b_8	1.895	10.088	11.523	–	-0.845	–	19.21	–	-1.794	–
b_9	1.718	–	1.673	–	-1.754	–	0.451	–	-0.643	–

Table 4.21: Regression assessment of BD with TEL loaded SNEDDS created by the BBD design

[a]FM, Full model; [b]RM, Reduced model; [c]df, Degree of freedom; [d]SS, Sum of squares; [e]MS, Mean of squares.

(a) Composition Elements' Impact on Responses

The regression analysis and Equation 8 demonstrated that X_1 (oil) had a positive influence on drop size, whereas X_2 (surfactant) and X_3 (co-surfactant) had negative impacts. Increasing oil content resulted in larger and more lipophilic droplets, maybe accelerating the emulsification process. For Self-Emulsification Time (Y_1), Droplet size (Y_2), % Rel 15 min (Y_3), (Y_4) and %T (Y_5) coefficients b_4 ,b_5 and b_6 were found to be insignificant ($P > 0.05$) and hence, these terms were separated from their respective full model in order to develop a reduced model. The removal of insignificant terms was further justified by executing an ANOVA test.

(I) Self-emulsification time

As can be seen from Equation 7, the efficiency and effectiveness of the emulsification process decreased with increasing oil content in the formulation, resulting in larger droplet sizes and an increased level of lipophilicity [47]. Increasing oil content resulted in larger and more lipophilic droplets, maybe speeding the emulsification process. In this manner, the nanoemulsion formation was a result of the composition of the system, where the presence of the nanoemulsion formation could be understood with the use of the ternary phase diagram.

Figure 4.22 presents a contour plot, whereas Figure 4.27 provides a 3D surface response plot. These figures indicate the influence of oil concentration, surfactant concentration, and co-surfactant concentration on the emulsification time. Emulsification of liquid SNEDDS preconcentrates results in a clear dispersion with a high percentage of transmittance (%T) as well as a tiny droplet size, which reveals a blue tint, as mentioned in Table 4.19. The %T was, in the majority of cases, >90%, which is an indication of a quick and reproducible emulsification process. The modified R^2 and the expected R^2 indicate significant agreement with each other's criteria.

(II) Droplet size

Model	df[c]	SS[d]	MS[e]	R^2
T_{emul} (sec) (Y_1)				
Regression				
FM[a]	9	1323.130	145.1475	0.9412
RM[b]	2	1190.905	545.1840	0.9205
Residual				
FM	5	75.7104	13.7023	**Fcal** = 1.267
RM	12	195.3410	15.5650	**Fcritical** = 4.12**, df=** (7,5)
D_{nm} (μ) (Y_2)				
Regression				
FM	9	1528.1657	190.3659	0.8725
RM	2	890.1590	365.5106	0.8540
Residual				
FM	5	450.7136	89.1531	**Fcal** = 1.4067
RM	13	165.5692	77.6934	**Fcritical** = 3.96, **df** = (7,5)
BD $_{\%Rel\ 15\ min}$ (Y_3)				
Regression				
FM	9	616.350	68.483	0.9229
RM	3	463.466	154.488	0.9109
Residual				
FM	5	107.208	21.441	**Fcal** = 1.1884
RM	11	260.092	23.645	**Fcritical** = 8.94, **df** = (6,3)
TEM $_{\%Rel\ 15\ min}$ (Y_4)				
Regression				
FM	9	525.950	65.102	0.9565
RM	1	394.676	134.877	0.9368
Residual				
FM	5	98.153	19.190	**Fcal** = 1.1960
RM	11	246.056	17.858	**Fcritical** = 7.75, **df** = (6,3**)**
%T (Y_5)				
Regression				
FM	9	210.107	76.109	0.9248
RM	1	97.706	84.347	0.9075
Residual				
FM	5	95.789	42.793	**Fcal** = 0.0642
RM	13	206.550	54.126	**Fcritical** = 3.17**,df** = (8,7**)**

Table 4.22: Outcomes of the ANOVA test for the BD-loaded SNEDDS.

[a]FM, Full model, [b] RM, Reduced model, [c]Non-significant ($P > 0.05$) coefficients

The droplet size was significantly dependent on the oil phase formulation, where the droplet size decreased as a result of the reduction in the percentage of the oil phase formulation [48]. Droplet size and polydispersity index increased as they increased oil content, as expected and observed in multiple studies, and this can also be seen from the polynomial equation 2 of the fitted model. Furthermore, the interaction between oil ratio and surfactant concentration was robust, with an exceptionally negative coefficient value on droplet size (Y_2). The surfactant and co-surfactant work together to reduce the size of the oil droplets in the system, as seen by the negative values of the interaction effects (X_2 X_3, and X_1 X_3).

Figure 4.23 displays a contour plot, whereas Figure 4.28 shows a 3D surface response plot. These figures show how oil concentration, surfactant concentration, and co-surfactant concentration affect the size of droplets. Nanoemulsion droplet size is a fundamental property of the self-emulsification process. A larger interfacial area for the release of the drug is formed by the nano-ranged droplets [48]. The droplet size varied from 176.24±1.90 to 194.20±2.10 nm, with Transcutol P adversely impacting drop size as its amount increased. The production of nanoemulsions with smaller droplet sizes is highly suggested, as it provides a particularly low surface tension for the entire system plus the interfacial tension of the o/w droplets.

(III) Drug release at 15 min

The oil concentration was the only independent variable whose change had a significant impact on CPR15. To generate a nanoemulsion, the compositions required to be mixed well; increasing the quantity of any one composition would have an influence on the system's overall balance, which was essential to keeping the medicines solubilized [44]. At a 15-minute interval, optimized batches resulted in drug percentages ranging from 91.5% to 93.5% for BD and 91.6% to 92.9% for TEL. The oil content has a major impact on CPR 15. The differing patterns of drug release demonstrated in different formulations could be attainable due to the presence of variable amounts of oil phase, surfactant, and cosurfactant. Proper mixing of components was critical to nanoemulsion production and drug solubilization [50]. Figure 4.24, contour plot, and Figure 4.29, 3D surface response plot, show the effect of concentrations of oil, surfactant, and co-surfactant on benidipine release, whereas Figure 4.25, contour plot, and Figure 4.30, 3D surface response plot, demonstrate the effect of concentrations of oil, surfactant,

and co-surfactant on telmisartan release. The quadratic polynomial equations 9 and 10 were utilized to calculate drug release at 15 minutes.

(IV) %Transmittance

Emulsification of liquid SNEDDS pre-concentrates resulted in a clear dispersion with a high percentage of transmittance (%T) and an extremely small droplet size. The percent transmittance is distinct from 86.50±0.95% to 99.60±0.70%. An almost 100% transmittance indicated a clean SNEDDS dispersion with nanoscale droplets, which is an indication of a quick and repeatable emulsification process. It may be realized from Equation 11 that a reduction in %T is connected with higher oil content, an inadequate amount of surfactant, and a co-surfactant in the formulation that decreases the droplet size.

Higher oil content resulted in decreased transmission as a consequence of greater lipophilicity along with decreased transparency [51]. Figure 4.27 displays a contour plot, while figure 4.31 shows a 3D surface response plot. These plots illustrate the impact of oil concentration, surfactant concentration, and co-surfactant concentration on the percent transmittance.

(a) Response Surface and Contour Plot Analysis

Two-dimensional contour plots and three-dimensional surface response plots have been constructed to illustrate the connection between the dependent and independent variables and study their interactions. Figures 4.22 to 4.26 exhibit contour graphs indicating the influence of oil concentration, surfactant concentration, and co-surfactant concentration on emulsification time, droplet size, percentage of drug release (BD and TEL) at 15 minutes, as well as percent transmittance. Figures 4.27–4.31 represent the response surface for the effects of oil concentration, surfactant concentration, and co-surfactant concentration on emulsification time, droplet size, drug release (BD and TEL) at 15 minutes, and transmittance%, respectively.

The corresponding fall in globule size with the decrease in oil concentration may be attributed to a fast increase in surfactant concentration, which has the potential to more quickly emulsify the oil phase and lower globule size. The time it took to emulsify increased as oil content increased, which may have been affected by the surfactant

shortage. Surfactant molecules attach to the outermost emulsion droplets in order to decrease the amount of free interfacial energy and produce a mechanical barrier that inhibits emulsion droplet coalescence of emulsion droplets. An effect formed as a spontaneous thermodynamic distribution formed as an effect. Therefore, higher concentrations increase emulsification and drug absorption [52].

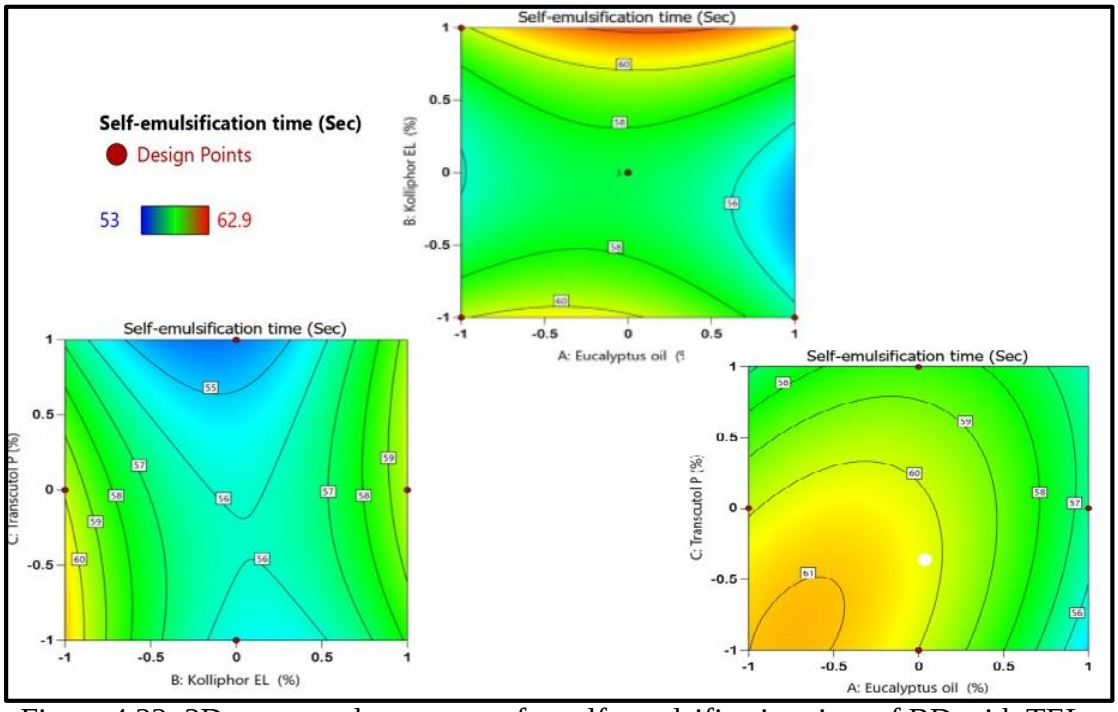

Figure 4.22: 2D contour plot response for self-emulsification time of BD with TEL-SNEDDS

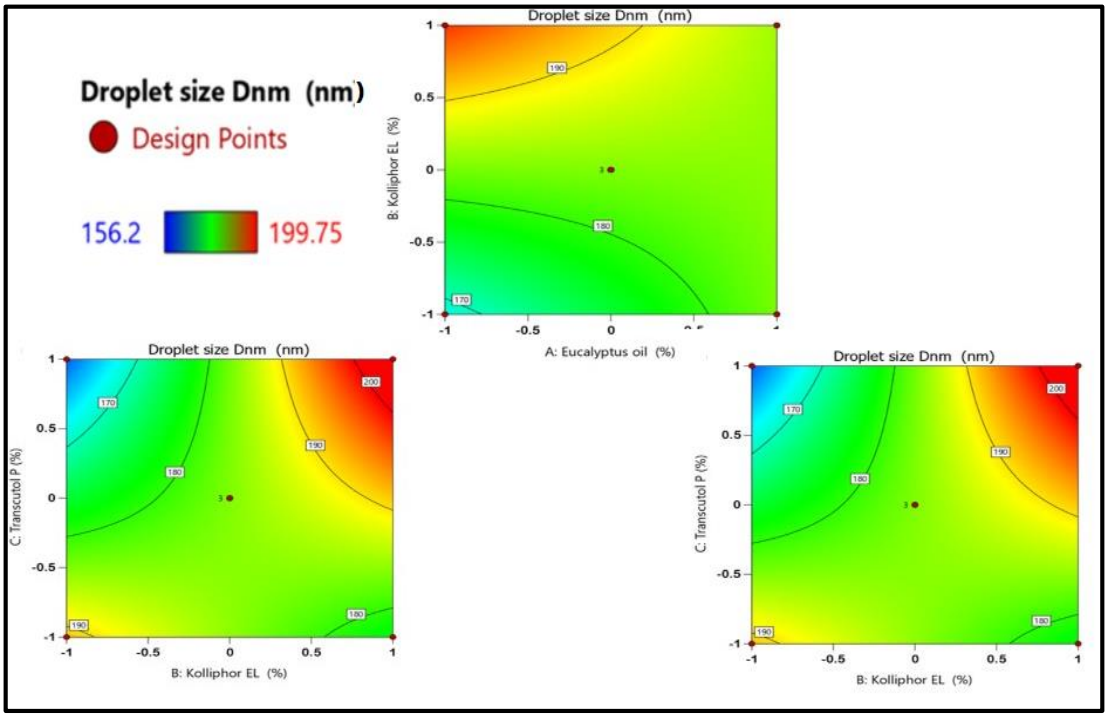

Figure 4.23: 2D contour plot response for droplet size of BD with TEL-SNEDDS

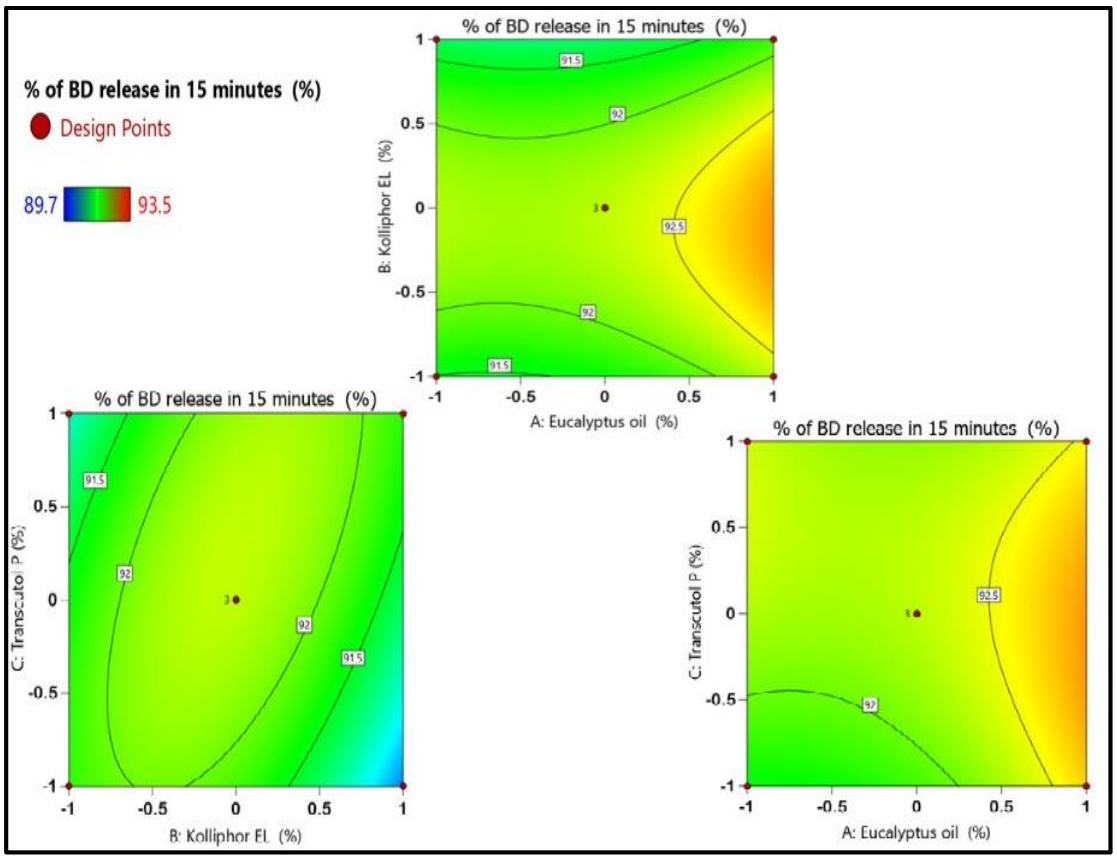

Figure 4.24: 2D contour plot response for % of BD release in 15 minutes of BD with TEL-SNEDDS

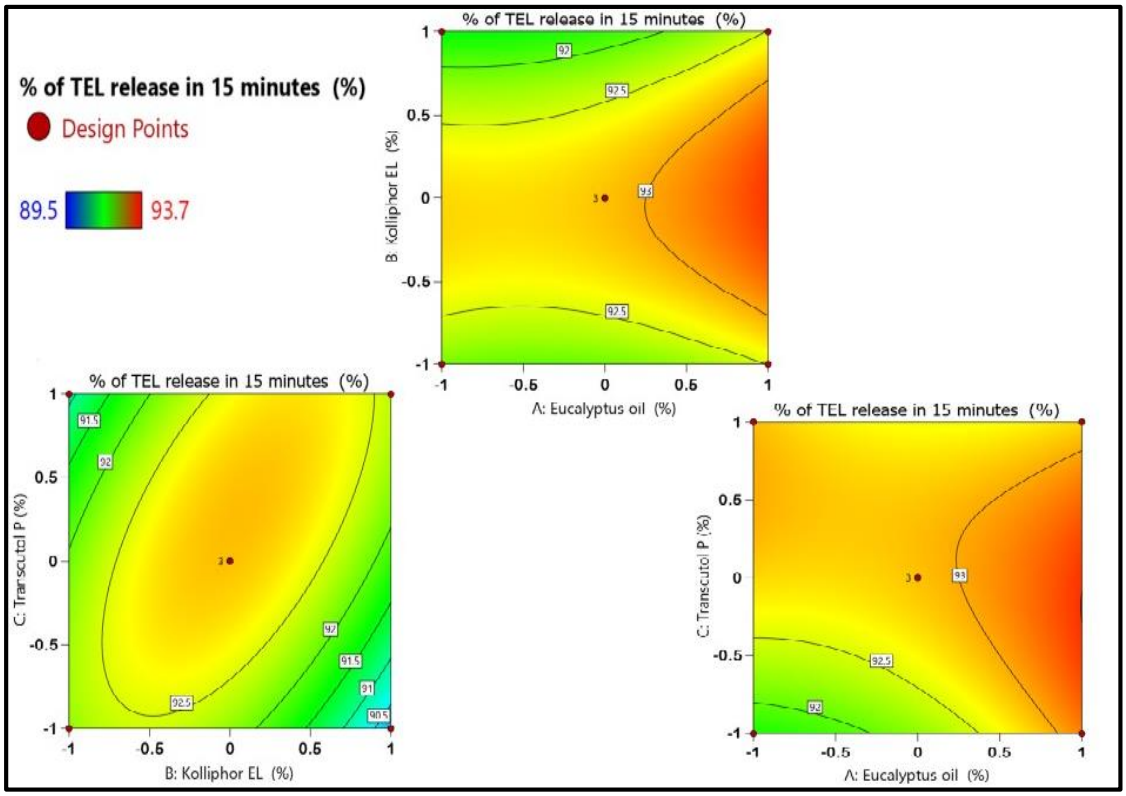

Figure 4.25: 2D contour plot response for % of TEL release in 15 minutes of BD with TEL-SNEDDS

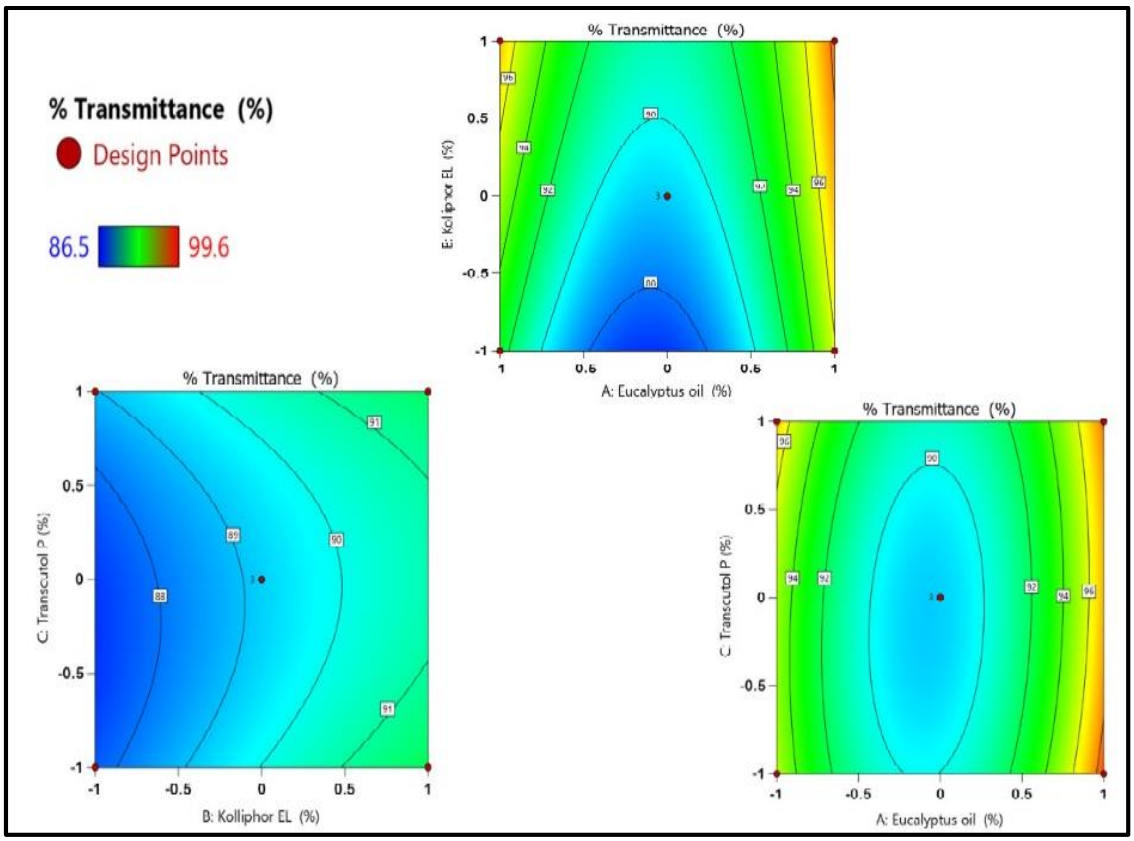

Figure 4.26: 2D contour plot response for % transmittance of BD with TEL-SNEDDS

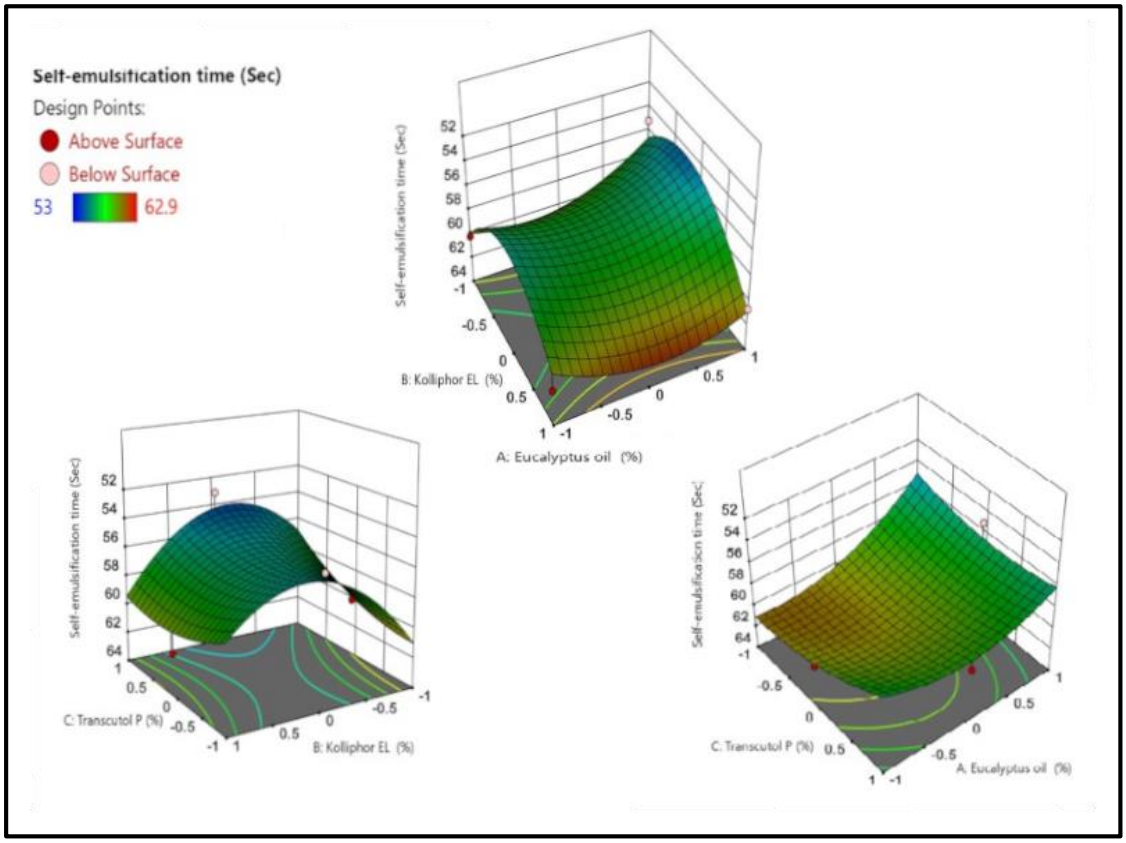

Figure 4.27: Response surface plots for emulsification time of BD with TEL-SNEDDS

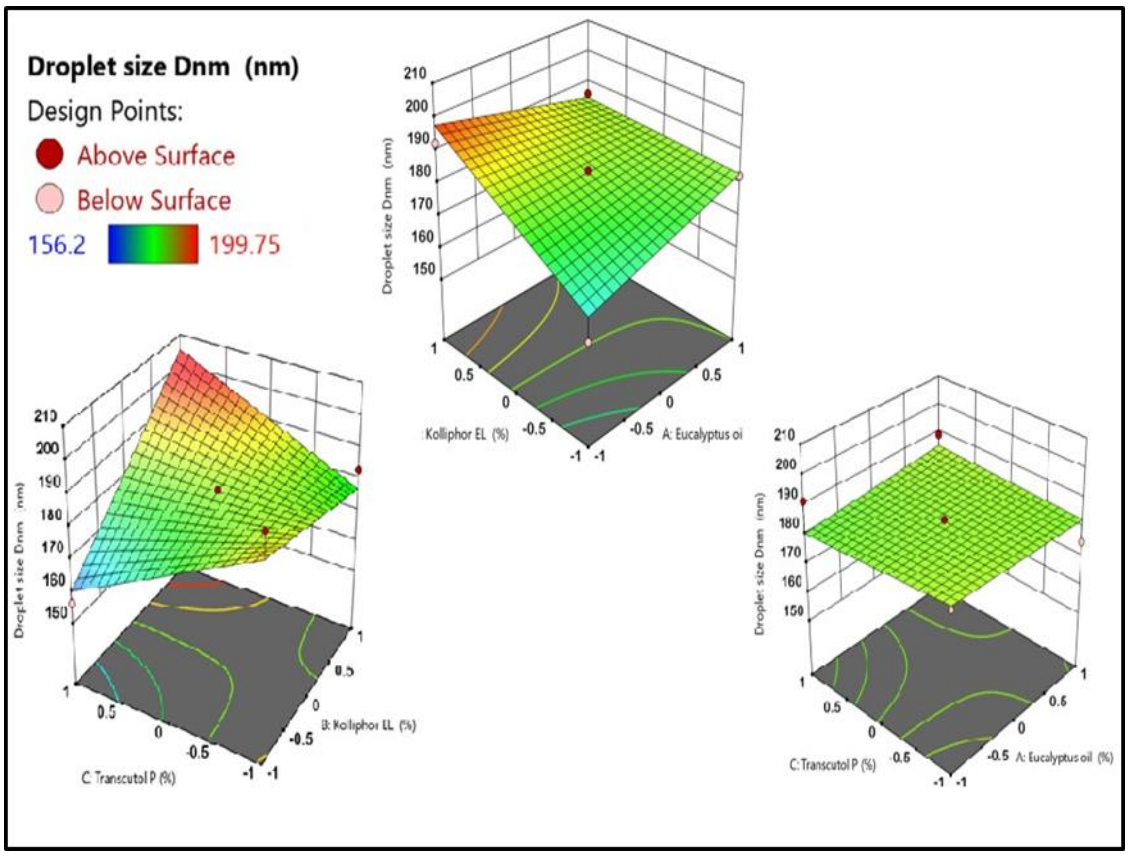

Figure 4.28: Response surface plots for droplet size of BD with TEL-SNEDDS

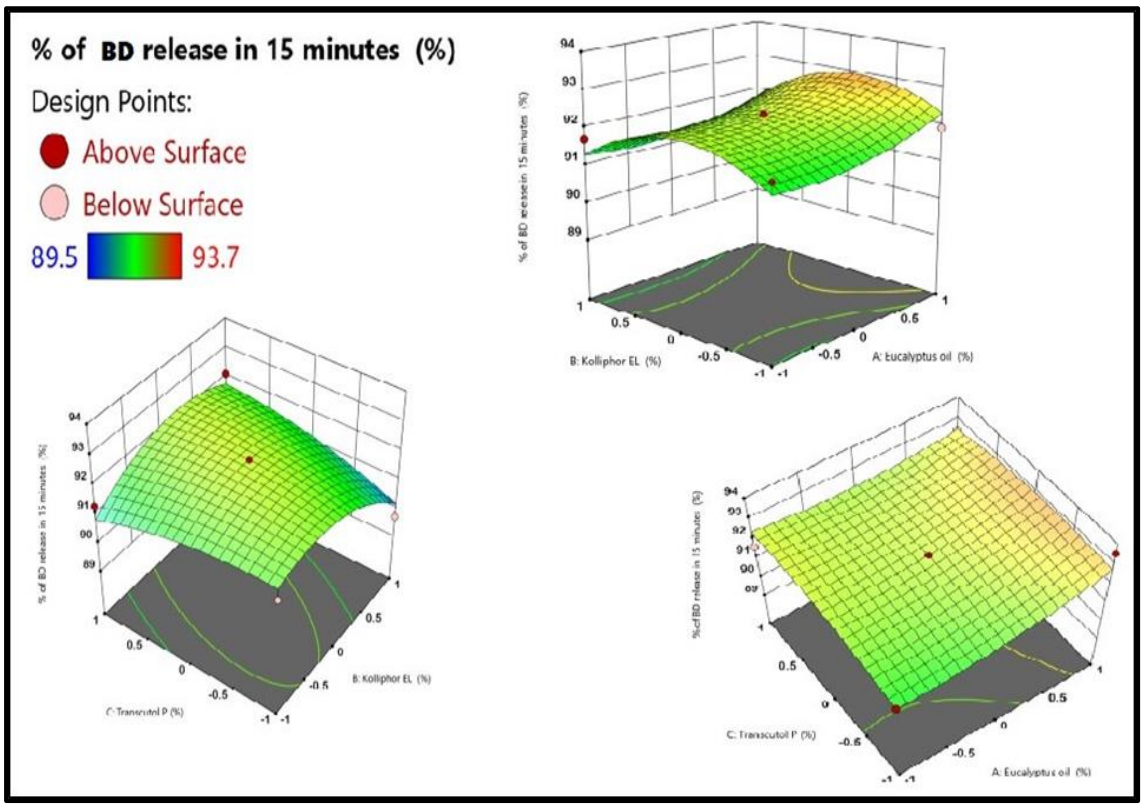

Figure 4.29: Response surface plots for % of BD release in 15 minutes of BD with TEL-SNEDDS

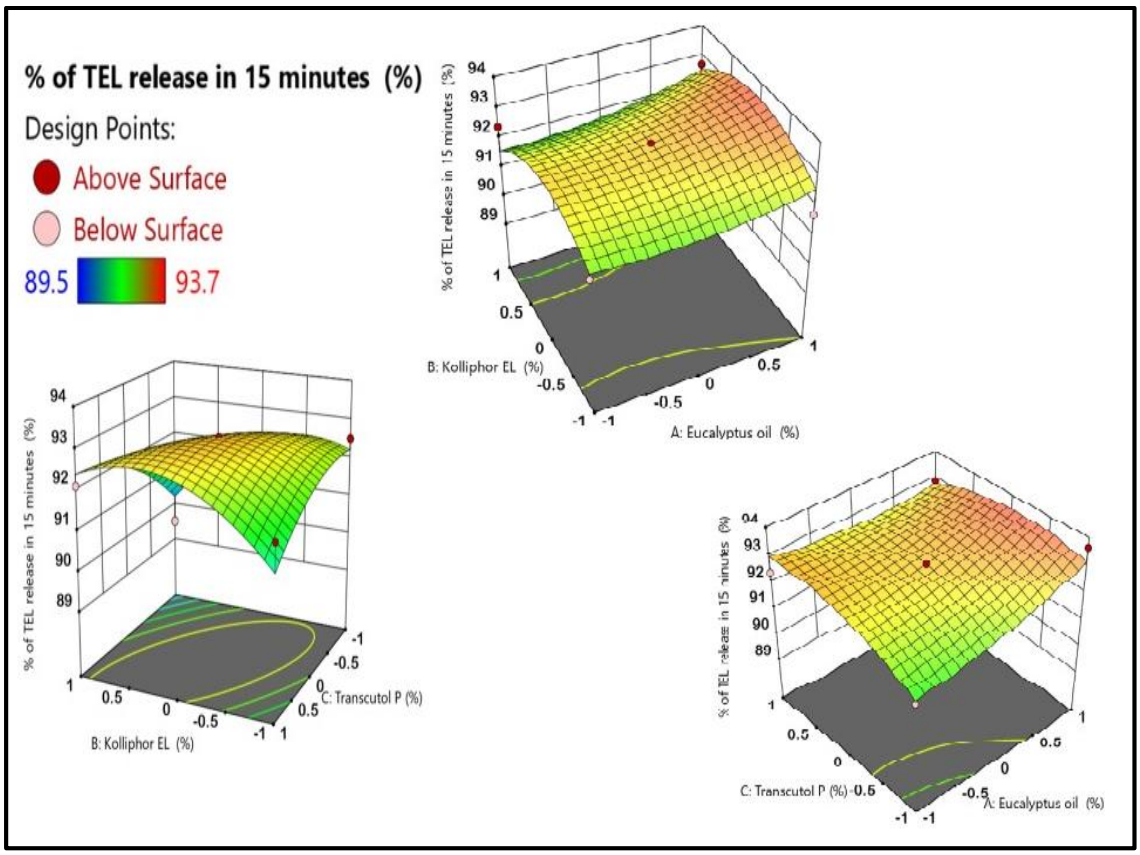

Figure 4.30: Response surface plots for % TEL release in 15 minutes of BD with TEL-SNEDDS

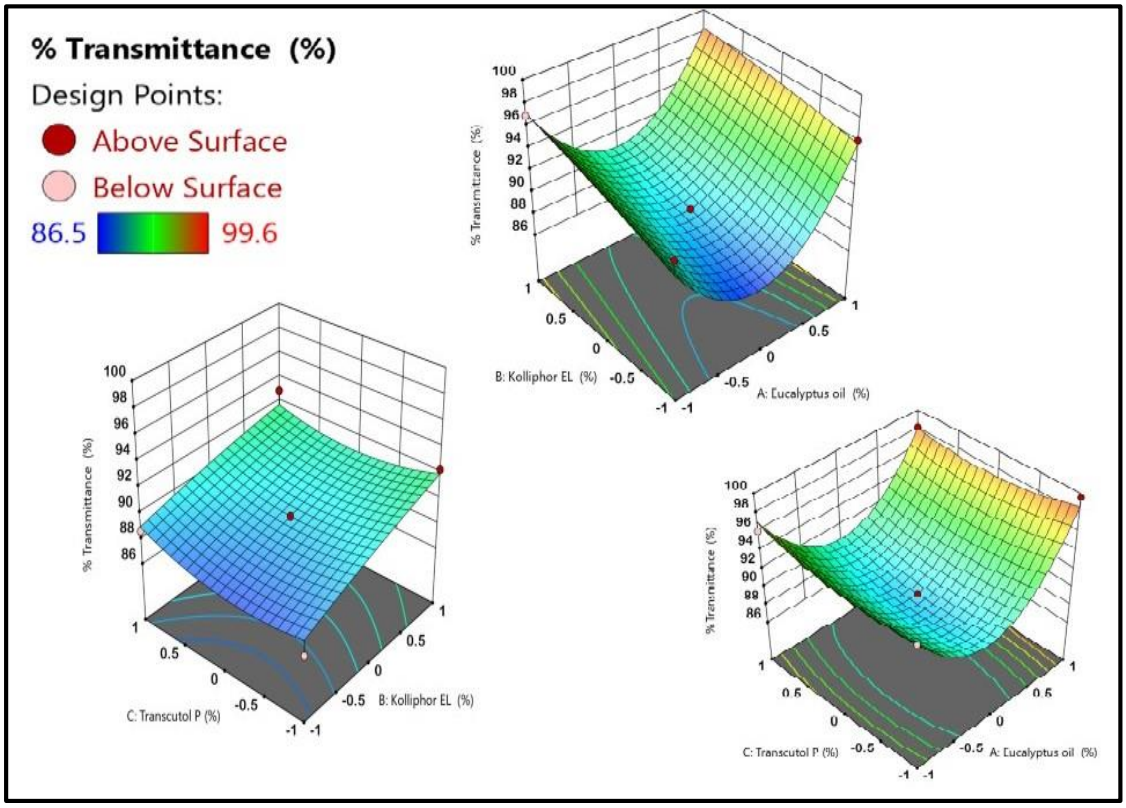

Figure 4.31: Response surface plots for % transmittance of BD with TEL-SNEDDS

(b) Identification and Evaluation of Optimum Formulation Using Desirability Function

To validate the proposed models, checkpoint formulations have been created and analyzed related to globule size, % transmittance, self-emulsification time, and % drug release (BD and TEL) in 15 minutes. All of the respondents in the present research were subject to limitations, and the optimum desirability function was determined [53].

Based on the necessary functions and response characteristics, an acceptable formulation was constructed. It was discovered that the design had sufficient predictability owing to the small variances between the predicted results and the average of the experimental outcomes observed for both of the responses (figure 4.32). For the selected formulation, X_1, X_2, and X_3 were assessed at percentages of 59.27%, 35.13%, and 12.50% w/w, respectively, resulting in an overall effect of 0.975. The expected and actual values for the responses toY_1, Y_2, Y_3, Y_4, and Y_5 are presented in Table 4.23.

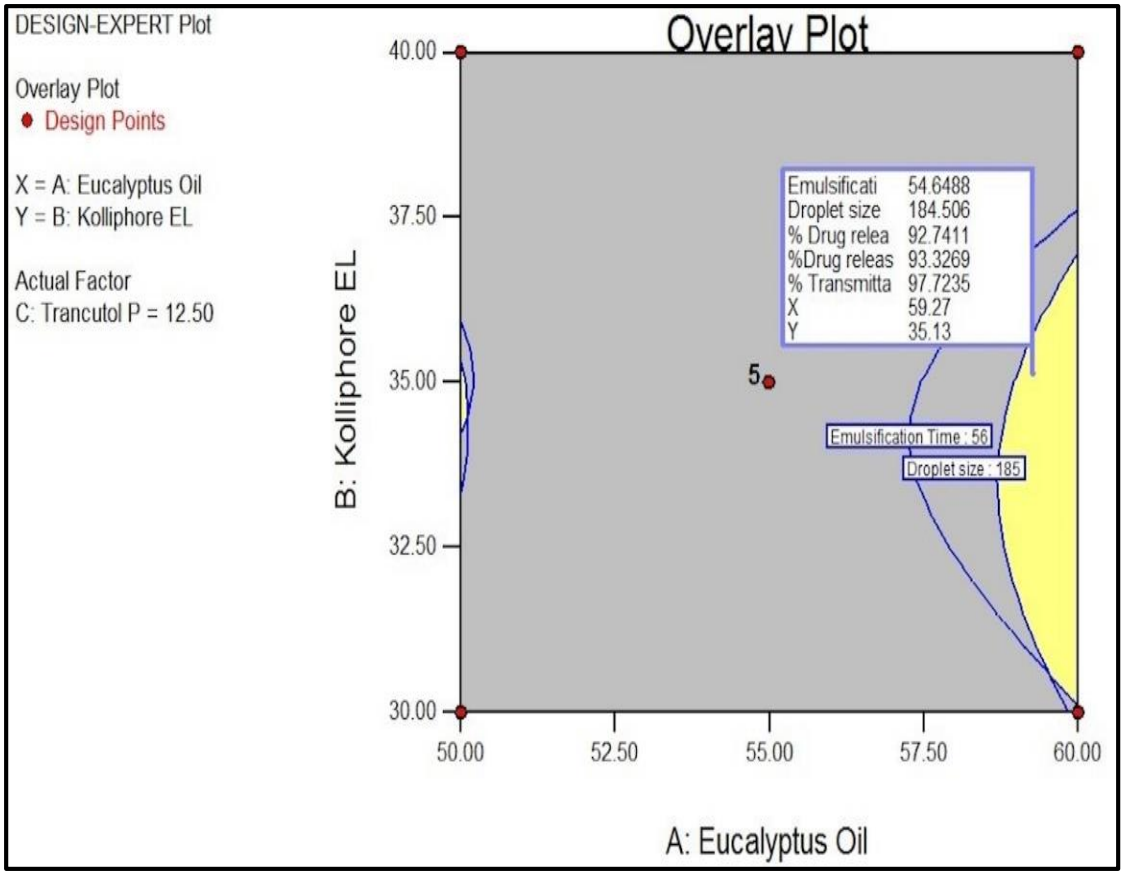

Figure 4.32: Overlay plot for optimized formulation of BD with TEL-loaded-SNEDDS

Response	Predicted value	Experimental value[a]	% Relative error
T_{emul} (sec) (Y_1)	54.6488	53.0±2.10	3.017
Dnm(μ) (Y_2)	184.506	175.12±2.70	5.087
%Rel $BD_{15\ min}$ (Y_3)	92.7411	93.5±0.8	-0.81
%Rel $TEL_{15\ min}$ (Y_4)	93.3269	93.7±0.7	-0.39
%T (Y_5)	97.7235	99.6±0.3	-1.92

Table 4.23: Predicted Values and measured values for optimized BD with TEL-loaded S-SNEDDS of BT11

[a]Values are of mean ± SD (n=3), SD: Standard deviation

The overlay plot of the optimized batch is presented in Table 4.22 and Figure 4.32. The predicted batch demonstrates significant reproducibility within the percentage deviation. From the result, it shows that the prediction value is close to the experimental value, therefore the design is significant.

Conclusion: Based on the desirability index, formulation BT11 was considered to be the most effective batch with a desirability value of 0.975. Formulation BT11 contained Benidipine (4mg), Telmisartan (40 mg), Eucalyptus oil (60%), Kolliphor EL (35%), Transcutol P (10%) with a globule size of 175.12 nm, release of drugs (BD and Tel) within 15 minutes (more than 90%), self-emulsification time of 53 sec, and %transmittance (99.60%).

4.4. Assessment of Drug-loaded Optimum Formulation

4.4A. Assessment of BD-Loaded Optimum Formulation

(I) Assessment and Changes in Opposition

The visual clarity of the optimized liquid SNEDDS (BD14) containing the drug was evaluated. It was proven to be homogeneous and optically clean, with a light blue color. There were no signs of precipitation or any sort of production activity.

(II) Resistance to Dilution

SNEDDS, or self-nanoemulsifying drug delivery systems, are concentrated formulations that form oil-in-water nanoemulsions only when diluted. However, problems with the separation of phases occur when the formulation is diluted indefinitely in gastrointestinal fluids. Pharmaceutical substances that have solubility depending on pH may form solid particles due to changes in pH [43]. To avoid this, the

most effective liquid self-nanoemulsifying drug delivery system (SNEDDS), BD14, was diluted in 0.1N hydrochloric acid and phosphate buffer with a pH of 6.8. The dilutions were made at volumes of 10, 100, 250, 500, and 900 times. No evidence of phase separation was observed in any of the formulations tested. Remarkably, the droplet size decreased as the pH level and the dilution factor increased from 10 to 500 times.

It was evident in Figure 4.33 that upon raising the availability of surfactants at the oil-water interface, droplet dispersion increased, which decreased the dilution factor to a particular value and resulted in the creation of uniform and smaller droplets. A small rise in zeta potential has been found concurrently with the change in pH and after increasing the dilution factor from 10 to 900 times. Despite this, the changes suggested the integrity of SNEDDS in nanoform when the gastrointestinal tract's volume and pH were changed. This confirmed the possibility of an optimized SNEDDS formulation for producing nanoemulsions at different physiological pH.

(III) Self-Emulsification Time

It is the amount of time required after dilution with water for the L-SNEDDS to produce a uniform dispersion. When exposed to dilution while still being gently mixed, the SNEDDS should disperse completely and quickly. The improved formulation's self-emulsification time was 65.21 ± 1.95 seconds. Reduced Temul levels in present investigations confirmed the spontaneous nature of the L-SNEDDS-generated nanoemulsions' process.

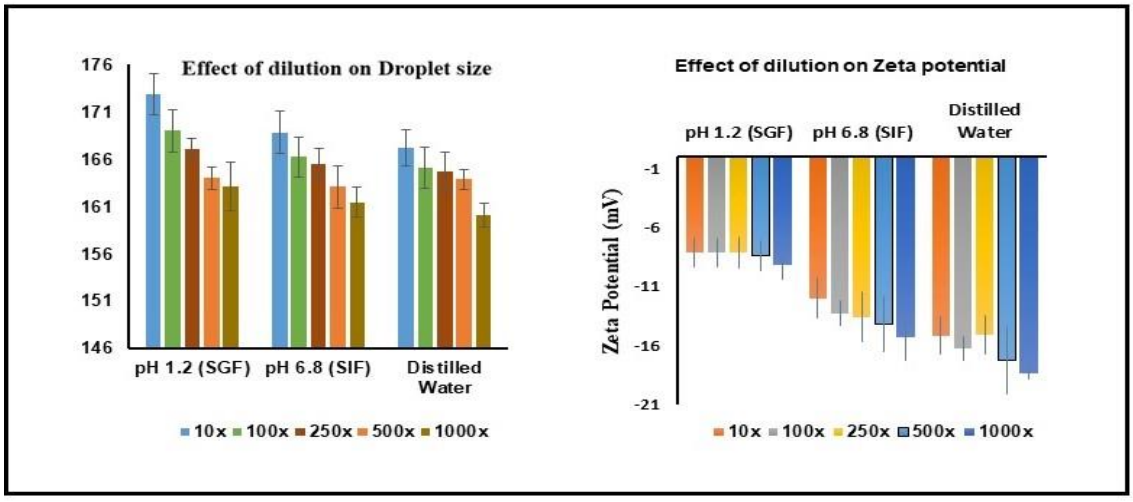

Figure 4.33: Effect of dilution on droplet size and zeta potential.

(IV) Drop size and Zeta potential

The nanoemulsion's particle size plays an important role in the self-emulsification process. The quantity of drug released from the most effective SNEDDS formulation is significantly determined by the drop size of the generated nanoemulsion. The expanded interfacial area for drug release is generated by the nanoscale droplets. The range of the permissible nanoemulsion definition (10 nm to 200 nm) was largely within the range of the average drop size of the nanoemulsion created by the drug-loaded optimized SNEDDS formulation, which was about 156.20 to 199.75 nm. According to Table 4.23, the PDI value was 0.250-0.450, illustrating the limited dispersion of decreased emissions.

The value of the zeta potential of −15.21 mV to -21.45 mV for the created nanoemulsion, as indicated in Table 4.24 and Figure 4.34, demonstrated remarkable stability. Phase separation is maintained as a result of a large electrostatic repulsive force that prohibits droplet coalescence. On the contrary, a reduction in electrostatic repulsive forces will produce phase separation. Several studies have indicated that the zeta potential plays a crucial role in the stability of microemulsion and nanoemulsions [45].

Formulation	**Average±SD (n=3)**				
	Liquification time(sec)	**Viscosity (Centi Poise)**	**Zeta potential(mV)**	**Cloud Point(ºC)**	**Refractive index**
BD1	70.50±2.50	140± 1.63	-15.23± 0.84	73.2±1.9	1.762±0.12
BD2	82.25±2.80	158± 2.55	-17.51± 0.60	73.9±1.7	1.789±0.18
BD3	65.10±2.30	132± 2.55	-20.52± 0.84	69.7±1.1	1.745±0.14
BD4	79.10±2.85	152± 1.40	-19.56± 0.85	74.4±1.5	1.752±0.13
BD5	66.15±1.80	137± 2.10	-21.21± 0.30	75.6±1.7	1.742±0.12
BD6	80.20±2.80	154± 2.40	-19.32± 0.64	72.8±2.2	1.761±0.12
BD7	65.10±2.10	125± 1.30	-18.95± 0.56	85.6±2.6	1.757±0.17
BD8	75.20±2.40	148± 2.40	-21.45± 0.30	83.7±2.8	1.780±0.18
BD9	64.75±1.87	110± 1.90	-18.63± 0.30	75.8±1.7	1.739±0.14
BD10	95.20±2.70	175± 2.20	-19.12± 0.20	79.6±1.7	1.773±0.17
BD11	72.20±2.60	141± 1.60	-16.12± 0.24	64.2±1.5	1.798±0.20
BD12	67.50±1.90	118± 1.92	-21.23± 0.18	71.5±2.2	1.765±0.19
BD13	69.25±1.95	145± 2.15	-15.21± 0.20	68.9±1.7	1.761±0.12
BD14	62.20±1.70	125± 1.50	-17.36± 0.18	69.9±1.5	1.752±0.14
BD15	64.50±1.65	136± 1.75	-16.50± 0.24	70.5±1.9	1.765±0.18

Table 4.24: Evaluation of SNEDDS BD1 to BD15 formulation of design

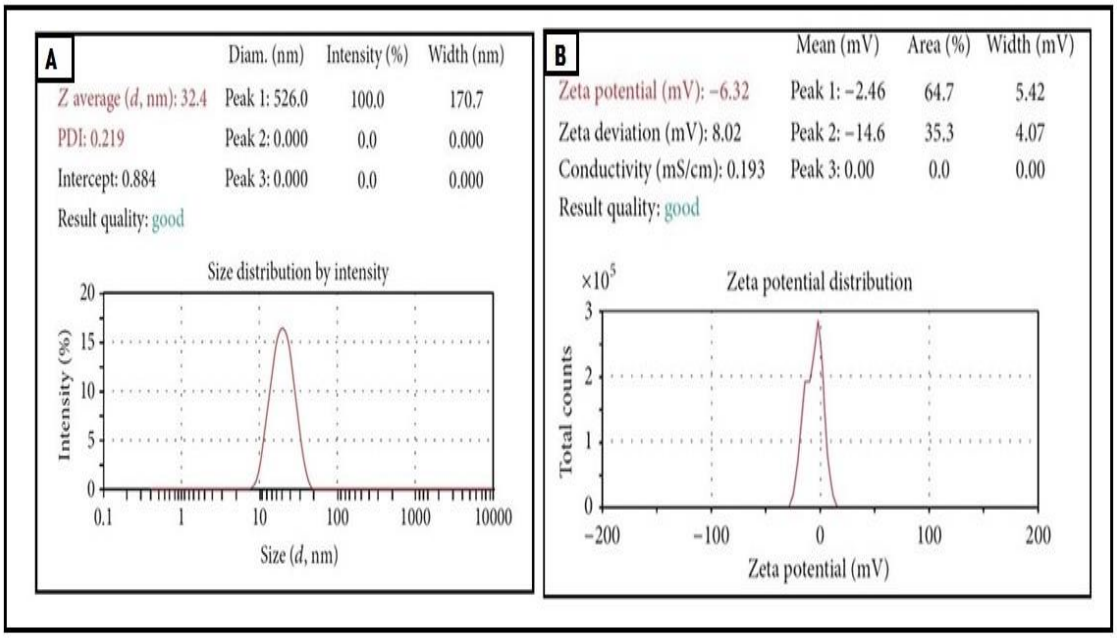

Figure 4.34: A) Droplet size distribution by intensity B) Zeta potential assessment of the augmented SNEDDS BD14 loaded with benidipine

(V) Transmittance Test

The clean, transparent, and nanosized globules have been observed, and the percent transmittance was 99.80±0.70%.

(VI) Cloud Point Measurement

The observed cloud point temperature is 69.9±1.5 °C, whereas the usual body temperature is 37 °C. In considering this, it can be claimed that the recently developed formulation remained stable in vivo at physiological temperature and did not show phase separation when stored at room temperature or when given via the digestive system [46].

(VII) Determination of the Refractive Index

The optimized formulation's refractive index turned out to be 1.752±0.14 (Table 4.23), experiencing the isotropy of the nanoemulsion. This value implied that the developed SNEDDS may produce an O/W type of nanoemulsion in vivo.

(VIII) Thermodynamic Stability Investigations

The impact of heating and cooling, centrifugation, and freeze-thaw cycling on the phase separation of nanoemulsions and the precipitation of drugs is illustrated in Table 4.25. All three accelerated tests are conducted to assess the stability of the nanoemulsion under stressful circumstances.

Batches that did not display any drug precipitation or phase separation after the heating and cooling cycles, along with centrifugation, displayed their stable nature. Similarly, batches that sustained freeze-thaw cycling were found to be reconstituted without any phase separation or drug precipitation after being subjected to freeze-thaw cycling.

When examined at various temperatures, these cycles demonstrated that the optimized formulation, BD14, was stable and did not exhibit any indication of drug precipitation or phase separation, while BD4, BD7, BD10, BD11, and BD12 failed the freeze-thaw cycling test with phase separation.

(IX)% Drug Content

The optimized formulation's percentage drug content of 99.22 ± 0.29% revealed that the SNEDDS formulation exhibited a consistent drug distribution.

Formulation	Heating Cooling Cycle	Centrifugation	Freeze thaw cycle
BD1	Pass	Pass	Pass
BD2	Pass	Pass	Pass
BD3	Pass	Pass	Pass
BD4	Pass	Pass	Fail
BD5	Pass	Pass	Pass
BD6	Pass	Pass	Pass
BD7	Pass	Pass	Fail
BD8	Pass	Pass	Pass
BD9	Pass	Pass	Pass
BD10	Pass	Pass	Fail
BD11	Pass	Pass	Fail
BD12	Pass	Pass	Fail
BD13	Pass	Pass	Pass
BD14	Pass	Pass	Pass
BD15	Pass	Pass	Pass

Table 4.25: Thermodynamic stability investigations of various Benidipine SNEDDS formulations

(X) Conductivity test

To predict the particular kind of nanoemulsion formed during dilution, the electrical conductivity of the optimal BD-loaded SNEDDS formulation was studied. The conductivity of o/w emulsions in BD-loaded systems was reported to be 0.193 µS/cm.

(XI) **Surface Morphology via TEM**

The microscopy of optimized SNEDDS formulation BD14 was studied using TEM micrographs. TEM studies confirmed that the modified SNEDDS formulation displayed a spherical shape and homogeneous size with no evidence of droplet aggregation, as depicted in Figure 4.35. These findings correspond with DLS data that confirm the practicability of SNEDDS formulations. The nanodroplets looked dark. These studies revealed the spontaneous creation of a nanometer-range nanoemulsifying system.

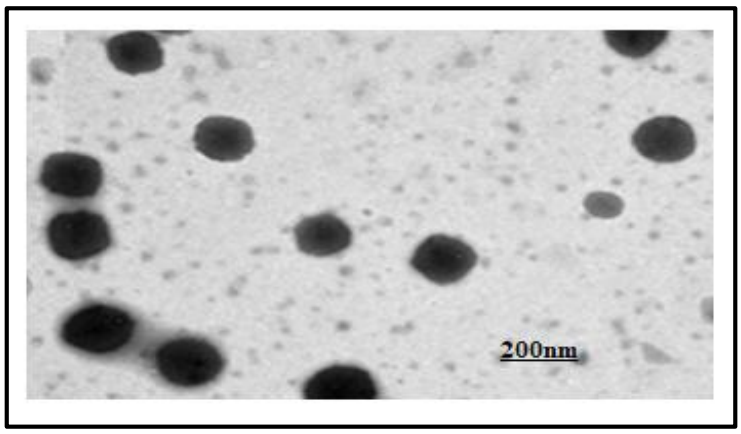

4.35: TEM images of the optimized benidipine SNEDDS - BD14

(XII) In Vitro drug release Study

To understand the features of drug releases from SNEDDS, in vitro release research has been conducted. When SNEDDS entered the aqueous medium, drugs existed in systems in many forms, including a free-molecule form, mixed in micelles, or in nanoemulsion droplets. Under this condition, it is essential to separate isolated drug molecules from those that are trapped by micelles or nanoemulsions for an accurate in vitro release test. Thus, it is not suitable to apply traditional release methods in this particular instance.

Comparisons of the dissolution profiles of different SNEDDS formulations with pure drugs are given in Tables 4.26 and Figures 4.36. Out of 15 formulation prepared as per experiment design BD14 release more than 95% at 20 min and 99.46±1.3 at 60 minutes. While, all produced batches had a drug release rate of around 90% within 60 minutes.

(XIII) Comparison of in vitro drug release between optimized batch BD14, pure drug powder, and marketed product

The benidipine release of the optimized batch (BD14) was measured contrasted to that of pure drug powder and the marketed product. The displayed product was Z-Bene, Corazon (a division of Arlak Biotech Private Limited), Punjab, India. Figure 4.37 depicts the findings of the study on the in-vitro drug release investigation of manufacturing batches BD14 (contained in HPMC capsules), pure drugs, and commercially available formulations. In essence, the pure drug and the marketed product could only release 45% and 40% of the drug, respectively, compared to the optimized batches. It's possible that the more considerable release of medicines from the targeted batches has been made possible through the SNEDDS formulation's potential to release the drug directly in its solubilized form in a dissolving medium [47].

Formulation	**Time(Minutes)**								
	0	**5**	**10**	**15**	**20**	**25**	**30**	**45**	**60**
Pure BD	0	28.21±0.4	36.12±0.6	41.23±0.7	47.23±0.6	52.12±0.5	58.24±0.5	62.2±0.5	64.27±0.5
BD1	0	78.21±0.6	80.21±0.8	82.17±0.9	83.25±0.7	84.14±0.6	88.21±0.5	90.14±0.6	91.24±0.7
BD2	0	78.14±0.8	79.17±0.9	83.14±1.2	85.14±0.8	86.12±0.6	89.15±0.6	90.99±0.5	92.14±0.8
BD3	0	80.14±1.7	81.14±1.2	82.11±1.4	82.89±0.5	83.14±0.8	85.15±0.7	91.11±0.7	92.78±0.5
BD4	0	80.65±0.8	82.19±1.7	83.12±1.4	84.21±0.7	85.31±0.6	85.99±0.5	88.9±0.5	92.9±0.6
BD5	0	88.12±1.9	89.99±1.8	90.12±1.3	90.98±1.2	91.12±0.9	93.41±0.8	94.12±0.8	94.9±1.1
BD6	0	86.12±1.8	89.12±1.9	89.65±1.2	90.97±1.3	92.05±1.2	93.78±0.6	95.21±0.9	96.31±1.0
BD7	0	80.12±0.6	81.17±1.2	82.59±1.5	84.23±1.2	90.52±1.3	92.15±0.5	95.65±1.2	96.25±1.2
BD8	0	76.25±1.7	78.26±1.7	80.45±1.1	85.12±1.4	87.96±1.5	89.23±0.4	91.21±1.1	96.66±1.3

BD9	0	82.32±1.7	85.23±2.0	87.25±1.3	88.21±1.5	92.14±1.4	92.99±0.9	95.23±1.2	96.78±1.2
B910	0	85.23±1.8	87.23±2.1	88.12±1.7	89.34±1.6	91.10±1.2	92.45±0.8	94.25±1.3	96.8±1.4
BD11	0	75.21±1.5	80.32±2.2	81.21±1.5	83.21±1.2	87.24±1.5	91.24±1.2	92.45±1.4	97.45±1.5
BD12	0	82.14±2.3	7.25±2.2	89.74±1.6	90.52±1.7	92.15±1.5	93.25±1.3	94.87±1.3	97.63±1.5
BD13	0	85.21±1.7	7.24±2.3	90.21±1.7	94.51±1.8	96.21±1.6	97.24±1.4	98.89±1.5	99.12±1.4
BD14	0	91.65±2.3	2.65±2.5	94.32±2.2	95.24±2.3	95.58±1.4	97.58±1.3	98.36±1.5	99.46±1.3
BD15	0	90.21±2.1	0.65±2.1	92.65±2.1	94.21±2.2	6.58±1.5	97.89±1.5	98.25±1.4	99.25±1.2

Table 4.26: Comparison of dissolution profile of various SNEDDS of benidipine formulation with pure drug

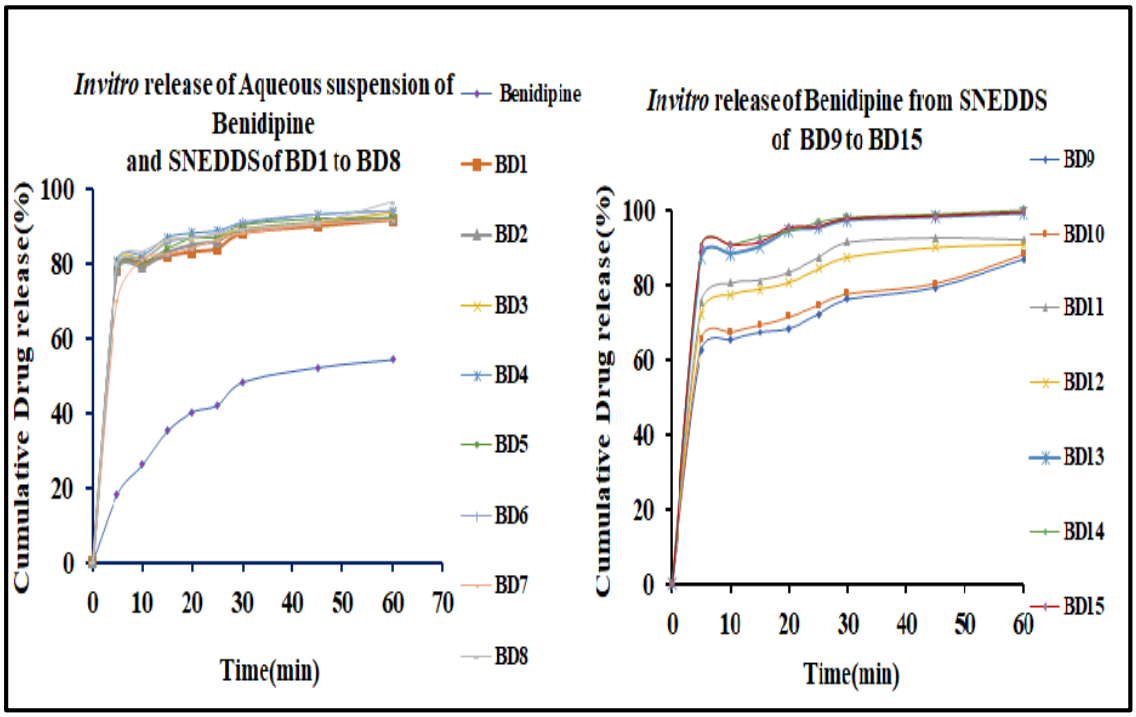

Figure 4.36: In-vitro drug released study of pure Benidipine and developed SNEDDS batches of Benidipine

When developing SNEDDS, surfactants and co-surfactants were utilized, which may spontaneously emulsify the oil into significantly smaller droplets (less than 500 nm) while providing a large surface area for drug release on objects. Compared to the pure drug's release profile of 42.40% and the marketed product's dissolution rate of 49.12%, all generated batches had a drug release rate of about 90% within 60 minutes.

It might be hypothesized that the SNEDDS formulation resulted in spontaneous production of a nanoemulsion with a very small droplet size, which facilitated a quicker

rate of drug release into the aqueous phase, significantly faster than that of plain Benidipine drug powder and marketed formulation. Thus, this enhanced availability of dissolved benidipine from the SNEDDS formulation could lead to better absorption and higher oral bioavailability [48].

From these findings, BD14 was chosen for optimization and future exploration owing to its smaller droplet size, reduced emulsification time, maximum drug release, and maximum transmittance.

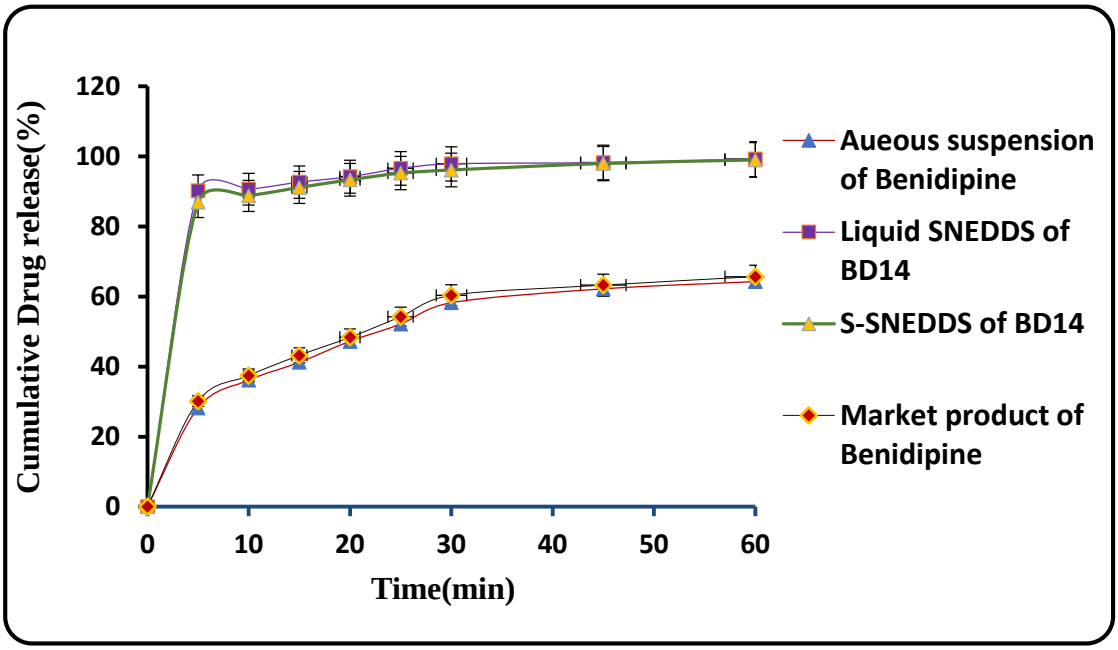

Figure 4.37: Comparative in vitro drug release studies of BD aqueous suspension, BD-L-SNEDDS, and BD marketed product

4.4B. Assessment of BD with TEL-Loaded Optimum Formulation

(I) Assessment and Changes in Opposition

The visual clarity of the optimized liquid SNEDDS (BT11)) containing the drug was evaluated. It was proved to be uniform and optical clean with a light blue color. It did not reveal any indication of precipitation or manufacture process.

(II) Robustness to dilution

The potential effects of different dilution ratios, including stability under varied pH conditions, were examined in vitro to verify SNEDDS emulsion stability following oral

administration and to minimize burst release of the integrated drug. Since SNEDDS are the pre-concentrates that simply develop into nanoemulsions after dilution, phase separation obstacles occur when the formulation experiences infinite dilution in the GI fluids. A drug that possesses pH-dependent solubility may precipitate as a result of these pH shifts. In order to check this, optimum liquid SNEDDS (BT11) was diluted 10, 100, 250, 500, and 900 times by volume in 0.1N HCl and phosphate buffer pH 6.8. There was zero evidence of phase separation in any of the formulations evaluated [45].No significant difference was noticed in the transmission of the produced nanoemulsion when diluted with 0.1N HCl, phosphate buffer pH 6.8, and saline phosphate buffer pH 7.4. This defined the ability of the enhanced SNEDDS formulation to form nanoemulsions at different physiological pH values.

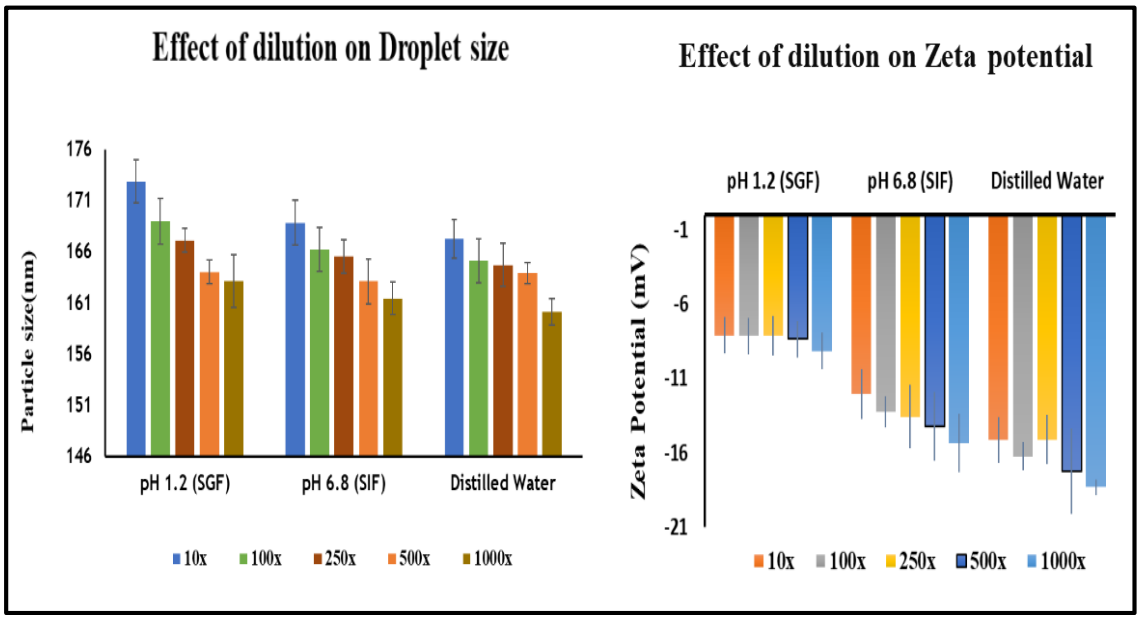

Figure 4.38: Effect of Dilution on Droplet size and Zeta potential in S-SNEDDS of BT11

Interestingly, as shown in Figure 4.38, a reduction in droplet size was observed with the change in pH as well as when the dilution factor increased from 10 to 500 times. It was observed that increasing the availability of surfactants at the oil-water interface increased droplet dispersion, which lowered the dilution factor to a given level and resulted in the generation of uniform and smaller droplets. A small rise in zeta potential has been noticed along with the change in pH and after increasing the dilution factor from 10 to 900 times. Despite this, the changes showed the integrity of SNEDDS in nanoform when the gastrointestinal tract's volume and pH changed (GIT). This proved

the capacity of the enhanced SNEDDS formulation to create nanoemulsions at different physiological pH [46].

(III) Drop size and Zeta potential

The nanoemulsion particle size serves a vital role in the self-emulsification process. The medication is released through the optimized self-nanoemulsifying drug delivery system (SNEDDS) formulation is significantly influenced by the size of the droplets in the nanoemulsion. The nanoscale droplets produce an increased interfacial area for drug release.

Formulation	Average ±SD (n=3)				
	Polydispersity Index	Cloud point(°C)	Zeta potential (mv)	Refractive index	Viscosity (Centi poise)
BT1	0.424	75.6±1.7	-24.26	1.798	190±3.6
BT2	0.332	72.8±2.2	-21.21	1.765	185±2.4
BT3	0.454	85.6±2.6	-23.24	1.745	180±2.8
BT4	0.258	83.7±2.8	-22.32	1.752	175±2.9
BT5	0.264	75.8±1.7	-20.65	1.742	178±3.4
BT6	0.425	73.2±1.9	-28.39	1.761	170±2.6
BT7	0.331	73.9±1.7	-22.14	1.762	184±2.8
BT8	0.256	69.7±1.1	-24.21	1.789	183±3.3
BT9	0.260	74.4±1.5	-24.36	1.739	196±2.5
BT10	0.265	68.7±1.4	-23.91	1.773	174±3.1
BT11	0.226	79.6±1.7	-17.20	1.742	187±3.2
BT12	0.421	64.2±1.5	-25.96	1.745	172±2.5
BT13	0.325	71.5±2.2	-22.62	1.761	185±2.7
BT14	0.299	68.9±1.7	-24.36	1.746	172±2.3
BT15	0.305	64.5±1.7	-23.63	1.734	179±2.8

Table 4.27: Evaluation of L-SNEDDS BT1 to BT15 Formulation of design

The acceptable range for defining nanoemulsion (10 nm to 200 nm) mostly lies within the average drop size of the nanoemulsion produced from the optimized SNEDDS formulation, including the drug, with a measurement around 176.24±1.3nm. According to the data provided in Table 4.27, the PDI value varied from 0.226 to 0.365, indicating a narrow dispersion of reductions. Smaller droplet sizes encourage drugs to flow across biological membranes, whereas oil droplets with a negative charge readily penetrate the charged mucus layer, enhancing drug bioavailability. The previously mentioned

qualities have been specifically identified as beneficial in the advancement of SNEDDS [53, 54].

The nanoemulsion showed a zeta potential ranging from -17.20 mV to -28.39 mV, as stated in Table 4.26 and depicted in Figure 4.39, which proved its stability. Zeta potential relies on the kind of surfactant employed in formulation. In BD with TEL-SNEEDS, non-ionic surfactant was utilized, and consequently, zeta potential was low. The Zeta Potential (ZP) readings were always negative across all formulations. This may be related to the composition of the oil-in-water (o/w) emulsion, which includes BD with TEL-SNEEDS. The negatively charged molecules on the surface of the emulsion indicate the existence of fatty acid esters in the oil phase. The presence of negative charges resulted in repulsive interactions between the nanoemulsion droplets, suggesting the physical stability of the formulations. This stability hindered the droplets from blending or breaking into separate phases, resulting in the clean and transparent look of the formulations [55].

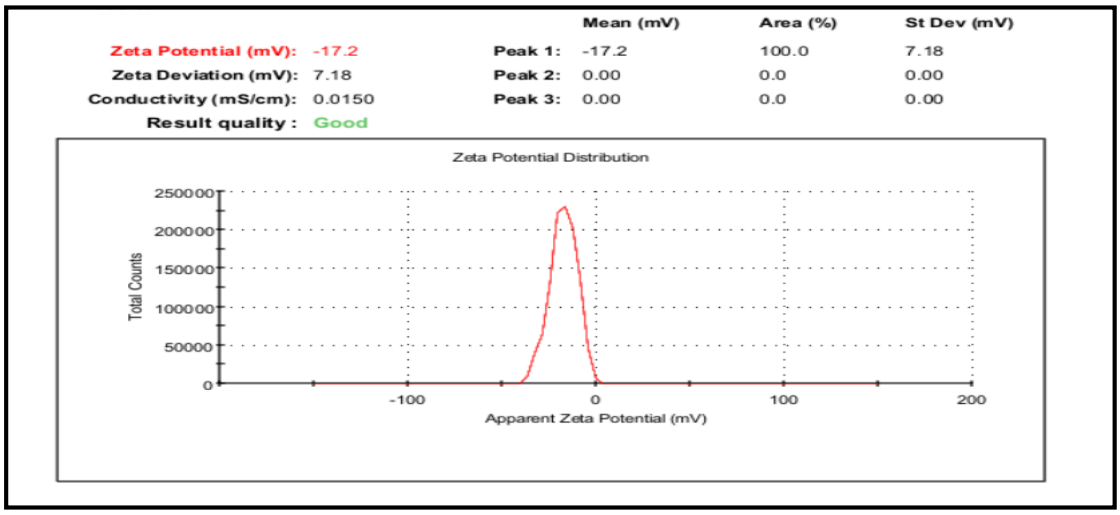

Figure 4.39: Zeta potential of optimized liquid SNEDDS of Benidipine with Telmisartan BT11

(IV) Transmittance Test

Emulsification of liquid SNEDDS preconcentrates resulted in a clear dispersion with a high percentage of transmittance (%T) and a small droplet size. The percent transmittance ranges from 86.50±0.95% to 99.60±0.70%. An almost 100% transmittance proposed a clean SNEDDS dispersion with nanoscale droplets, which is a sign of a fast and reproducible emulsification process.

(IV) Cloud Point Measurement

The cloud point temperature is the temperature above which the micelles produced in the aqueous solution begin to expand and distort. A further increase in temperature presumably leads to a complete reversal of the system: water gets solubilized in micelles and oil becomes an exterior phase, resulting in the precipitation of the solubilized drug. The cloud point temperature of the optimized formulation was recorded at 79.6±1.7 °C, which is much higher than the typical body temperature of 37 °C. This shows that the newly developed formulation was stable in vivo at physiological temperature and displayed no phase separation when stored at ambient temperature or in the GI tract [47].

(V) Determination of the Refractive Index

The negative charges caused repulsive interactions between the nanoemulsion droplets, which indicated the physical stability of the formulations in terms of their absence of droplet combination or phase separation that resulted in the clear and translucent appearances of the formulations. The mean RI of the optimized formulations was determined to be 1.742 ± 0.14, which indicates that the nanoemulsion is isotropic.

(VI) Thermodynamic Stability Investigations

A thermodynamic stability analysis was carried out to assess the effects of fluctuations in temperature on SNEDDS formulations and discover any signs of phase separation. The influence of heating and cooling, centrifugation, and freeze-thaw cycling on the phase separation of nanoemulsions and the precipitation of drugs is depicted in Table 4.28. Each of the three accelerated tests have been carried out to examine the stability of the nanoemulsion under stress conditions. Batches that did not display any drug precipitation or phase separation after the heating and cooling cycles, as well as centrifugation, showed their stable nature. Similarly, batches that survived freeze-thaw cycling were found to be reconstituted without any phase separation or drug precipitation after exposure to freeze-thaw cycling.

Upon evaluation at various temperatures, it was observed that the optimized formulation, BT11, and almost all batches were stable without any signs of drug

precipitation or phase separation. However, BT3 and BD12 exhibited phase separation and failed the freeze-thaw cycling test.

It was found that all formulations passed the three tests. A lack of proof of phase separation, flocculation, or precipitation was observed in the formulation. All formulations are stable at each temperature.

So we finally concluded that prepared SNEDDS is thermodynamically stable, keeping a specific concentration of oil, surfactant, and water with no phase partitions, creaming, or breaking [48].

(VII) Drug Content

The percentage drug content in the optimal dosage form BT11 was 99.10±0.29% w/w for BD and 99.25±0.35% w/w for TEL, suggesting continuous drug dispersion in the SNEDDS formulation.

Formulation	Heating Cooling Cycle	Centrifugation	Freeze thaw cycle
BT1	Pass	Pass	Pass
BT2	Pass	Pass	Pass
BT3	Pass	Pass	Fail
BT4	Pass	Pass	Pass
BT5	Pass	Pass	Pass
BT6	Pass	Pass	Pass
BT7	Pass	Pass	Pass
BT8	Pass	Pass	Pass
BT9	Pass	Pass	Pass
BT10	Pass	Pass	Pass
BT11	Pass	Pass	Pass
BT12	Pass	Pass	Fail
BT13	Pass	Pass	Pass
BT14	Pass	Pass	Pass
BT15	Pass	Pass	Pass

Table 4.28: Thermodynamic stability investigations of various Benidipine with Telmisartan SNEDDS formulations

(VIII) Conductivity Test

Conductivity tests are utilized to predict the kind of nanoemulsion formed during dilution, techniques of evaluating whether a nanoemulsion is oil-continuous or water-continuous, as well as a means of monitoring phase inversion processes. The electrical conductivity of the optimum BD with TEL-loaded SNEDDS formulations BT11 was examined. The conductivity of o/w emulsions in BD with TEL-loaded systems was reported to be 0.0150 µS/cm.

(IX) Surface Morphology via TEM

The microscopy of the improved SNEDDS formulation BT11 was studied using TEM micrographs. TEM studies confirmed the improved SNEDDS formulation displayed a spherical shape and homogeneous size with no evidence of droplet aggregation, as represented in Figure 4.40. These findings link with DLS data that confirms the authenticating of SNEDDS formulations. The nanodroplets looked dark. These studies revealed the spontaneous creation of a nanometer-range nanoemulsifying system.

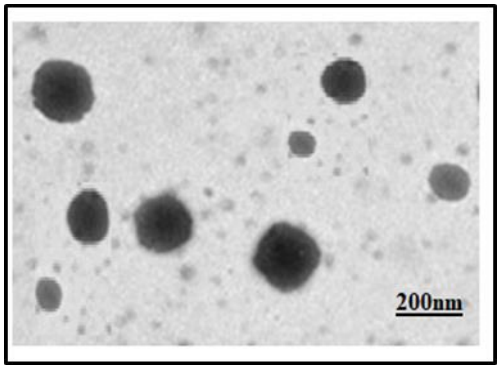

Figure 4.40: TEM images of the optimized BD with TEL-loaded SNEDDS

(X) In Vitro drug release Study

The benidipine with telmisartan release of the optimized batch (BT11) has been compared with that of pure drug powder and the commercially available tablet Benidip T 4 mg/40 mg Tab (Precia Pharma Pvt. Ltd.) in Thane, India. Figure 4.41 demonstrates the in-vitro release of drug behavior of BD with TEL-SNEDDS. The findings showed that BD with TEL-SNEDDS had a greater percentage of drug release during the initial stages of the trial as compared to BD with TEL pure drugs. During the first hour of the examination, all the BD with TEL SNEDDS batches released BD and TEL more than 95% of the drug, as contrasted to the BD with TEL pure drug, which released simply 48.7% of the BD and 50.1% for TEL.

All developed SNEDDS formulations continued to release the medication slowly until the steady state was established at 1 h. By that time, the cumulative drug release for formulations BT4, BT7, BT9, BT11, BT13, and BT15 was >99%, while for formulations BT1, BT2, BT3, BT5, BT8, BT10, BT12, and BT14, it was> 98%.

From these data, BT11 was selected for optimization and future exploration due to its smaller droplet size, shorter emulsification time, most significant drug release, and maximum transmittance.

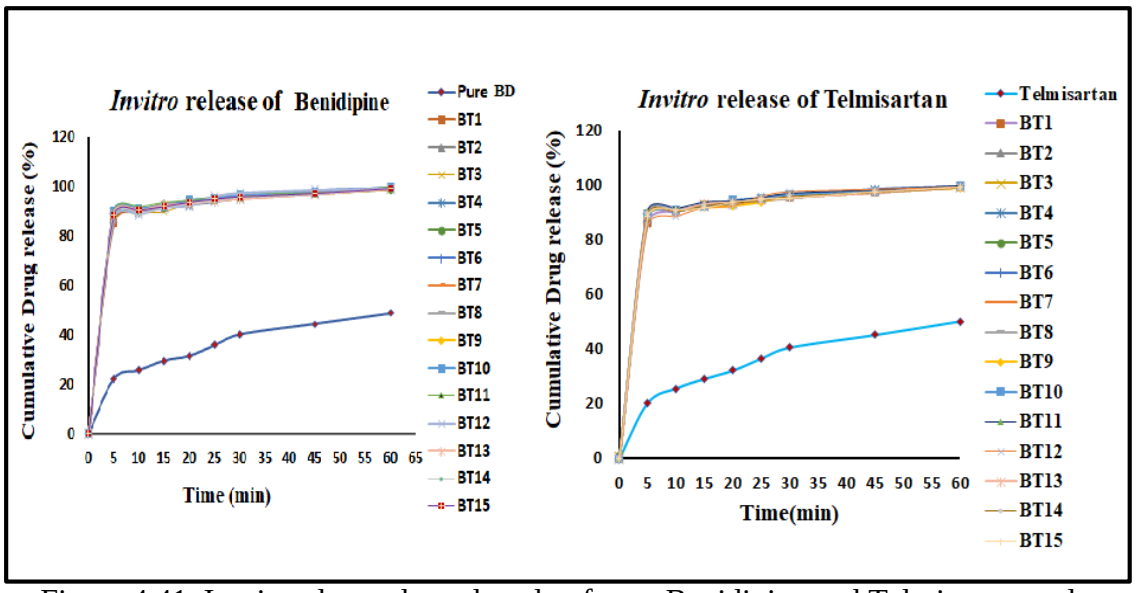

Figure 4.41: In-vitro drug released study of pure Benidipine and Telmisartan and developed SNEDDS batches of Benidipine with Telmisartan

(XI) Comparison of in vitro drug release between optimized batch BT11, pure drug powder, and marketed product

The benidipine with telmisartan release of the optimized batch (BT11) has been compared with that of pure drug powder BD with TEL and the marketed product. The marketed product was (Precia Pharma Pvt. Ltd.) in Thane, India. Figure 4.42 shows the in-vitro release of drugs behavior of BD with TEL-SNEDDS, BD with TEL pure drug, and the market formulation. The data have shown that BD with TEL-SNEDDS had a greater proportion of drug release during the initial hours of the experiment as compared to BD with TEL pure drugs as well as market formulation. It's possible that the more considerable release of medicines from the targeted batches has been made possible

through the SNEDDS formulation's potential to release the drug directly in its solubilized form in a dissolving medium [47].

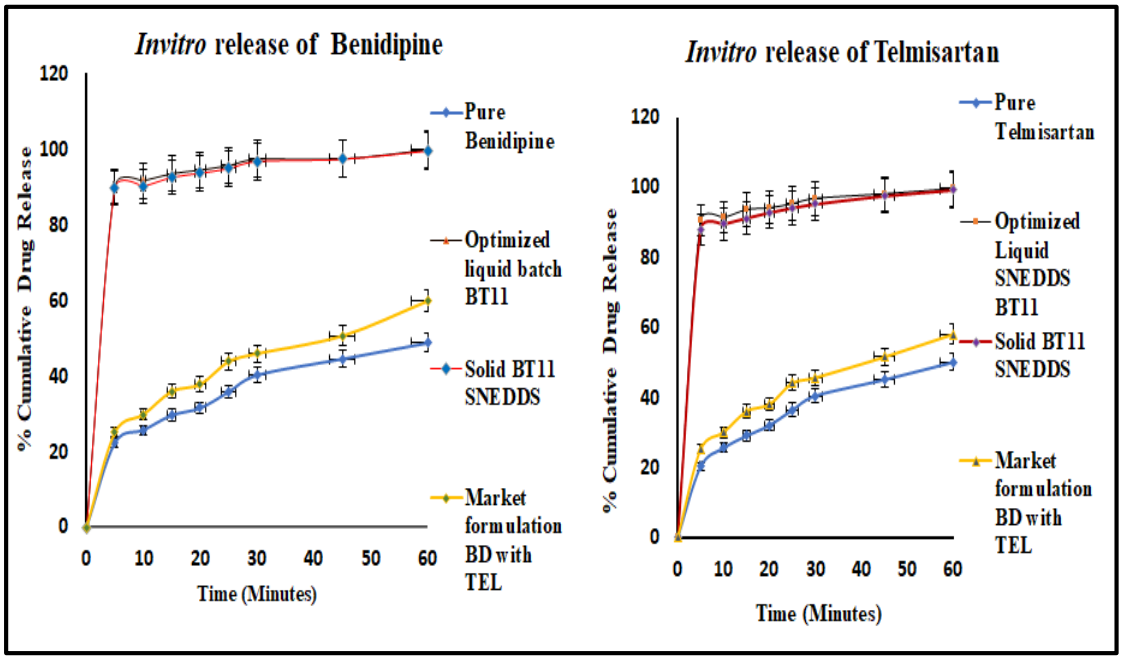

Figure 4.42: Comparative in vitro drug release studies of Benidipine with Telmisartan pure drug, Benidipine with Telmisartan liquid SNEDDS, BT11, and Market formulation (Benidip T 4 mg/40 mg Tab)

When developing SNEDDS, surfactants and co-surfactants were utilized, which may spontaneously emulsify the oil into significantly smaller droplets (less than 500 nm) while providing a large surface area for drug release on objects. During the first hour of the investigation, all the BD with TEL SNEDDS batches released BD and TEL more than 95% of the drug, as opposed to the BD with TEL pure drug, which released only 48.7% of the BD, and 50.1% for TEL. A similar approach to market formulation demonstrated a release of 59.8% for BD and 58.1% for TEL.

From these findings, BT11 was chosen for optimization and future exploration owing to its smaller droplet size, reduced emulsification time, maximum drug release, and maximum transmittance.

4.5 Preparation of S- SNEDDS

The most effective liquid SNEDDS for Benidipine-BD14 and for benidipine with Telmisartan-BT11 formulation was effectively converted into a solid SNEDDS in the form of a free-flowing powder by adsorbing it onto a solid carrier. This approach is

known for its high lipid absorption capacity, reaching up to 80% [41, 42]. So, picking the right solid carrier material is very important for creating a solid SNEDDS formulation that works very well for both BD and BD with TEL.

The commonly utilized porous solid carriers are Aerosil 200, Aeroperl 300, and Neusilin US2. During the initial stage of our studies for both liquid SNEDDS of BD14 and BT11, we first analyzed solid carriers to determine their capacity for adsorbing oil. This was done to find the most appropriate solid carrier according to the ratio of SNEDDS and their oil adsorption characteristics. According to the data shown in Table 4.29 for BD and Table 4.30 for BD with TEL, the drug formulation L-SNEDDS: adsorbent (1:1.5) had the smoothest and driest appearance. It was observed to have excellent flow characteristics and flow rate in Neusilin US2, in comparison to the L-SNEDDS adsorbent formulations with ratios of 1:1 and 1:2.

Solid SNEDDSs were further optimized, emphasizing their micromeritic properties, including bulk density, tapped density, Hausner's ratio (HR), Carr's index (CI), and angle of repose (AR)AR, CI, HR, and flow rate, in addition to self-emulsification efficacy.

Formulation No.	**L-SNEDDS Composition**	**Carriers**	**L-SNEDDS : Adsorbent**	**Appearance**
S-SNEDDS-1	4mg BD in 1 g of BD14 (30% Labrafil M2125 Cs, 45% Kolliphor EL and 33.4% Transcutol P)	Aerosil 200	1:1	Caking and Wet
S-SNEDDS-2			1:1.5	Caking and Wet
S-SNEDDS-3			1:2	Fine
S-SNEDDS-4		Neusilin US2	1:1	Fine and Dry
S-SNEDDS-5			1:1.5	Fine and Dry
S-SNEDDS-6			1:2	Dusty
S-SNEDDS-7		Aeroperl 300	1:1	Fine
S-SNEDDS-8			1:1.5	Fine
S-SNEDDS-9			1:2	Fine and Dry

Table 4.29: Solidification of Optimized Liquid SNEDDS of Benidipine BD14
S-SNEDDS: Solid –Self Nanoemulsifying Drug Delivery System

Based on the details that have been obtained from the parameters affecting flow table 4.31 of the solid SNEDDS formulation for BD and Table 4.32 for BD with TEL, powder flow can be regarded as acceptable, according to the European Pharmacopeia.

Formulation No.	L-SNEDDS Composition	Carriers	L-SNEDDS : Adsorbent	Appearance
S-SNEDDS-1	4mg BD with 40 mg TEL in 1 g of BT11 (60% Eucalyptus oil, 35% Kolliphor EL and 10% Transcutol P)	Aerosil 200	1:1	Caking and Wet
S-SNEDDS-2			1:1.5	Caking and Wet
S-SNEDDS-3			1:2	Fine
S-SNEDDS-4		Neusilin US2	1:1	Fine and Dry
S-SNEDDS-5			1:1.5	Fine and Dry
S-SNEDDS-6			1:2	Dusty
S-SNEDDS-7		Aeroperl 300	1:1	Fine
S-SNEDDS-8			1:1.5	Fine and Dry
S-SNEDDS-9			1:2	Fine and Dry

Table 4.30: Solidification of Optimized Liquid SNEDDS of Benidipine with Telmisartan BT11
S-SNEDDS: Solid –Self Nanoemulsifying Drug Delivery System

Formulation No.	Angle of repose (θ)[a]	Carr's index[a]	Hausner's ratio[a]	Flow rate (g/s)[a]	Flowability[a]
S-SNEDDS-1	34.35±1.16	29.94±0.04	1.36±0.06	1.05±0.65	Poor
S-SNEDDS-2	33.12±2.15	28.25±1.02	1.32±1.11	1.26 ±0.21	Poor
S-SNEDDS-3	32.35±1.17	28.94±1.01	1.34±0.04	1.65 ±0.02	Passable
S-SNEDDS-4	24.31±2.21	16.34±0.21	1.22±0.05	2.15±0.34	Excellent
S-SNEDDS-5	22.11±1.98	16.21±0.27	1.21±0.01	2.50 ±0.12	Excellent
S-SNEDDS-6	24.07±1.06	16.24±0.25	1.33±0.11	2.30±0.13	Good
S-SNEDDS-7	26.48±0.89	22.67±0.65	1.66±1.01	1.45±0.21	Good
S-SNEDDS-8	24.51±0.45	22.18±0.89	1.68±1.20	1.88±0.05	Good
S-SNEDDS-9	24.00±0.42	23.92±0.78	1.70±0.02	1.38±0.23	Passable

Table 4.31: Micromeritic Properties of S-SNEDDS of BD14
[a]All the values are in mean ±SD (n=3),
S-SNEDDS: Solid –Self Nanoemulsifying Drug Delivery System

Formulation No.	Angle of repose (θ)[a]	Carr's index[a]	Hausner's ratio[a]	Flow rate (g/s)[a]	Flowability[a]
S-SNEDDS-1	35.10±1.10	29.12±0.14	1.34±0.06	1.15±0.65	Poor
S-SNEDDS-2	33.30±2.20	28.57±1.32	1.33±1.13	1.56 ±0.21	Poor
S-SNEDDS-3	32.08±1.58	28.51±1.41	1.32±0.06	1.68 ±0.02	Passable
S-SNEDDS-4	24.86±2.21	16.87±0.15	1.20±0.07	2.35±0.34	Excellent
S-SNEDDS-5	22.58±1.98	16.41±0.50	1.23±0.05	2.40 ±0.12	Excellent
S-SNEDDS-6	24.97±1.43	16.20±0.35	1.36±0.09	2.15±0.13	Good
S-SNEDDS-7	26.23±0.54	22.36±0.56	1.64±1.12	1.95±0.21	Good
S-SNEDDS-8	24.36±0.41	22.05±0.51	1.66±1.17	1.98±0.05	Good
S-SNEDDS-9	24.27±0.35	23.92±0.62	1.67±0.07	1.28±0.23	Passable

Table 4.32: Micromeritic Properties of S-SNEDDS of BT11
[a]All the values are in mean ±SD (n=3),
S-SNEDDS: Solid –Self Nanoemulsifying Drug Delivery System.

Conclusion: Therefore, Neusilin US2, L-SNEDDS: Adsorbent (1:1.5), was chosen as the carrier for pores in the mixture with excellent flow rate, flow ability, highest drug content, and drug release in order to facilitate further study of BD14 and BT11.

4.5.1. Characterization of S-SNEDDS of BD and BD with TEL

A) Characterization of S-SNEDDS of BD

(I) Fourier Transform Infrared Spectroscopy (FTIR) Study

The FTIR spectra of Neusilin US2, BD, a physical mixture of Neusilin US2 and BD, and S- SNEDDS of BD14 are presented in Figure 4.43. The S-SNEDDS of BD14 displayed the typical peaks of both BD and Neusilin US2, suggesting that the drug was still present in the mixture and had not suffered any molecular modifications or interactions with carriers (Labrafil M2125 CS, Kolliphor EL, Transcutol P, and Neusilin US2).

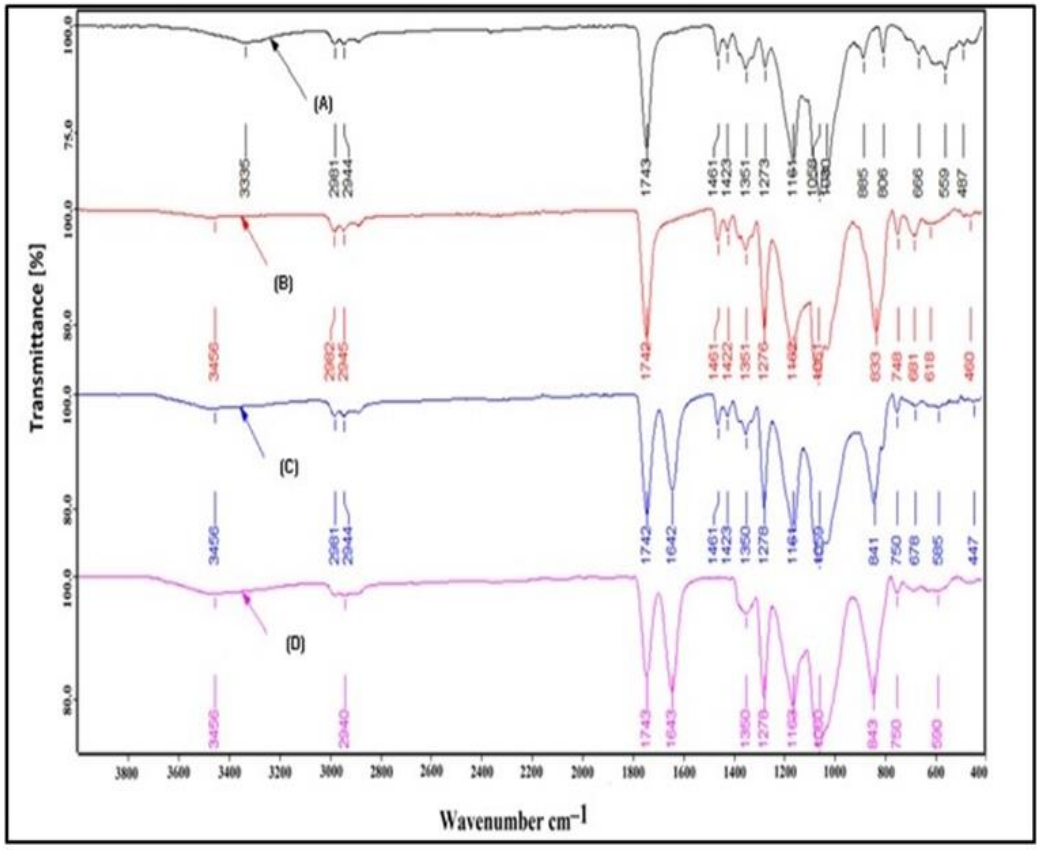

Figure 4.43: FTIR spectra of (A) Neusilin US2, (B) physical mixture of BD and Neusilin US2, (C) BD, and (D) S-SNEDDS BD14

(II) DSC

A significant endothermic peak was found in the pure BD DSC thermogram at exactly 226.02°C, which correlates to the melting point of the mater as depicted in Figure 4.44. In the specific case of S-SNEDDS BD14, the drug's endothermic peak was 106.21°C. The ability of SNEDDS to prevent BD crystallization and solubilization may be associated with BD's higher melting behavior. It may subsequently appear to transition from a crystalline to an amorphous state, which may significantly improve water solubility [92]. However, no unexpected peak of the drug was detected in S-SNEDDS, which can be interpreted as shifting from crystalline to amorphous form, which might ultimately result in an improvement in water solubility. The absence of any new peaks in S-SNEDDS shows the compatibility of excipients and BD in the present formulation.

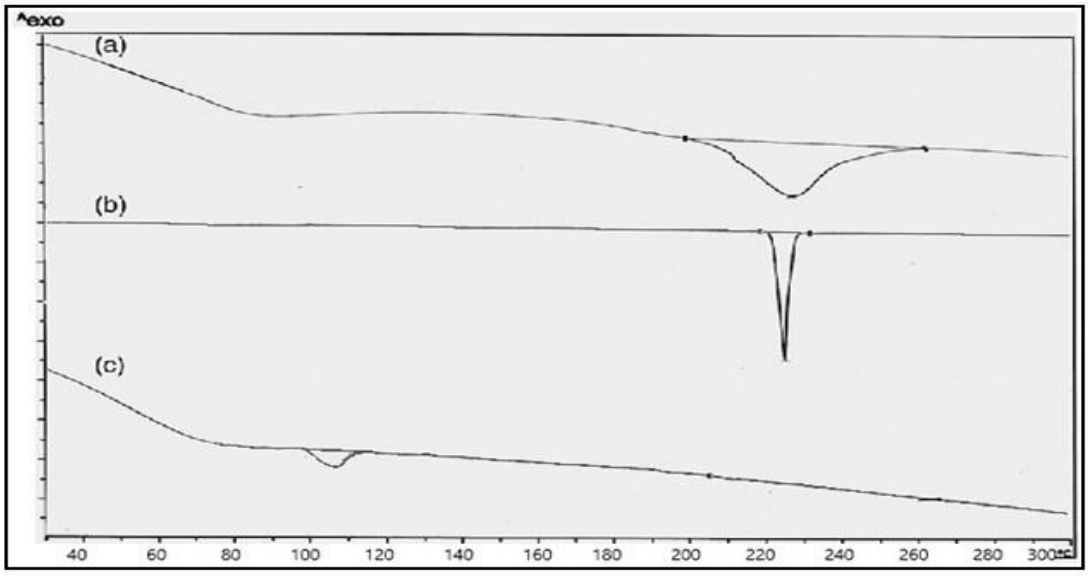

Figure 4.44: DSC Thermogram of (a) Neusilin US2, (b) BD, and (c) optimized S-SNEDDS BD14

(III) Morphology Evaluation of SSNEDDS

SEM images of BD (Figure 4.45A) and S-SNEDDS BD14 can be observed in Figure 4.45B. Since S-SNEDDS of BD had smooth surface particles that aggregated to create larger particles without crystalline morphology, the drug showed up in SEM images as tiny, irregularly shaped particles with a rough exterior surface. This revealed that L-SNEDDS could have had significant effects on the Neusilin US2 surface.

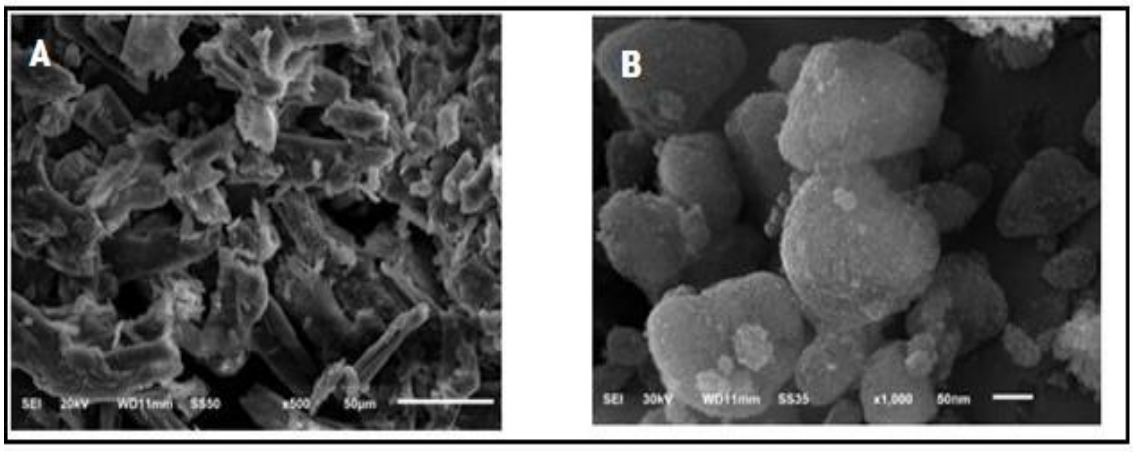

Figure 4.45: SEM image of (A) Pure drug and BD (B) S-SNEDDS of BD14

(IV) PXRD

Figure 4.46 represents the X-ray diffraction patterns of BD and S-SNEDDS. X-ray diffraction patterns of benidipine displayed prominent and powerful peaks notably at 2θ diffraction angles of 9.9819°, 17.2137°, 18.6489°, 19.8632°, 21.5225°, 23.8034°,

25.5001°, 27.7464° and 29.1848°. The findings demonstrated the lack of prominent peaks showing crystalline BD in the optimal formula (S-SNEDD), suggesting that the drug was in an amorphous or disordered crystalline phase in the oily inner core. The XRPD of the S-SNEDD formula exhibited only three prominent diffraction peaks at 2θ angles of 15.6217°, 20.5113°, and 22.5252°. The drug's shift from its original crystalline state to an amorphous or molecularly dispersed state in the S-SNEDDS formulation, as depicted in Figure 4.46, has been validated by the lack of significant peak representations of such a crystallized nature in the BD of the S-SNEDDS diffractogram.

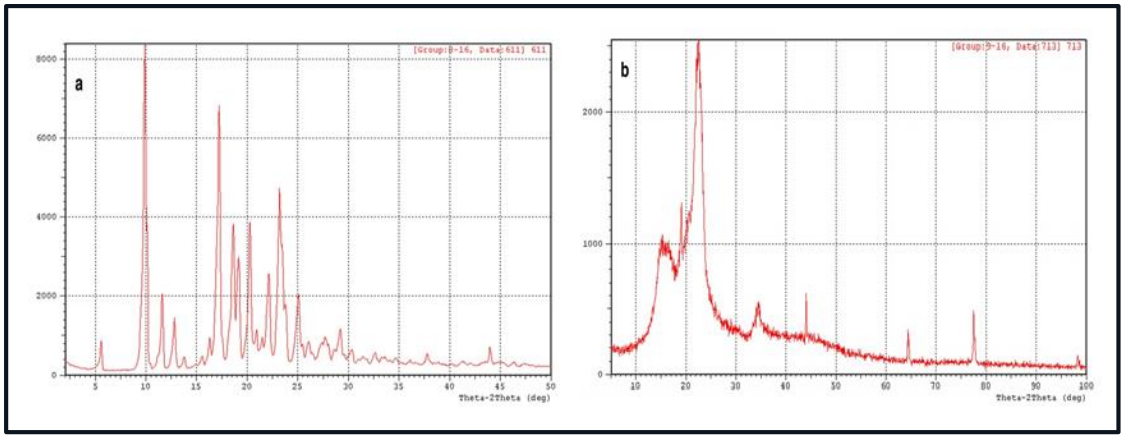

Figure 4.46: XRD patterns of (A) BD and (B) S-SNEDDS BD14

(V) In Vitro Characterization of S-SNEDDS of BD

Research was done to find out how much the composition of BD as S-SNEDDS may speed up the process of dissolution. When S-SNEDDS are exposed to the dissolving fluid, their solid structure dissolves, and L-SNEDDS are capable of being released from adsorbent gaps. L-SNEDDS were subsequently freely dispersed into tiny globules with large interfacial areas, which displayed enhanced solubilization [90]. In contrast to the percentages of 58.80% and 60.15% for the pure drug and a commercial specimen of BD that Figure 4.47 indicated, L-SNEDDS and S-SNEDDS showed that BD released more than 85% of its contents after 15 minutes and 100% after 60 minutes (f2< 50).

The drug released in liquid SNEDDS in 0.1 N HCl during the first 5 minutes was more than from the S-SNEDDS formulation. This delay in drug release for S-SNEDDS might be attribute to the desorption process from the adsorbed carriers. The capacity of the SNEDDS formulation to release the drug directly in its solubilized state in a dissolving fluid may have attributed to the in-creased release of drugs from the optimized batches

[91]. The release of drug kinetics of L-SNEDDS of BD 14 and S-SNEDDS of BD14 follow 1st-order kinetics, which suggests the drug release from the porous matrix corresponds to the quantity of drug remaining in its interior [91].

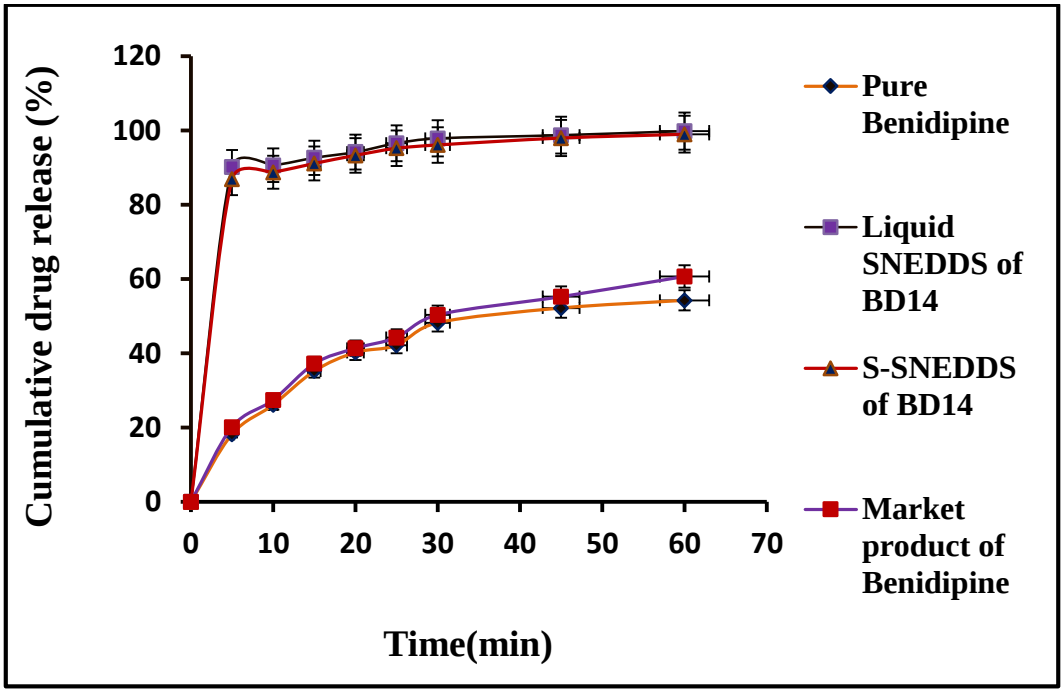

Figure 4.47: Comparative in vitro drug release studies of BD aqueous suspension, BD-L-SNEDDS, BD14-S-SNEDDS, and BD marketed product

B) Characterization of S-SNEDDS of BD with TEL

(I) Fourier Transform Infrared Spectroscopy (FTIR) Study

The FTIR spectra of Neusilin US2, a physical combination of Neusilin US2, BD, and TEL, and S-SNEDDS of BT11 are displayed in Figure 4.48. The S-SNEDDS of BT11 displayed the typical peaks of both BD, TEL, and Neusilin US2, demonstrating that the drug continued to exist in the combination and had not suffered any molecular modifications or interactions with carriers (Eucalyptus oil, Kolliphor EL, Transcutol P, and Neusilin US2). The minor change in some of the peaks could be caused by the overlapping of the excipients' peaks. These results demonstrate the lack of compatibility issues between BD, TEL, and other chemicals utilized for the creation of prepared S-SNEDDS.

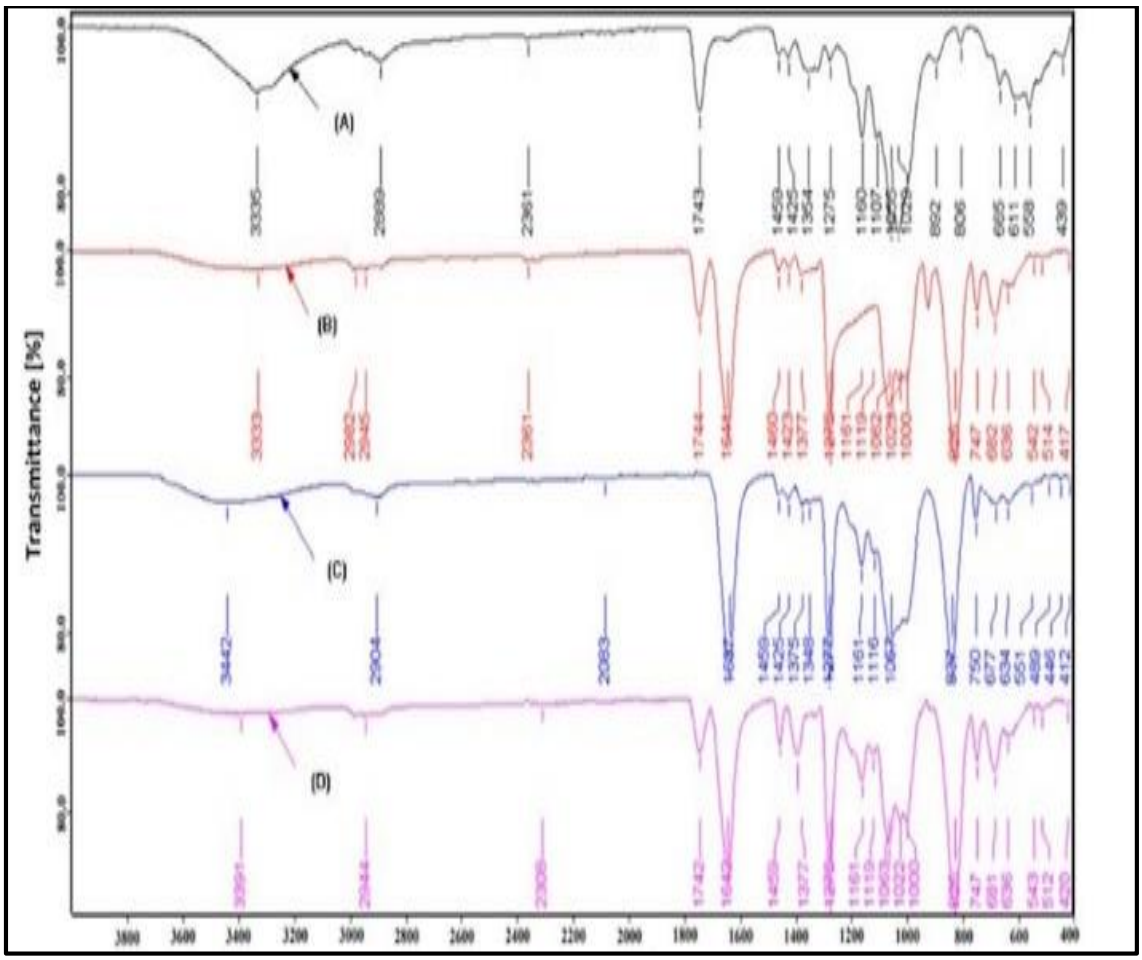

Figure 4.48: FTIR spectra of (A) Neusilin US2, (B) Physical mixture of Benidipine, Telmisartan and Neusilin US2, (C) Benidipine with Telmisartan and (D) S-SNEDDS of Benidipine with Telmisartan

(II) DSC

A thermoanalysis technique employing DSC has been performed to validate the physical characteristics of the drug resulting from distinct orders of molecule conversion from crystalline and amorphous components present within the powder mix. The prominent melting endotherm peak demonstrates the crystalline form of benidipine and telmisartan at 189.08 and 278.10 °C, respectively, as represented in Figure 4.49. Similarly, the physical mixture also revealed an evident drug peak at 184.22 and 273.37 °C, respectively. Still, no unexpected peak of the drug was identified in S-SNEDDS, which could potentially examine as transitioning from crystalline to amorphous form, which could ultimately result in an improvement in water solubility. The absence of any extra peaks in S-SNEDDS demonstrates the compatibility of excipients and BD with TEL in this present formulation [90].

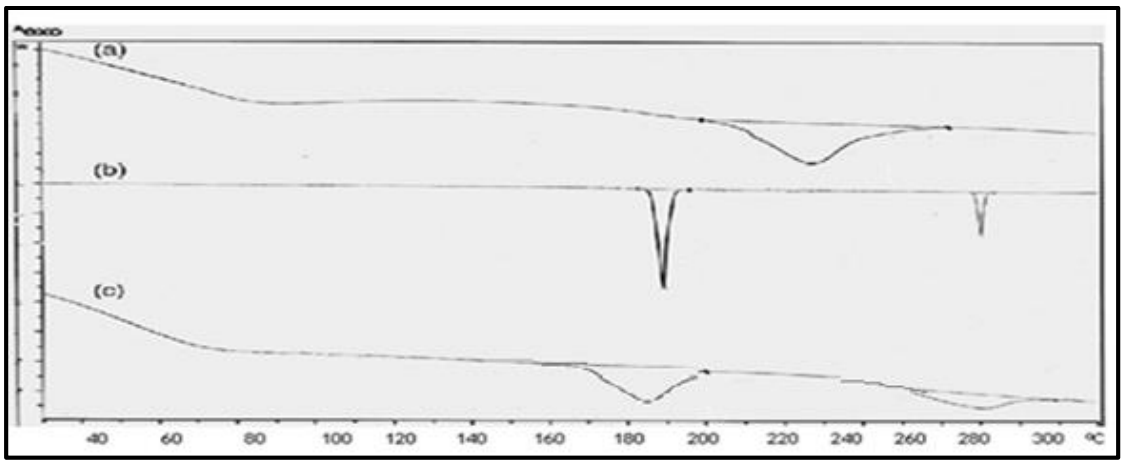

Figure 4.49: DSC Thermogram of (a) Neusilin US2, (b) Benidipine with Telmisartan and (c) Optimized S-SNEDDS of Benidipine with Telmisartan

(III) Morphology Evaluation of S-SNEDDS

SEM Images from of BD with TEL and S-SNEDDS BT11 can be seen in Figure 4.50. BD and TEL developed as irregular rod-form crystals. Liquid SNEDDS was adsorbed on the surface of Neusilin US 2, which is evident as small adsorbed particles on Neusilin US2.

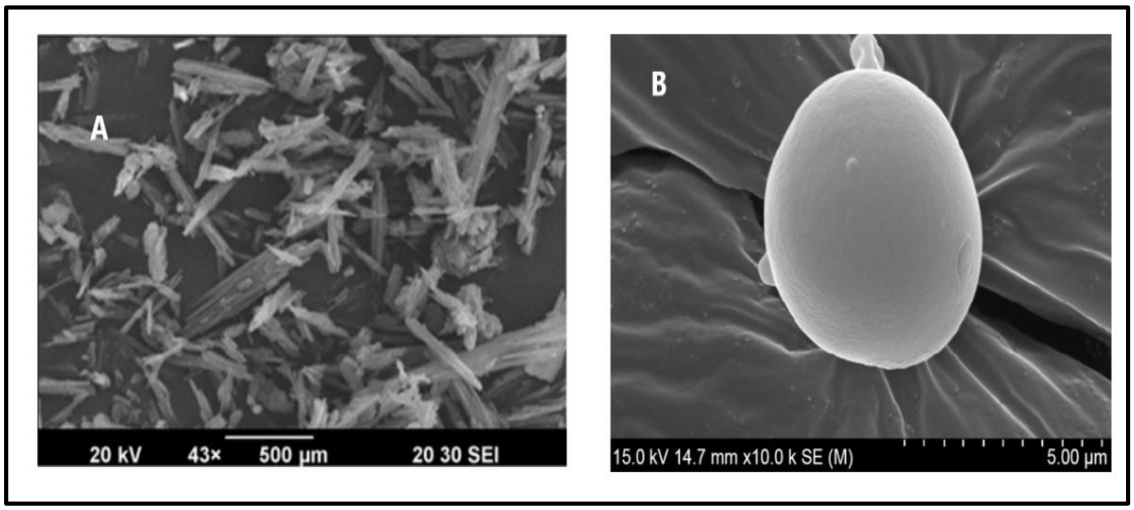

Figure 4.50: SEM image of (A) Pure drug Benidipine with Telmisartan (B) S-SNEDDS of BT11

Irregular crystals of drug BD and TEL have been eliminated in the scanning electron micrograph of S-SNEDDS of BT11, suggesting that the drug is totally dispersed in the S-SNEDDS of BT11 formulation, with neither precipitation nor crystallization. Scattered tiny holes and pores are also noticeable on the matrix structure, which may also enhance the quick entry of water and hence allow for quick dispersion in the gastrointestinal environment [92]. Additionally, the findings reveal full adsorption of

L-SNEDDS into the carrier materials, which has been noticed by the absence of any oil globules in the S-SNEDDS.

(IV) PXRD

X-ray diffraction patterns of benidipine and telmisartan revealed prominent and strong peaks at 2θ diffraction angles of 4.4523°, 8.1456°, 9.9819°, 17.2137°, 18.6489°, 19.8632°, 21.5225°, 23.8034°, 25.5001°, 27.7464°, 29.1848°, 36.2450° ,40.5628°,48.5634° and 54.1674°. The XRPD of the S-SNEDD formula exhibited one sharp diffraction peak at 2θ angles of 20.5113°, as illustrated in Figure 4.51. The results showed that there were no prominent peaks for the BD and TEL drugs in the S-SNEDDS diffractogram, which suggests that the drug was in an amorphous or disordered crystalline phase in the oily core [93].

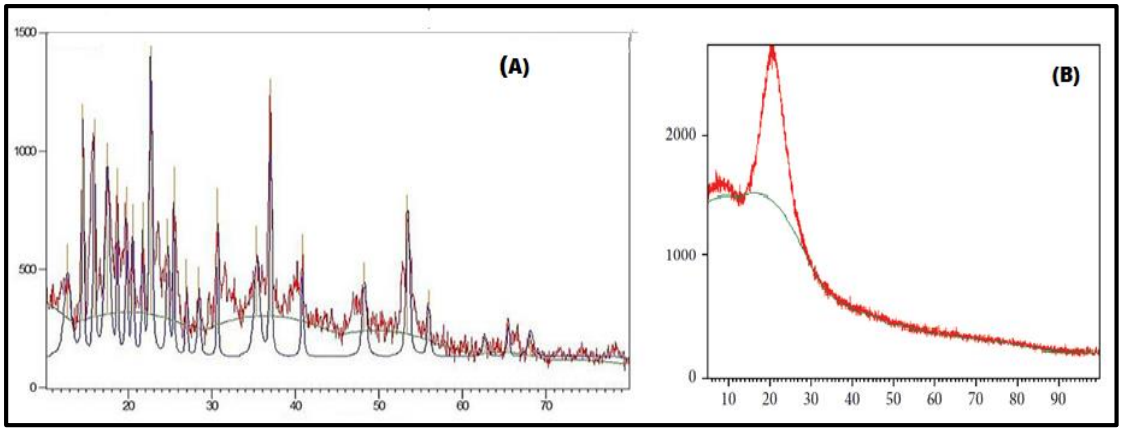

Figure 4.51: PXRD of (A) Drug: Benidipine with Telmisartan (B) S-SNEDDS of BD with TEL

(V) In Vitro Characterization of S-SNEDDS of BD with TEL

Research has been undertaken in order to find out how much the composition of BD with TEL as S-SNEDDS may speed up the process of dissolution. When S-SNEDDS come into contact with the dissolving fluid, their solid structure dissolves, and L-SNEDDS have the potential to be released from adsorbent gaps. L-SNEDDS were then quickly dispersed into small globules with large interfacial surfaces, which demonstrated improved solubilization [93]. In contrast to the percentages of 50.1% and 58.1% for the pure drug BD and a commercial specimen of BD with TEL that Figure 4.52(a) displayed, L-SNEDDS and S-SNEDDS demonstrated that BD released more than 85% of its contents after 15 minutes and 100% after 60 minutes (f2< 50). Similarly,

when compared to the percentages of 48.7% and 59.8% for the pure drug TEL and a commercial specimen of BD with TEL that Figure 4.52 (b) displayed, L-SNEDDS and S-SNEDDS showed that TEL released more than 85% of its contents after 15 minutes and 100% after 60 minutes (f2< 50).

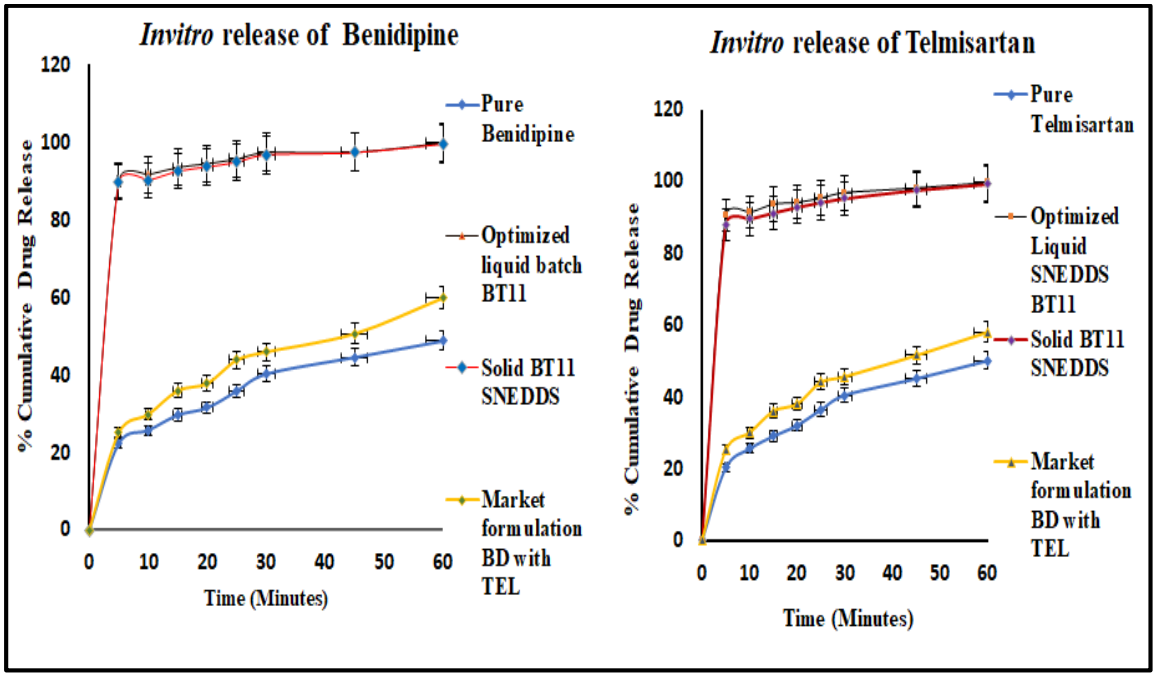

Figure 4.52: Comparative in vitro drug release studies of pure Benidipine, Telmisartan, Benidipine with Telmisartan liquid SNEDDS, BT11, S-SNEDDS of BT11 and Market formulation (Benidip T 4 mg/40 mg Tab)

The amount of drug released in liquid SNEDDS in 0.1 N HCl within the first 5 minutes was greater than the amount released by the S-SNEDDS formulation. This delay in drug release for S-SNEDDS may be attributed to the desorption process from the adsorbed carriers. The potential of the SNEDDS formulation to disperse the medicine successfully in its solubilized state in a dissolving fluid may have contributed to the greater release of drugs throughout the optimized batches [90]. The release of drug kinetics of L-SNEDDS of BT11 and S-SNEDDS of BT11 follows 1st-order kinetics, which suggests the drug release from the porous matrix corresponds to the quantity of drug remained in its interior [91].

4.6. Pharmacodynamics Research of Benidipine and Benidipine with Telmisartan

When fructose delivery was used to induce hypertension in experimental rats, the effectiveness of this induction was evident in Group II, III, IV, V, and VI rats, as demonstrated by the highly significant differences ($p < 0.01$) in blood pressure (BP) in contrast to the negative control Group I, as depicted in Figure 4.39. Group I served as the negative control and displayed normal blood pressure levels. The hypertensive model rats in Group II, administered 66% w/v D-Fructose, showed a substantial rise in systolic blood pressure (SBP) by 40 mmHg, diastolic blood pressure (DBP) by 20 mmHg, and mean arterial pressure (MAP) by 30 mmHg from their basal levels, as we observe from Tables 4.31 and 4.53.

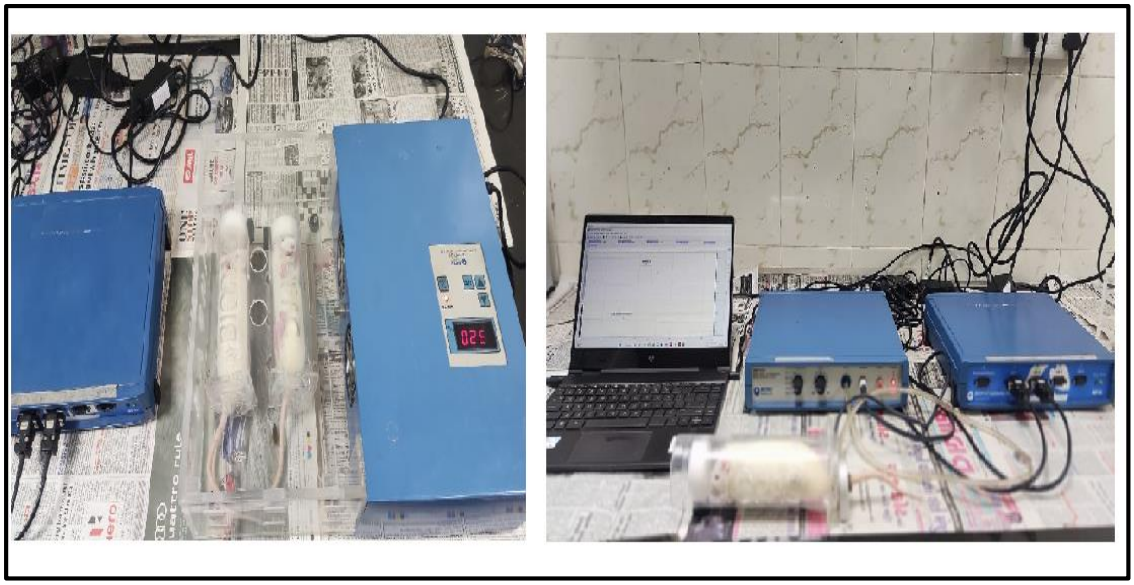

Figure 4.53: Instrumental setup for measurement of Systolic blood pressure, Mean Arterial pressure and Diastolic blood pressure

Conversely, the positive control groups receiving self-emulsifying drug delivery systems (S-SNEDDS) of BD, pure Benidipine as individual drugs, self-emulsifying drug delivery systems (S-SNEDDS) of TEL, and pure Telmisartan as individual drugs, all administered simultaneously with 66% w/v D-Fructose, effectively prevented the rise in SBP, DBP, and MAP among the fructose-consuming rats, as shown in figure 4.54.

Table 4.33 displays the systolic, mean, and diastolic blood pressure values with standard error of measurement (SEM) for each group, comprising the normal control group (G1), hypertensive control (G2), benidipine SNEDDS (G3), and pure BD (G4). Table 4.34 displays the systolic, mean, and diastolic blood pressure readings with standard error of measurement (SEM) for each group, comprising the normal control

group (G1), hypertensive control (G2), benidipine with telmisartan SNEDDS (G5), and pure TEL (G6).

The studies suggest that S-SNEDDS of BD and BD with TEL demonstrated higher bioavailability compared to both pure BD and BD with TEL drugs. This enhanced bioavailability might be related to the enhanced solubility of BD and BD with TEL obtained with the S-SNEDDS formulation. This difference in hypertensive response is suggestive of the higher drug solubility and absorption kinetics achieved by the S-SNEDDS formulation.

Treatments	Blood pressure (mm Hg)						
	Types	**0 hr**	**1 hrs**	**2 hrs**	**4 hrs**	**6 hrs**	**8 hrs**
Normal control (G1)	Systolic	117.0±1.633	112.83±1.40	110.33±2.201	107.00±1.155	103.83±1.851	106.17±3.070
	Mean	92.67±1.232	88.17±0.864	89.89±0.901	87.78±0.918	87.50±0.576	86.83±0.373
	Diastolic	80.50±1.408	75.83±1.195	79.50±0.885	78.17±1.078	79.33±1.174	77.17±1.078
Hypertensive control (G2)	Systolic	162.67±1.667$^{@}$	157.83±1.740$^{@}$	155.50±1.648$^{@}$	162.667±1.764$^{@}$	155.50±1.821$^{@}$	162.83±3.060$^{@}$
	Mean	126.22±1.655$^{@}$	121.94±1.543$^{@}$	121.94±1.703$^{@}$	123.33±1.167$^{@}$	117.83±1.659$^{@}$	121.28±0.218$^{@}$
	Diastolic	108.00±1.770$^{@}$	104.00±2.221$^{@}$	105.17±2.040$^{@}$	103.67±1.308$^{@}$	99.00±1.966$^{@}$	100.50±1.544$^{@}$
Benidipine SNEDDS (G3)	Systolic	158.0±0.856	138.50±1.118*	131.83±0.946*	128.33±1.054*	124.50±1.147*	126.00±1.770*
	Mean	123.11±1.365	107.83±0.864*	102.72±0.777*	99.89±0.991*	97.61±1.013*	99.33±1.029*
	Diastolic	105.67±1.820	92.50±1.648*	88.17±1.515*	85.67±1.282*	84.17±1.078*	86.00±1.033*
Pure Benidipine (G4)	Systolic	157.17±2.561	144.50±1.258*	139.17±1.014*	132.50±1.500*	134.50±1.668*	138.83±1.701*
	Mean	123.17±2.506	111.39±1.477*	108.94±1.240*	105.17±0.453*	106.83±1.179*	107.28±1.418*
	Diastolic	106.17±2.522	94.83±2.272*	93.83±1.797*	91.50±1.088*	93.00±1.506$^{\$}$	91.50±1.784*

Table 4.33: Pharmacodynamics study of BD-SNEDDS and Pure Benidipine
All the values are in mean ±SD (n=6)
$^{@}$P<0.01, when compared to normal control group; $^{\$}$P<0.05, *P<0.01, when compared to hypertensive control group (Annova followed by Dunnett's multiple't' test)

The inclusion of surfactants in the S-SNEDDS formulation likely contributed to the enhanced water solubility of BD and BD with TEL and promoted the quick dispersion of drug globules. This result is consistent with the potential of SNEDDS to deliver drug molecules at the nanoscale scale, therefore increasing the surface area accessible for oral absorption. This corresponds with the concept that smaller particle sizes and a higher surface area contribute to better dissolving behavior and enhanced absorption [140-142].

Treatments	Blood pressure (mm Hg)					
	Blood pressure	0 hr	2 hrs	6 hrs	12 hrs	24 hrs
Normal control (G1)	Systolic	117.0±1.633	110.33±2.201	103.83±1.851	101.00±2.477	110.83±3.683
	Mean	92.67±1.232	89.89±0.901	87.50±0.576	85.44±1.219	89.17±1.468[@]
	Diastolic	80.50±1.408	79.50±0.885	79.33±1.174	77.67±1.706	78.33±2.155
Hypertensive control (G2)	Systolic	162.67±1.667[@]	155.50±1.648[@]	155.50±1.821[@]	153.33±2.860[@]	148.33±3.833[@]
	Mean	126.22±1.655[@]	121.94±1.703[@]	117.83±1.659[@]	120.78±1.833[@]	115.28±2.140[@]
	Diastolic	108.00±1.770[@]	105.17±2.040[@]	99.00±1.966[@]	104.50±2.754[@]	98.50±2.262[@]
Benidipine+ Telmisartan SNEDDS (G5)	Systolic	159.33±1.085	133.33±1.667*	122.83±1.493*	119.50±2.766*	124.50±3.423*
	Mean	124.55±1.207	102.55±1.472*	98.17±1.765*	97.61±1.013*	100.94±2.147*
	Diastolic	107.17±2.023	87.17±1.922*	85.83±2.386*	83.50±1.996*	89.17±2.482[$]
Pure Benidipine + Telmisartan (G6)	Systolic	156.83±2.183	137.83±1.515*	127.17±1.424*	126.50±2.045*	131.33±2.654*
	Mean	123.28±2.296	105.94±1.013*	101.72±1.679*	99.83±1.964*	103.11±1.703*
	Diastolic	106.50±2.705	90.0±1.633*	89.00±2.309*	86.50±2.884*	89.00±2.840[$]

Table 4.34: Pharmacodynamics study of Benidipine with Telmisartan-SNEDDS and Pure Benidipine with Telmisartan

All the values are in mean ±SD (n=6),

[@]P<0.01, when compared to normal control group; [$]P<0.05, *P<0.01, when compared to hypertensive control group (Annova followed by Dunnett's multiple't' test)

Statistical analysis was performed using one-way ANOVA followed by Dunnett's post hoc test, with statistical significance defined at $p < 0.05$. Moreover, the normotensive rats provided S-SNEDDS of BD and BD with TEL displayed a noteworthy drop ($p < 0.05$) in systolic blood pressure, mean arterial blood pressure, and diastolic blood pressure. This observation further highlights the potential antihypertensive efficacy of the S-SNEDDS formulation even in normotensive situations.

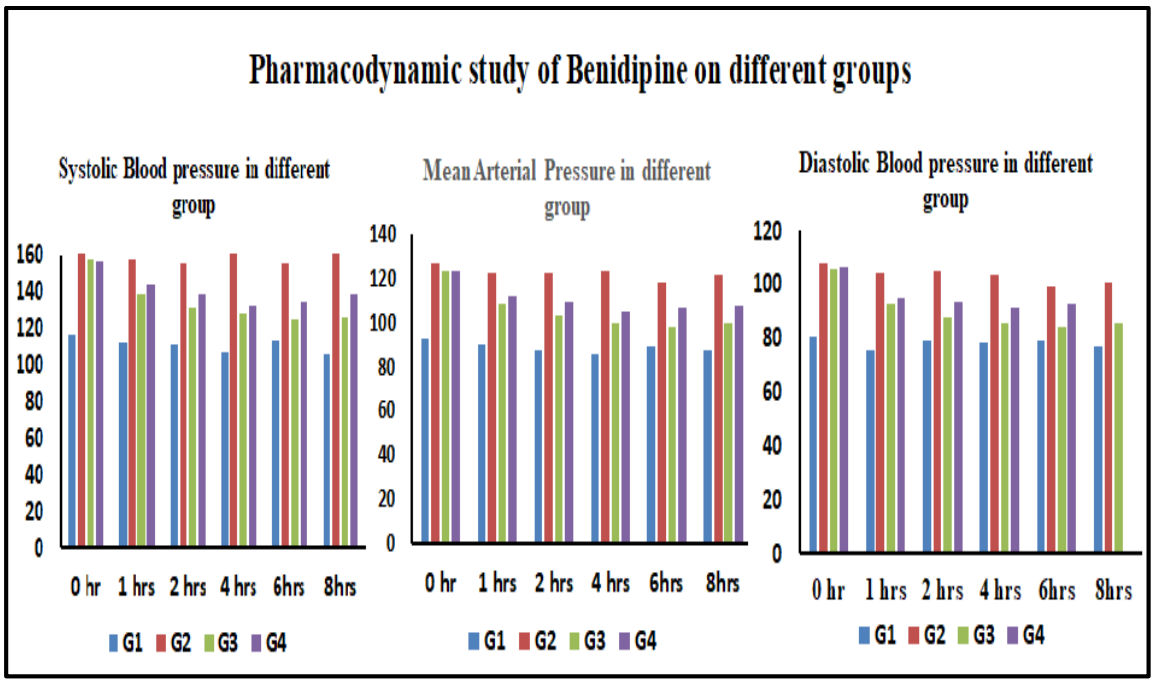

Figure 4.54: Systolic blood pressure, Mean Arterial pressure and Diastolic blood pressure values before and after benidipine treatment to different group (n=6 rats/group)

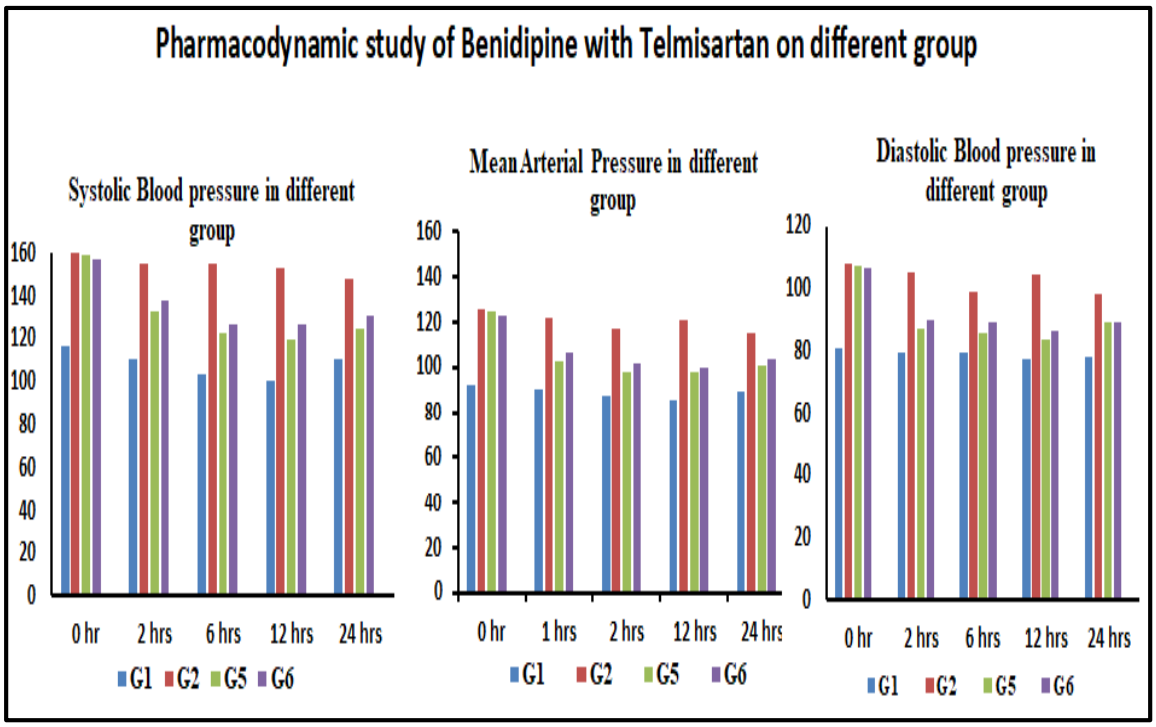

Figure 4.55: Systolic blood pressure, Mean Arterial pressure and Diastolic blood pressure values before and after benidipine with telmisartan treatment to different group (n=6 rats/group)

Accelerated stability study

A stability study was done on the optimized formulations BD14 for Benidipine SNEDDS and BT11 for Benidipine with Telmisartan SNEDDS. The investigation included keeping the formulations at a temperature of 40±2°C and a relative humidity of 75±5% for a period of six months. A stability chamber was used to create accelerated conditions. Periodic assessments were conducted to evaluate the stability of benidipine and telmisartan in the formulation under different storage conditions. These assessments included measuring changes in globule size, emulsification efficiency, % transmission, and drug release at 15 minutes.

After six months of storage at 40±2°C and 75±5% relative humidity, the BD-loaded S-SNEDDS of BD14 samples and the BD with TEL-loaded S-SNEDDS of BT11 exhibited no observable changes in emulsification efficacy, size of the globules, percentage of transmission, or release of the drug over a period of fifteen minutes. These findings indicate that BD14 and BT11 in the augmented S-SNEDDS exhibit chemical and structural stability. Table 4.35 presents the stability characteristics of the S-SNEDDS formulation including benidipine in BD14, whereas Table 4.36 shows the stability characteristics of the S-SNEDDS formulation containing benidipine with telmisartan in BT11.

Parameters	**Formulation at 40± 2°C and 75 ± 5% RH.**				
Months	**0**	**1**	**2**	**3**	**6**
Visual appearance	Transparent	Transparent	Transparent	Transparent	Transparent
Emulsification time T_{emul} (sec)	65.21±1.1	65.85±1.7	66.20±1.4	67.80±1.2	68.10±0.5
Droplet size (D_{nm})	156.20±2.4	158.10±1.4	158.85±1.3	159.45±1.7	160.15±1.1
% Drug release Benidipine in 15min	92.65±1.70	91.80±1.35	91.06±1.14	90.20±1.1	90.05±1.22
%Transmittance	99.80±0.70	99.60±0.60	99.20±0.15	98.50±0.25	98.15±0.40

Table 4.35: Stability investigation of optimized BD-loaded S-SNEDDS
Each of the values is in Mean ± SEM (n=3)

Parameters	**Formulation at 40± 2°C and 75 ± 5% RH.**				
Months	**0**	**1**	**2**	**3**	**6**
Visual appearance	Transparent	Transparent	Transparent	Transparent	Transparent
Emulsification time T_{emul} (s)	50.18±1.95	50.76±1.7	51.20±1.4	51.80±1.2	52.10±0.5
Droplet size (D_{nm})	176.24 ±2.40	175.90±1.4	158.85±1.3	177.45±1.7	178.15±1.1
% Drug release BD in 15min	93.56±1.10	92.94±1.3	91.15±1.4	90.89±1.1	90.05±1.22
% Drug release TEL in 15min	93.74±0.7	92.9±1.95	91.30±1.40	90.85±1.07	90.15±1.17
%Transmittance	99.6±0.3	99.50±0.50	99.10±0.35	98.95±0.65	98.15±0.40

Table 4.36: Stability investigation of optimized BD with TEL-loaded S-SNEDDS
Each of the values is in Mean ± SEM (n=3)